Survey of Ophthalmology

Imaging of vascular abnormalities in ocular surface disease

--Manuscript Draft--

Manuscript Number:	SURVOPH-D-21-00026R2
Article Type:	Review article
Section/Category:	Cornea/External Disease
Keywords:	ocular surface; vascularization; corneal neovascularization; OCT-A; angiography; fine needle
Corresponding Author:	Vito Romano, MD University of Liverpool Liverpool, UNITED KINGDOM
First Author:	Vito Romano, MD
Order of Authors:	Vito Romano, MD
	Bernhard Steger
	Mohammad Ahmad, FRCOphth
	Giulia Coco
	Luca Pagano, MD
	Sajjad Ahmad
	Yitian Zhao, PhD
	Yalin Zheng, PhD
	Stephen B Kaye, MD
Abstract:	The vascular system of the ocular surface plays a central role in infectious, autoimmune, inflammatory, traumatic and neoplastic diseases. The development, application and monitoring of treatments for vascular abnormalities depends on the in vivo analysis of the ocular surface vasculature. Until recently, ocular surface vascular imaging was confined to biomicroscopic and color photographic assessment, both limited by poor reproducibility and the inability to image lymphatic vasculature in vivo . The evolvement and clinical implementation of innovative imaging modalities including confocal microscopy, intravenous and OCT-based angiography now allows standardized quantitative and functional vascular assessment with potential applicability to automated analysis algorithms and diagnostics.
Response to Reviewers:	

Title: Imaging of vascular abnormalities in ocular surface disease

Short title: Ocular surface vascularity

Authors: Vito Romano[1,2*],MD, Bernhard Steger[3*],MD, Mohammad Ahmad[1], FRCOphth, Giulia Coco[1,4],MD, Luca Pagano[1,5], MD, Sajjad Ahmad[6],PhD, Yitian Zhao[2,7], PhD, Yalin Zheng[2], PhD, Stephen B Kaye[1,2] MD

*Vito Romano and Bernhard Steger contributed equally.

Affiliations:

[1] The Royal Liverpool University Hospital, Liverpool, UK

[2] Department of Eye and Vision Science, Institute of Life Course and Medical Sciences, University of Liverpool, Liverpool, UK

[3] Department of Ophthalmology, Medical University of Innsbruck, Innsbruck, Austria

[4] Department of Clinical Science and Translational Medicine, University of Rome Tor Vergata, Rome, Italy

[5] Humanitas Clinical and Research, via Manzoni 56, 20089 Rozzano (Mi) - Italy

[6] UCL Institute of Ophthalmology, London, UK

[7] Cixi Institute of Biomedical Engineering, Ningbo Institute of Materials Technology and Engineering, Chinese Academy of Sciences, Ningbo, 315300, China

Correspondence:

Vito Romano, MD

Corneal and External Eye Disease Service,

Royal Liverpool University Hospital,

Liverpool, United Kingdom L7 8XP

Email: Vito.Romano@liverpool.ac.uk

Tel: 0151 706 3997

Abbreviations: CoNV: Corneal neovascularization; FA: Fluorescein angiography; ICGA: Indocianin green angiography, ICG: Indicianin green; IVCM: *In vivo* confocal microscopy; OCT: Optical coherence tomography; OCT-A: Optical coherence tomography angiography; HSV: Herpes simplex virus; MCA: Marginal corneal arcades; LCA: Lymphatic corneal arcade ; FSLB: Functional slit lamp biomicroscocpy ; PAM: Photoacoustic microscopy; ROI: Region of interest ; DSA: Digital subtraction analysis ; VBR: Validated Bulbar Redness ; PDI: Pixel densitometry index ; HSK: Herpes simplex keratitis; LSCD: Limbal stem cell deficiency; OSN: Ocular surface neoplasia; AI: Artificial intelligence

Abstract

The vascular system of the ocular surface plays a central role in infectious, autoimmune, inflammatory, traumatic and neoplastic diseases. The development, application, and monitoring of treatments for vascular abnormalities depends on the *in vivo* analysis of the ocular surface vasculature. Until recently, ocular surface vascular imaging was confined to biomicroscopic and color photographic assessment, both limited by poor reproducibility and the inability to image lymphatic vasculature *in vivo*. The evolvement and clinical implementation of innovative imaging modalities including confocal microscopy, intravenous, and optical coherence tomography-~~OCT~~-based angiography now allows standardized quantitative and functional vascular assessment with potential applicability to automated analysis algorithms and diagnostics.

Keywords: Ocular surface; vascularization; corneal neovascularization; OCT-A; angiography; fine needle

Disclosure

None of the authors have any potential conflict of interest

1. Introduction

The vascular system of the ocular surface is essential for the homeostasis of the cornea and conjunctiva. It delivers nutrients and removes catabolites and aids the defense responses of the ocular surface to infectious, inflammatory, traumatic, and neoplastic disease. The vasculature normally covers the entire ocular surface except for the cornea, although it does extend into the corneal periphery. Pathologic vessel formation such as corneal neovascularization (CoNV) and abnormal neoplastic vessel formation~~,~~ or peri-limbal vessel loss [27,134] following chemical or radiation injury, represent significant causes of visual loss [9]. Although the global impact is not known, the incidence rate of CoNV has been estimated to be 1.4 million per year in the United States [33]. The development, application, and monitoring of treatments for vascular abnormalities depend~~s~~ on the *in vivo* analysis of the ocular surface vasculature. ~~The purpose of this literature review is to~~We provide a picture of current methods for imaging and quantifying vascular abnormalities in ocular surface diseases and~~,~~ their clinical applications and highlight future perspectives.

2. History of imaging of vascular abnormalities of the ocular surface

Documentation of vascular conditions of the ocular surface has been underpinned by accurate drawing and image annotation. Advances in ocular surface imaging follows the improvements in photography, such as lighting systems and magnification. Use of fluorescein in ophthalmology dates back to 1881~~,~~ when Ehrlich observed that the dye appeared in the anterior chamber following injection into the blood stream [41]. Jensen and Lundbaek in 1968 described the use of fluorescein angiography (FA) for studying iris vascularization [62]. In 1969, Mitsui an ~~coworkers~~co-workers~~et al.,~~ used FA to study CoNV, highlighting the vascular patterns associated with trachoma and herpes simplex virus (HSV) [94]. In 1971, Bron and Easty, in a large study of 250 patients, concluded that 'fluorangiography', was the only investigation able to identify CoNV, which would otherwise be difficult to visualize with photography or slit lamp biomicroscopy. They also noted the ability of FA to identify vascular leakage and its limitation in visualizing vessels underneath corneal scars [86]. In the 1980's, Goldberg and Bron [48], Meyer and Watson, [92] and others [94,141,19,35] were able to describe in detail the features of the limbal palisades using FA. Image analysis programs and the dependency on analogue systems, limited the analysis that could be undertaken. Following improvements in digital imaging systems, corneal and anterior segment angiography gained new interest in the second decade of the 21st century~~2000'~~, with the quality of image analysis software enabling more reliable and reproducible methods for quantifying CoNV [70,8,139]. Further steps in the imaging of the ocular surface vasculature came with developments of *in vivo* confocal microscopy (IVCM). In 1998, Yaylali and ~~coworkers~~co-workers~~et al.,~~ first described CoNV using IVCM, [147] followed In 2009 by Guthoff and

Formatted: Superscript

~~coworkers~~co-workers~~et al.,~~ who were able to obtain depth selective high-resolution *in vivo* optical images [51]. More recently developments in optical coherence tomography angiography (OCT-A) ha~~ve~~s allowed visualization of blood flow in vessels via motion contrast imaging of blood cell movement across sequential B-scans [133,7,21].

3. Anatomy of the ocular surface vasculature

The blood supply to the anterior segment of the eye is derived from both an extraocular and an intraocular circulation~~route~~ [91]. The medial and lateral long posterior ciliary arteries that run within the globe~~,~~ arise from the ophthalmic artery and travel forward to supply the iris, ciliary body, and anterior part of the choroid. The external route consists of anterior ciliary arteries that~~, which~~ are continuations of the muscular arteries from the ophthalmic artery. The anterior ciliary arteries run forward along the tendons and divide within the episcleral tissue to form an anterior episcleral arterial arcade that~~, which~~ supplies the anterior conjunctival and episcleral capillary bed. The anterior ciliary arteries give rise to the episcleral branches, which in turn give rise to the recurrent conjunctival arteries, the palisadal vessels~~,~~ and the marginal arcades (terminal capillary loops) of the cornea that~~, which~~ are the most centrally located vessels [48,92] (Figure 1).

The superior and inferior medial palpebral arteries (from the ophthalmic artery) anastomose with the corresponding superior and inferior lateral palpebral arteries (from the lacrimal artery) to form the marginal and peripheral tarsal arcades in the upper and lower lid. These supply the palpebral conjunctiva and the fornixes. The ascending branches from the peripheral tarsal arcade pass around the fornixes as the posterior conjunctival arteries. These vessels anastomose with conjunctival arteries from the anterior ciliary arteries and supply the bulbar conjunctiva. The conjunctival veins largely accompany the corresponding arteries. The episcleral venous plexus also receives blood from the anterior uveal circulation as well as aqueous from the Schlemm~~'s~~ canal. The venous blood then primarily drains into the superior ophthalmic vein, which empties into the cavernous sinus [17]. There is, however, significant anatomical variation am~~o~~ng~~between~~ individuals [124].

3.1 Limbal vascular complex and the marginal corneal arcades (MCA)

The limbal vasculature helps to maintain the homeostasis of the limbal palisade stem cell niche. Biomicroscopy and anatomical methods such as vascular casting have informed much of our understanding of this vasculature [101,49]. In the 1980's, Goldberg and Bron used FA to demonstrate that the vessels of the palisades are derived from the anterior ciliary arteries, [48] and Meyer and Watson showed that the limbal arcades are supplied by anterior branches from the episcleral circle

[92]. Peng Li and ~~coworkers~~co-workers~~et al.~~, using optical microangiography, suggested that a fraction of the conjunctival plexus become terminal vessels which reach the palisades of Vogt to supply the peripheral corneal arcades [77]. They also noted recurrent vessels in the conjunctival plexus, which run posteriorly to supply the perilimbal area [77]. The vessels within the peripheral cornea (0.2 to 0.3mm) are the marginal corneal arcades [129] (MCA, Figure 1 and 2). Until recently, little was known about the MCA, particularly in the living human eye, because of~~due to~~ limitations in image acquisition and analysis systems [16,35]. The introduction of indocyanine green angiography (ICGA) with increased magnification, computerized digital angiography, and image analysis systems [8] has greatly improved our understanding of the corneal marginal arcades *in vivo*. The MCA are a network of vessels rather than a vascular tree, consisting of vascular loops with between 3 and 4 branches, approximated by an elliptical shape with the major axis twice as long as the minor axis (Figure 2). There is, however, considerable variation in loop size and branching both within and between subjects and quadrants. The internal row of loops appears to have a slightly larger diameter than the average of the external 4-5 rows. It is possible that the larger diameter, together with an increased path length, leads to a reduced velocity of blood flow, allowing for better oxygen exchange. In fact, the total capillary loop area of the marginal capillaries varies between 10.44 x10^{-3}mm^2 and 11.87 x10^{-3}mm^2 (F~~f~~or comparison, the capillary loop area in the perifovea varies between 3.95x10^{-3}mm^2 and 6.87x10-^{3}mm^2 [25]).

While MCA are clinically visible and well described, lymphatic vessels are biomicroscopically invisible and therefore elude clinical observation [4]. The presence of limbal lymphatic vasculature has been visualized~~described with~~ immunohistochemistry using LYVE-1 antibodies to selectively stain the lymphovascular endothelium in murine and human tissues [99,103]. High resolution, cross-sectional and volumetric images of the human corneo-scleral limbus using spectral domain OCT has allowed the visuali~~z~~sation, but not the differentiation, of limbal and scleral blood and lymph vasculature [14]. The lymphatic corneal arcade (LCA) is more pronounced in the nasal compared to the temporal limbal region [36]. *In -vivo* confocal microscopy has been used to image corneal blood and lymphatic vasculature in human beings [119] (Figure 3). This technique was also applied to describe the LCA in human corneoscleral tissue [103]. Palme and coworker~~et al.,~~ showed~~,~~ that the LCA overlaps with the MCA, but terminates slightly more peripherally, and is located at a mean depth of 43 ± 12 µm~~;~~. ~~which~~This is deeper than~~compared to~~ the hematic arcade that has a mean depth of 24 ± 9 µm [103]. Morphometric characteristics as observed on *in vivo* confocal microscopy are useful to differentiate blood and lymphatic limbo corneal vasculature, with LCA showing shorter and larger vessel segments (Figure 3).

3.2 Conjunctival vascular complex [27,134]

The conjunctival vascular network is sensitive~~very responsive~~ to local irritants including contact lenses, immune and allergic reactions, infections and systemic disease such as diabetes and hypertension [102,52,1,28]. Different ~~imaging~~ methods, including digital imaging [55] and angiography, [144] have been used to try and image the conjunctival vascular network, such as digital imaging using serial displacement of red blood cells, etc.

Recently, OCT-A has been employed in imaging the anterior segment and for aiding the diagnosis of vascular lesions of the cornea and conjunctiva [7]. Akagi and ~~coworkers~~co-workers~~et al.,~~ investigated conjunctival and intrascleral vasculature using OCT-A and suggested comparable results with FA and ICGA [3]. Liu and ~~coworkers~~co-workers~~et al.,~~ carried out quantitative analysis of bulbar conjunctival microvascular density acquired using OCT-A and compared with vessel density using functional slit lamp biomicroscopy (FSLB). Vessel density measured by fractal analysis (box counting) as well as by pixel counting (per centage~~%~~) was found to be significantly lower when using OCT-A compared with FSLB [84]. Although OCT-A is considered a promising tool for evaluating conjunctival and intrascleral vasculature, further developments are required to improve axial and lateral resolution.

4. Modalities of reporting vascular abnormalities

4.1. Drawing and annotating

Hand drawing or digital image annotation can be used to record vascular pathology, and with the advent and popularity of electronic patient records it is important to have a standard method to annotate images and notes. The observer can draw or annotate any ocular surface vascular abnormality visible on the slit lamp. A generally accepted convention for documentation of corneal conditions was standardized in 1973, with frontal and slit sketches of the cornea and color-coding [18,143]. In the frontal view~~,~~ a black circle is used to represent the corneal limbus and a red color to represent vessels. Superficial corneal vessels are drawn as wavy lines originating from outside the limbus, while deep vessels are straight lines beginning at the limbus. Ghost vessels are represented as ~~straight~~ dashed lines. Corneal scars and degenerations, including lesions such as droplet keratopathy and lipoid degeneration, are black [18,143]. In the slit view~~,~~ a freehand drawing of two parallel curved lines indicating the corneal contour are first drawn. Corneal vessels are represented as red lines in the longitudinal section or as red dots in the cross section at the appropriate depth [143]. Annotation of digital images (manual, semi-automated or automated) can now be performed and may become the norm in the future (Figure 4). Hand drawings are easy to perform but are lack the

precision or reproducibility of digital images. Digital annotations of colo~~u~~r images can be time consuming if done manually, but may be performed semi-automatically in the future with further developments in artificial intelligence.

4.2. Photography

Slit lamp biomicroscopy typically uses a white light source (>100,000 lux) modulated by different filters (such as red-free and polarization filters) and different illumination patterns. In general, slit lamp biomicroscopy can provide magnifications ranging from 6x to 40x and a best resolution of approximately 20 µm. Color photographic images are popular because they match to some extent what is seen clinically using slit lamp biomicroscopy. Advantages include speed and ease of acquisition, ~~-~~as well as superior reproducibility compared to~~with~~ hand annotations. Larger vascular abnormalities of the ocular surface such as feeder vessels of tumo~~u~~rs, corneal neovascularization, and conjunctival hyperemia can be visualized. Current photography of ocular surface disease, including color, red free, and infrared, however, has limited reproducibility and image quality due to the convex ocular surface, lighting (environment, dimmer settings, diffuser, slit-beam angle), camera definition (magnification, number of pixels of the lens, diaphragm diameter and shutter speed), and patient-dependent factors [11]. Fine details however can be lost in transparent media, and slit lamp color photographs tend to favor larger venous vessels, as these vessels are more numerous, and have a larger diameter with more red blood cells, thereby making them more prominent than the smaller, less abundant, faster flowing, and more deeply located arteries. As a consequence, many studies delineating the anatomy of the normal and abnormal ocular surface using color photography~~,~~ tend to evaluate the efferent or venous system. These limitations have meant that other techniques such as angiography and optical coherence tomography are more desirable because of their ability to highlight the presence of vessels, despite also their limitations in focusing on a convex surface [8] (Figure 5).

Photoacoustic microscopy (PAM) is another emerging imaging technology that allows vasculature visualization in 3D[64] as a result of~~due to~~ its depth-resolving imaging capability [149]. It relies on a photoacoustic effect generated when light is absorbed by an exogenous contrast agents or endogenous molecules within a medium. It utilizes the inherent optical absorbance of hemoglobin itself to provide a~~n ocular~~ vascular image [34]. This can aid ophthalmic diagnosis by providing morphologic information on ocular vasculature[63]. Liu and ~~coworkers~~co-workers~~et al~~ previously demonstrated segmentation of corneal vascularization using this technique using local regression smoothing[80]. Jeon and ~~coworkers~~co-workers~~et al.,~~ combined *in vivo* PAM imaging and an ocular surface imaging estimation method using machine learning to visualize ocular vasculature[66]. Similar

Formatted: Font: Italic

to OCTA, an advantage is the lack of side effects associated with contrast agents[56]. The presence of opaque and scarred tissue, however, affects image quality, and imaging speed are slow [66]. On the other hand, current PAM imaging requires physical contact between the eye and its ultrasonic detector that ~~which~~ may cause patient discomfort ~~of patients~~ in a similar way as a confocal microscope, and ~~their~~ resolution is ~~are~~ not sufficient to image the capillaries. It is expected that technical advances will improve the speed, depth, ~~and~~ resolution, and the need for ~~of~~ physical contact [65,81]

4.3 Angiography

Anterior segment angiography using FA and or ICGA provides accurate images of the vascular network of the ocular surface. It has been shown that anterior segment angiography allows for a 3 to 4 times greater visibility of ocular surface vessels compared to color photographs [8]. Fluorescein is an orange-red crystalline hydrocarbon that ~~. It~~ travels through vascular structures 80% bound to plasma proteins, mainly to plasma albumin, and 20% unbound. This latter component transits freely and spreads rapidly in tissues where blood-tissue barriers are altered and can therefore be visualized. Fluorescein fluoresces in the green light spectrum (520–530 nm) when the molecule is excited by a blue light (465–490 nm). Following injection into a peripheral vein of 3 ml of 20% fluorescein (Martindale Pharmaceuticals, Essex, United Kingdom), the mean time to appearance of fluorescein in CoNV is approximately 20 ± 7 seconds ,depending on the age and cardiovascular status of the patient. A combination of videography and single images acquired every three to five seconds for three minutes and late images at 5 and 10 minutes provides good detail [73,12] usually with the most informative images acquired at 47 ± 19 seconds [8] (Figures 5, 6 and 7).

ICGA uses a water-soluble~~,~~ tricarbocyanine dye that travels almost completely bound to plasma proteins (98%) after intravenous injection. This limits its diffusion through small capillary fenestrations ~~which is very limited~~, thus remaining confined into the intravascular space [59]. This accounts for the absence of leakage (before 10 minutes) and excellent vessel delineation [70,8]. After injection of 5 ml of indocyanine green at a concentration of 5mg/ml (Pulsion Medical Systems, Feldkirchen, Germany) into a peripheral vein, images are similarly acquired by videography every three or five seconds for three minutes, followed by later acquisitions at five and ten minutes. ICG in the corneal vessels appears approximately 17 ± 6 seconds after injection. Best image quality is obtained at 64 ± 41 seconds [8]. It fluoresces in the near-infrared range (790–805 nm), less than fluorescein, ~~(4% of fluorescein)~~ and can therefore be detected only with specialized infrared angiography systems [59]. Owing to the peak of indocyanine absorption in the near-infrared range, ICGA images allow a better visualization of corneal vessels in opaque corneas and corneal scars

compared to color photographs and FA [70,8] (Figure 5). ICG is then metabolized in the liver and excreted into the bile [59]. Given the different characteristics of FA and ICGA, angiography that which uses both fluorescein and indocyanine green provides better visualization of CoNVs and vessel maturity [8]. As fluorescein and ICG both travel within the vessel lumen, the differences in vessel diameter seen on angiographic images compared to color photographs may reflect vessel wall thickness [11,70,8]. Unfortunately, both FA and ICGA require intravenous dye injection and are therefore invasive, time-consuming, and can be associated with adverse reactions in some patients such as nausea, itching, and very rarely, anaphylaxis [73,54].

FA and ICG are particularly useful in delineating abnormal corneal vessels, extent of limbal ischaemia following injury, as well as vascular supply of surface tumours.

Fluorescein angiography provides important information on time to leakage, which is useful when assessing vessel maturity and late reuptake by lymphatics. Although leakage can affect image quality, the extent of leakage can help decide between medical and surgical treatment, as timing and extent of leakage are an indirect indicator of vessel maturity.

4.4 *In vivo* confocal microscopy (IVCM)

Formatted: Font: Italic

IVCM is a non-invasive imaging technique for imaging the cornea at high resolution. IVCM is based on the confocal principle discovered by Marvin Minsky in the 1950s [88]. Using point illumination, a pinhole is introduced in an optically conjugate plane to selectively allow only light reflected from the focal plane to pass through. This configuration blocks the light that is out-of-focus and significantly improves the axial and lateral resolution. Depending on the scanning pattern, there are slit-based systems such as the Nidek instrument and laser scanning such as the Heidelberg HRT3 [61,37]. TheHRT3 uses spotlights at near infrared range (about 670 nm) to scan the tissues in a raster scan pattern. IVCM can normally provide a magnification >400x and a lateral resolution of about 1um/pixel. It requires the lens or a cap to applanate the cornea of the patients in order to achieve high resolution. By moving the focal points in the axial direction, a series of images of the corneal structures at different depths can be acquired. Romano and coworkersco-workerset al., showed larger corneal vessels filled with erythrocytes using IVCM, while the intravascular cell types could not be determined in the small vessels [120]. Figure 3 shows an exemplary IVCM image of large corneal vessels. Although the resolution is very high, image quality is limited by low contrast. IVCM also requires contact with the cornea provides a very small field of view that which can be of limited value when assessing large area of vascularizsation. Moreover, while IVCM allows in vivo microscopic evaluation of the cornea, it only provides morphologic information and requires careful interpretation and clinical correlation. Limited reproducibility means that, at present, it is not

routinely used to evaluate ocular surface vascular abnormalities such as staging or differentiating corneal vascularizsation, tumour progression, or ischaemic changes following chemical injury.

4.5. Optical coherence tomography angiography

OCT-A is an innovative application of the OCT technique that was initially introduced in 1991 [58] as part of the rapid development of OCT [45]. OCT uses an interference principle similar to ultrasound to acquire high-resolution images of biological tissues with near infrared light in a non-invasive manner. It can provide axial resolution down to ~~to~~ 1-2 µm [74] (Figure 8). OCT-A, is a functional extension of OCT imaging that enables visualization of microvasculature down to capillary level [132]. OCT-A reconstructs blood vessels by detecting moving particles such as red blood cells in the tissue by detecting phase [44] or amplitude [67] differences from the repeated OCT scans at the same location. By conducting continuous cross-sectional OCT-A scans of the tissue, a 3-dimensional OCT-A map can be produced. In order to facilitate the visualization of retinal vessels, projections of the acquired 3D OCT-A map into 2D enface images are frequently used. Compared with FA and ICGA, OCT-A is preferred for its non-invasive nature, however, it is not able to show the dynamic patterns of leakage offered by FA and ICGA especially when assessing corneal vascularizsation. Recent studies have suggested that measurement of ocular surface vessel density by OCTA in eyes with pterygia and pinguecula is repeatable [150]. It should be noted that, while the scan only takes a few seconds, involuntary movements of the eye could affect the quality of CoNV images. Although at present, its main applications clinically are in retinal imaging [47], a recent literature has demonstrated applicability of OCT-A in assessing abnormal vasculature in pterygium and corneal neovascularization invading corneal graft [7,26]. Currently there are four OCT-A devices: AngioVue RTVue XR Avanti (Optovue, Fremont, California, USA), Angioscan RS-3000 Advance (Nidek, Gamagori, Aichi, Japan), Triton Prototype DRI-OCT (Topcon Corporation, Tokyo, Japan), and PLEX Elite 9000 (Carl Zeiss Meditec, Dublin, California, USA) [76]. Figure 8 shows an OCTA image obtained with AngioVue and a FA/ICG angiograph of CoNV [22]. Table 1 summarizes the applications, benefits, and limitations of each of the imaging modalities.

5.0 Analysis

5.1 Quantitative image analysis

Quantitative analysis of images is essential for the characterization of lesions and in aiding management plans [134,8,70]. In general, these analyses involve a number of techniques in the field of image analysis [8]. Firstly, image enhancement or restoration may be required when the image quality is poor or there is too much noise for the subsequent analysis. Following image enhancement, an

automated process of threshold binarization allows ~~to~~ enhancement of the vessel's pixels compared to the surrounding pixels. Vessel segmentation is then applied to the enhanced images so as to separate the pixels of vessels from the background. The segmentation is often represented by a binary image where white pixels represent vessels and black pixels represent non-vessels. After the segmentation a skeletonization process is often required in order to extract the center ~~re~~ lines of the vessels for the detailed analysis of vessel parameters (Figure 4).

In the situations where there are several images of the same structure or pathology taken at different times, a process called image registration can be applied to align them into the same spatial coordinates. This process is essential to obtain digital subtractions (subtraction between images after alignment) [119], or to measure flow by detecting the movement of particles in the same vessel [152].

5.2 Definitions of vessel parameters

Ocular surface vessels often appear as a vascular network. In order to characterize these networks, ~~in general~~ a top-down approach is generally adopted, and the whole vascular segmentation is divided into individual vessel segments by the knowledge of branching or intersection points. Once we derive the center lines of the vessels, then the tail (end) points are defined as the pixels that only have one neighbor vessel pixel, while branching points are defined by pixels that have three neighboring vessel pixels. Due to ~~the~~ projection artefacts, intersections (pixels with more than three vessel pixel neighbors) between vessels may appear, and ideally these need to be removed. Figure 4 illustrates the segmented vessels with center lines, branching, tail and intersection points. For each segment then we can then measure its length, diameter and tortuosity. For instance, the length of a segment is the length along the path between its two end points. Given the vessels are often not straight, tortuosity is used to measure the curviness of a vessel segment. There are many definitions, however, the one defined by the ratio of the path length against the Euclidian distance between the two end points is most commonly used (the smallest value is 1 when it is a straight line) [8]. The diameter at each point along the path is the distance between two intersection points on the edge of the vessels of the perpendicular line passing the point under consideration. The mean diameter can then be estimated by averaging the diameters along the path. The area of a segment is the total number of pixels between the two end points of a segment. After all the parameters of each individual vessels are extracted, an overall picture of the whole vasculature can be produced using statistical analysis [152].

5.3. Program, software design and datasets

At present, there are no proprietary programs that can be used for the quantitative analysis of vessel parameters. Programs described in the literature are often semi-automated, customized for specific applications, or even certain types of images. In addition, there are no publicly available datasets to evaluate the programs, thus it is difficult to validate these techniques and widen their applications. Future developments in technology may overcome these limitations.

6. Vascular parameters

A multimodal approach is very helpful in providing most of the detail needed to adequately delineate the vascular abnormality. Slit lamp biomicroscopy and drawing or annotating color images are necessary to ask the clinical question and then to define what is known as the region of interest (ROI). Functional slit lamp biomicroscopy consists of a slit lamp and digital camera. It can assess vessel diameter, blood flow velocity and also generate vascular perfusion maps. It is typically used in contact lens and dry eye disease to study change in microvasculature on the ocular surface. [130] ICGA delineates the anatomy of the vascular network, location and number of afferent vessels and FA vessel maturity. OCT-A differentiates between superficial and deep CoNV [21] (Figure 8).

Changes in the area of CoNV, vessel diameter, branching, and tortuosity have been shown to be particularly evident on angiography, and the analysis provides a reliable measure of change. [70,11] Although some of these parameters may be present in color images, they are much less evident and are inconsistent. Angiography and OCT-A in conjunction with computer-assisted automated analysis, have enabled the measurement of individual vessels across ROI for each patient before and after treatment. This type of analysis enables construction of frequency histograms and statistical testing of changes in vessel parameters for each patient. For example, following treatment of microbial keratitis, the frequency distributions of individual vessel parameters such as diameter and tortuosity for an individual patient, show a reduction in vascular parameters accompanied by a reduction in the spread of vessel size.

6.1 Filling patterns

Angiographic methods have shown that limbal vessels and MCAs do not fill at the same rate around the circumference of the cornea [152]. The inferior vessels fill first, followed by those of the superior, nasal, and temporal regions [152]. There is a 6 second difference in filling of the inferior MCAs to those of the temporal region. In cases of carotid stenosis, delays in filling of the limbus and surrounding conjunctiva may be expected [137].

6.2 Origins of corneal neovascular complexes

Angiography is essential for the investigation of the origin of the vascular complex. Arterioles or afferent vessels may be differentiated clinically from venules or efferent vessels, as they are a usually thinner, straighter, deeper and less tortuous. There are generally fewer afferent than efferent vessels and, in the presence of large vascular complex, they can be very difficult to find. CoNV may potentially arise from the MCA, the limbal vessels and or the surrounding conjunctival and episcleral vascular arcades. The location and severity of the disease will usually determine their respective origin. For example, CoNV resulting from disease confined to the cornea, such as inflammatory or infective conditions, may arise from the intact limbal and MCA. In situations where there is injury to the MCA and limbal arcades, such as in a chemical injury resulting in limbal ischemia, CoNV may develop from the in-growth and or originate from conjunctival and episcleral vessels. Determining the origin of the vascular complex helps plan treatment, especially for selective fine needle diathermy. [116136118114] (Figure 9 and 10, video 1 and 2)

6.3 Area

Defining and measuring the area of an abnormal vascular network is important for both characterizing the condition and measuring the response to treatment [79]. For example, the number of 'quadrants' of CoNV is significantly associated with an increased risk of corneal graft rejection [87]. Corneal angiography compliments slit lamp biomicroscopy as it has a wide field of view which helps to precisely quantify the area of CoNV. At present, OCT-A has a limited field of 6x6 mm and still presents artifacts that limit its ability to quantify the area (Figure 8).

6.4 Drop-out

Defining an area of ischemia and or vessel loss ~~particularly~~ following a chemical injury is essential for planning clinical management. It can be very difficult to discern between the unaffected and damaged vessels with no blood flow by simple observation on slit lamp biomicroscopy and accompanying photography. Determining the extent of limbal ischemia for example, is crucial for assessing the risk of limbal stem cell failure or neovascular response following a chemical injury. Using anterior segment angiography (OCT-A, FA and ICGA) provides the best definition of the ischemic area, residual vascular damage with leakage, degree of flow, and capillary drop out [113,46](Figure 11).

6.5 Vessel parameters (diameter, branching, tortuosity)

ICGA provides excellent vessel delineation even in the presence of stromal scars to measure vessel parameters~~,~~ such as branch pattern, segment length, diameter, and tortuosity. Appropriate

computer software is essential for this type of analysis. Kirwan and ~~coworkers~~co-workers~~et al.~~ found~~showed~~ a statistically significant reduction in mean vessel diameter in patients treated for active keratitis, -that was more evident when analyzed with ICGA (reduction from 44.77μm to 33.29μm), compared to color images (reduction from 29.10μm to 25.17μm [70]).

6.7 Flow

Digital angiography measures vascular flow (rate and direction), which is useful for disease monitoring. For example, direction of flow is important in planning treatment such as fine needle diathermy. Digital angiography is gaining importance especially in cases of ocular surface neoplastic lesions where the intralesional formation of shunt vessels and the filling time can be considered as a parameter in malignant lesions [23]. Tissue perfusion is proportional to the transit time across a capillary bed which in turn governs the time available for the exchange of respiratory gases. Alfred and Nuttal noted that the greatest velocities occurred in feeder vessels, which are vessels that divide into two or more capillaries at the apical border [98]. A problem in measuring blood flow velocity through capillaries by observation is the need for a mark by which blood motion along the vessel can be observed [60]. Ivanov used gaps (plasma) between erythrocyte flow to measure velocity [60]. It is difficult, however, to appreciate gaps with the use of dyes such as ICG and FA. Although only based upon one patient, the average speed of flow in the marginal corneal arcade of 0.22 mm/second or 0.79m/hour, is similar to the velocity of blood flow in the capillaries of the cochlea which has been measured from below 0.1 mm/s to about 0.3-0.4 mm/s with an average velocity of 0.22 mm/s [98,109]. Although the flow velocity in the limbal vessels is unknown, it would be expected to be greater than in the MCA.

6.8 Angiographic dye leakage

6.8.1 Corneal neovascular complex (CoNV)

Apart from the MCA, all corneal vascularization is pathological. CoNV evolves as a result of a disruption of the balance between pro- and anti-angiogenic factors, with loss of the corneal angiogenic and immune privilege [27,93]. The time to leakage of FA or ICGA provides a measure of vessel staging and maturity. Fluorescein usually leaks at 42 ± 23 seconds depending on the maturity of the CoNV. The earlier the leakage (about 30 seconds), the more immature the vessel and the later the leakage (about 50 seconds), and the more mature and stable the vessel [8] (Figure 7). For example, time to first appearance of FA dye leakage significantly increases following treatment and resolution of the keratitis and is consistent with the clinical impression of reduced vascular leakage as the inflammation responds to treatment. Topical fluorescein before intravenous fluorescein injection

interferes with good angiographic image quality and should be avoided [8]. Palme and ~~coworkers~~co-~~workers~~~~et al.,~~ demonstrated a significant association between the time to ICG leakage and clinical staging of CoNV and the age of CoNV [104]. ICG leakage within 10 minutes was observed significantly more frequently in cases with active compared to inactive CoNV (100% vs 9%, p<0.001), supporting the use of FA and ICGA to ~~objectively~~ stage objectively the activity of CoNV and to guide treatment. The use of a five-grade biomicroscopic staging scale of CoNV by Faraj and ~~coworkers~~co-~~workers~~~~et al.,~~ was found to be of limited value due to reliance on easily seen large vessels which are usually efferent (venous) with little attention to afferent (arterial) vessels that~~which~~ are fewer and much more difficult to discern ~~as acknowledged by the authors~~ [43]. This limitation underlines the need for objective measures reflecting functional stages and maturity of CoNV and the need to distinguish afferent and efferent vessels, especially for guiding treatment [116]. Palme and ~~coworkers~~co-~~workers~~~~et al.,~~ therefore suggested 3 clinical stages of CoNV: a~~A~~ctive CoNV, i~~I~~nactive CoNV and r~~R~~egressed CoNV (ghost vessels) (Figure 6 and 7).

This simplified clinical three-stage classification ~~(active, inactive, and regressed CoNV)~~ was found to be supported by the angiographic features (leakage, pattern, and size) and age of CoNV. In both patients with active and inactive CoNV, there is perfusion of the corneal vessel plexuses on angiography with no differences in segment length, branching, and tortuosity. Time to leakage of both fluorescein and ICG helps to define active from inactive CoNV. For example, leakage of ICG dye within 10 minutes was identified in 100% of active, but only in 6.3% of inactive or regressed CoNV. At late stages of inactive CoNV, angiography showed cessation of red blood cell traffic but persistent acellular flow in corneal plasma vessels confirmed by IVCM. The intravascular lumen of plasma vessels was found to be large enough to potentially carry red blood cells (average diameter, 21 mm), and the mean vessel diameters did not differ between plasma vessels and active CoNV.

Corneal hematic angiogenesis is mostly accompanied by the formation of lymphatic neovessels.[78,32,145,31] These lymphatic vessels, however, have long eluded *in vivo* detection because of the transparency of lymphatic endothelial cells and the lymph fluid [108]. Based on these findings Romano and ~~coworkers~~co-~~workers~~~~et al.~~ [120]~~,~~ proposed to image corneal lymphatic vessels using IVCM and digital subtraction analysis of intravenous angiograms, showing that dye leaks out from vessels into the surrounding tissues and is then reabsorbed into the venous or lymphatic system or both [117] (Figure 3). They ~~authors~~ suggested that ~~the~~ uptake into the lymphatic micro vessels in the cornea will occur in less than an hour, enabling the visualization of micro-lymphatic vessels. Digital subtraction analysis (DSA) was used to objectively identify newly appeared corneal vessels with reuptake of ICG from the interstitial space. It was shown that, similar to the mouse model used by

Yuen and ~~coworkers~~co-workers~~et al.~~, corneal neovascular lymphatic vessels are co-localized to blood vessels [148]. This method, however, has limitations such as imaging at exactly the same angle and focus of a 3-dimensional CoNV on the spherical cornea, which can be difficult to perform. Technological developments to improve alignment may enhance the ability to more consistently identify such a vascular structure with DSA.

6.8.2 Conjunctival vessels and inflammation

Conjunctival capillaries are fenestrated, allowing more rapid passage of luminal contents in inflammation [138]. After intravenous injection of fluorescein, conjunctival vessels ~~can be seen to~~ leak in a time and concentration sequence similar to that of the choroidal capillaries. The vessels at the palisades of Vogt may be more competent and leak less than conjunctival vessels elsewhere. Conjunctival inflammation, infections, irritation, or severe intraorbital inflammation cause the conjunctival capillaries to leak plasma proteins faster than the fluid can pass between the epithelial cells [30,96,85]. This phenomenon can be used to stage the activity of ocular surface inflammatory disease such as e.g. cicatrizing keratoconjunctivitis [57,42]. Steger and ~~coworkers~~co-workers~~et al.~~ [135] described new angiographic parameters that may help evaluate inflammatory activity using IVCM and anterior segment angiography. In cases with active inflammation, the trans-vascular migration of inflammatory cells into the interstitial tissue, known as leukocyte diapedesis, can be observed (Video 2). Using tarsal conjunctival FA and ICGA there was both increased transvascular and even transepithelial leakage of intravenous dyes on FA and ICGA in active atopic keratoconjunctivitis, which correlated closely with the clinical degree of disease activity [135] (Figure 12). This is supported by reports using a rat model, where the activity of allergic conjunctivitis correlated with the degree of Evans blue-albumin complex extravasation from conjunctival vessels [111]. Invasive angiography should, however, be used with caution in non-vision threatening~~,~~ mild inflammatory disease as it has side effects, including allergic reactions ranging from mild to ~~serious such as~~ anaphylaxis.

Clinical grading of conjunctival redness is used for monitoring inflammatory ocular surface disease [90,39]. Biomicroscopic grading of vascular alterations is widely based on the assessment of conjunctival redness but is limited by intra- and inter-observer variability, poor reproducibility and image quality [10,110,142,29].

Frequently used photographic scales for estimating bulbar redness include the McMonnies and Chapman-Davies scale (M-CD scale) [90], the Efron scale [38], and the Validated Bulbar Redness (VBR) grading scale. [123] There are many differences among these scales, including the number of reference images, the range of redness, the linearity of the scores as a measure of redness, and the conjunctival region displayed in the reference images [40,107,121,110,29,122]. To overcome these limitations,

the ocular redness index and CLAHE algorithm (contrast-limited adaptive histogram equalization) have been proposed~~, which are~~ based on automated digital analysis of nasal conjunctival digital slit lamp photographs [5,131]. Both indices are observer-independent but cannot correct for quality and color deficiencies of the conjunctival photographs used. Recent literature has suggested that OCTA maybe useful when assessing ocular surface vasculature when compared with invasive angiograph [6] and slit lamp photography [2]. The quality of OCTA images however may~~can~~ be limited by artefacts [21,6]. Ang and ~~coworkers~~co-workers~~et al~~ observed underestimation of corneal vessel area on~~from~~ ICGA compared with OCTA was likely of minimal clinical significance and may need reconfirming in further studies. It may be due to fundamental differences in image acquisition techniques and discrepancies in image analysis like non-parallel segmentation or projection artefacts that can cause a superficial vessel to appear thicker that it actually is. Furthermore, light scatter from corneal scars can also overestimate areas of vascularisation.[6] Romano and ~~coworkers~~co-workers~~et al.,~~ proposed a pixel densitometry index (PDI) based on early ICG angiographic images to ~~objectively~~ quantify obkectively ocular hyperemia. PDI is calculated from the number of white and black pixels in analyzed angiograms, where vessels with dye are seen as white pixels [115] (Figure 13). Use of FA or ICGA enables the assessment of additional vascular parameters including flow direction and vascular permeability, [104,119] which can be helpful in disease activity and differentiating episcleritis, scleritis and scleral necrosis [50,97,53,144]. ICGA in particular provides anatomical details of the ocular vessels giving the opportunity to highlight even systemic conditions such as generalized essential telangiectasia [146] (Figure 14).

7. Imaging vascular features of specific conditions

7.1 Vascular abnormalities associated with infective conditions

Corneal neovascularization (CoNV) is a common accompaniment of microbial keratitis. This is typically seen in *Herpes simplex* ~~virus~~ keratitis (HSK), *Pseudomonas aeruginosa* and *Staphylococcus aureus* keratitis, and acanthamoeba ~~-~~associated keratitis. Herpetic keratitis has been associated with the most severe CoNV and with more frequent lipid keratopathy while a~~A~~canthamoeba keratitis leads to less severe CoNV~~:~~.[43] h~~H~~owever, a more detailed analysis on the extent of variation of the pattern of development of CoNV between these microbiological causes is unclear. Typically, with recurrent disease as in HSK and *Staphylococcus aureus* further CoNV occurs adjacent to or in a new area of the cornea. The associated exudation and scarring associated with the keratitis and CoNV leads to loss of vision. [75] Identifying and characterizing the neovascular complex enables one to monitor the disease and plan treatment aimed at reducing the exudation and scarring associated with the CoNV. It can be difficult to determine whether the CoNV is helping to negate the infection,

Formatted: Font: Italic

and or is~~are~~ contributing to loss of vision. This is often dependent on the stage of the microbial keratitis.

Corneal angiography in the presence of microbial keratitis, provides information on many aspects of the neovascular complex so that the clinician is able to make a decision on whether and when to treat the CoNV. Time is important as CoNV may be an important part of the host's immune response to helping clear the infection and too soon an intervention may be deleterious. Treatment may comprise medical treatment, for example the response of immature vessels to steroids or antivascular treatment or response of mature vessels to angiographically assisted fine needle diathermy of the feeder vessel. Analysis of the neovascular complex (area, vessel length, tortuosity, leakage times) can be used to monitor the response of the disease to treatment as in the following examples of an HSK, bacterial and acanthamoeba keratitis [134], although potential side effects and time required for repeated corneal angiographies should be kept in mind and careful evaluation of their appropriateness performed [73,54]. (Figure 10).

7.2. Non-infectious~~ve~~ diseases.

FA and ICGA are particularly suited to delineating vessels in congenital lesions of the cornea, assessing corneal grafts or pre-corneal transplantation, or in determining the prognosis of nasal conjunctival disorders [150]. ICGA has also been used to show that the fan-shape vascular plexus of a pterygium forms from a single feeder vessel of the anterior conjunctival circulation [24]. Both ICGA and OCTA have also been utilized to investigate the progress and pattern of vascularization of autografts used for conjunctival reconstruction after pterygium excision [69,82,151].

7.2.5 Limbal stem cell deficiency

Limbal stem cell deficiency (LSCD) is a clinical and or cytological diagnosis where the corneal epithelium is replaced by conjunctival tissue, including conjunctival epithelium and blood vessels. Conversely, chemical burns and radiation damage to the limbus can result in limbal ischemic changes and subsequent LSCD. There are many causes of LSCD including genetic, trauma (chemical burns), inflammatory and iatrogenic causes. The presence of superficial corneal vascularization as well as the loss of limbal vessels is important in the grading and therefore subsequent management of LSCD using limbal stem cell therapies. CoNV in LSCD has been studied using slit lamp biomicroscopy, as well as more recently fluorescein and OCT angiography [100,46,103,68,13]. Without angiography it can be very difficult to detect and quantify the associated vascularization and plan treatment. (Figure 15) Reconstructive surgery in LSCD requires limbal transplants (either whole tissue or cultured cells), and

for these to succeed the vascular supply to the ocular surface is important in bringing blood borne growth factors and cytokines to the transplanted limbal stem cells.

7.2.6 Neoplasms~~tic:~~ (benign and~~,~~ malignant)

Pathological angiogenesis is a known hallmark of tumor growth. High densities of new vessel formation in neoplastic tissues are associated with aggressive invasive growth and metastatic disease [72]. Both vascular architecture and function are impaired in malignant neoplastic disease. Nonhomogeneous Videovessel density, decreased regularity, loss of vessel hierarchy, shunt vessel formation [112], and blind ending capillaries are seen in a variety of malignant tissues [71]. Defective angiogenesis leads to an anomalous vessel wall structure with multi-layered basement membrane, incomplete and loose pericyte coverage leading to chronic transvascular hyperpermeability.

Clinical assessment of ocular surface neoplasia (OSN) includes the identification of risk factors associated with dysplastic or malignant disease, including vascular features such as the presence of hemorrhage, feeder vessels or visible intrinsic tumor vasculature [125,126].

FA, ICGA and OCT angiography have been used to characterize both vascular patterns and functional alterations seen in vascular OSN [127,128,83]. Using ICGA, afferent feeders can clearly be discerned from efferent vessels [23]. Under physiologic circumstances arterioles can be differentiated clinically from venules by thinner vessel diameter and less tortuosity. This, however, is not always possible with ocular surface vessels in OSN. Flow velocity and vessel diameter in efferent venules are increased due to the frequent intralesional formation of shunt vessels, bypassing the capillary system [112]. Thus, flow and pressure differences between arterioles and venules are reduced, leading to morphologically similar appearance of these vessels, as shown by Brunner et al. [23]. They reported that the vessel diameter ratio of afferent to efferent vessels was significantly different between benign and malignant melanocytic OSN and that the angiographic filling time was significantly shorter in benign and non-invasive lesions compared to invasive melanocytic and squamous cell OSN [23]. In a further recent study, the angiographic characteristics of OSN included focal or sea_fan-shaped intra-tumoral and conjunctival feeding vessels on ICGA, and angiography proved useful to monitor vessel regression as a measure of treatment response to subconjunctival and perilesional 5-fluorouracil injection [140]. Additionally, the observation of ICG dye leakage has proved to be useful in the diagnostic evaluation of OSN. While ICG does not usually leak from conjunctival vessels, a recent report describes extensive ICG leakage from intrinsic but not feeding conjunctival tumor vessels or surrounding healthy conjunctival tissues in a case of in situ conjunctival squamous carcinoma [106,105](Figure 16). Likewise, the extravascular leakage of ICG was significantly associated with conjunctival melanoma in a series of 32 cases of melanocytic OSN [15] (Figure 17). The observed increased dye leakage on intravenous

angiography is likely to be caused by trans-vascular hyperpermeability in tumor vessels [96] due to pathological tumor angiogenesis with incomplete or absent pericyte coverage, and abnormal basement membrane structure [89]. OCT angiography has recently been proposed as a non-invasive method for visualizing and quantifying vessel structure and density within, under, and surrounding ocular surface squamous neoplasia [83] and melanocytic lesions of the conjunctiva and iris. [20] Angiographic assessment of OSN thus enables early diagnosis and grading of OSN in vivo by the detecting active intralesional tumor angiogenesis and abnormal transvascular permeability. The most notable vascular features differentiating benign from dysplastic or malignant OSN are summarized in Table 2.

8.0 Conclusion

Over the past several decades, ophthalmology as a whole has witnessed a rapid development in terms of new imaging technologies and novel analysis techniques. Recent advances in artificial intelligence (AI) offers further potential in developing new imaging technologies for the management of ocular surface disease. While predicting the future is difficult~~fraught with risks~~, we expect that new hardware development will allow improved imaging of the structures of interest and their functions (e.g. flow velocity) in real time at much higher resolution with a deeper and wider field of view. A single device may eventually be capable of providing all the diagnostic information needed currently provided by multiple devices and reduce the need for multimodal imaging. We expect that there will be improved image analysis programs that will be able to automatically extract useful clinical information from the large volume of raw data on the device for the clinician. AI will be the key enabler for the invention of new camera devices and novel analysis algorithms. In order, however, to reach~~fulfil~~ the full potential of AI, some key issues have to be addressed ~~sooner rather than later~~, such as availability of data, interpretation, validation, and reliability [95], regulatory approval and ethical considerations, as well as acceptance by patients and clinicians. This should lead to improvements in the management and treatment of conditions associated with abnormal ocular surface vascularization.

Funding: This research did not receive any specific grant from funding agencies in the public, commercial, or not-for-profit sectors.

Methods of Literature Search

Literature search was conducted on PUBMED and Google Scholar for the topic “corneal neovascularization”. The authors analyzed original studies, reviews, and case reports. Keywords used

were: corneal neovascularization/neovascularisation (CoNV), CoNV imaging, CoNV review, CoNV angiography, CoNV fluorescein angiography/FA, CoNV indicianine green angiography/ICGA, CoNV in vivo confocal microscopy/IVCM, CoNV optical coherence tomography, CoNV optical coherence tomography angiography/OCT-A, CoNV photography, CoNV drawing. Animal and human studies were included in this review and adhered to the Helsinki Declaration.

References:

1. Abelson MB, Schaefer K. Conjunctivitis of allergic origin: Immunologic mechanisms and current approaches to therapy. *Surv Ophthalmol*. 1993;38(SUPPL. 2):115-132. doi:10.1016/0039-6257(93)90036-7
2. Aicher NT, Nagahori K, Inoue M, Itoh Y, Hirakata A. Vascular density of anterior segment of eye determined by optical coherence tomography angiography and slit-lamp photography. *Ophthalmic Res*. 2020;63(6). doi:10.1159/000506953
3. Akagi T, Uji A, Huang AS, et al. Conjunctival and Intrascleral Vasculatures Assessed Using Anterior Segment Optical Coherence Tomography Angiography in Normal Eyes. *Am J Ophthalmol*. 2018;196:1-9. doi:10.1016/j.ajo.2018.08.009
4. Albuquerque RJC, Hayashi T, Cho WG, et al. Alternatively spliced vascular endothelial growth factor receptor-2 is an essential endogenous inhibitor of lymphatic vessel growth. *Nat Med*. 2009;15(9):1023-1030. doi:10.1038/nm.2018
5. Amparo F, Wang H, Emami-Naeini P, Karimian P, Dana R. The ocular redness index: A novel automated method for measuring ocular injection. *Investig Ophthalmol Vis Sci*. 2013;54(7):4821-4826. doi:10.1167/iovs.13-12217
6. Ang M, Cai Y, Macphee B, et al. Optical coherence tomography angiography and indocyanine green angiography for corneal vascularisation. *Br J Ophthalmol*. 2016;100(11):1557-1563. doi:10.1136/bjophthalmol-2015-307706
7. Ang M, Sim DA, Keane PA, et al. Optical Coherence Tomography Angiography for Anterior Segment Vasculature Imaging. *Ophthalmology*. 2015;122(9):1740-1747. doi:10.1016/j.ophtha.2015.05.017
8. Anijeet DR, Zheng Y, Tey A, Hodson M, Sueke H, Kaye SB. Imaging and evaluation of corneal vascularization using fluorescein and indocyanine green angiography. *Investig Ophthalmol Vis Sci*. 2012;53(2):650-658. doi:10.1167/iovs.11-8014
9. Bachmann B, Taylor RS, Cursiefen C. Corneal neovascularization as a risk factor for graft failure and rejection after keratoplasty: An evidence-based meta-analysis. *Ophthalmology*. 2010;117(7). doi:10.1016/j.ophtha.2010.01.039
10. Baudouin C, Barton K, Cucherat M, Traverso C. The measurement of bulbar hyperemia: Challenges and pitfalls. *Eur J Ophthalmol*. 2015;25(4):273-279. doi:10.5301/ejo.5000626
11. Benayoun Y, Rosenberg R, Casse G, Dallaudière B, Robert PY. Imagerie et quantification de la néovascularisation cornéenne. *J Fr Ophtalmol*. 2013;36(8):693-703. doi:10.1016/j.jfo.2013.04.006
12. Berkow J, Flower R, Orth D, Kelley J. Fluorescein and Indocyanine Green Angiography: Technique and Interpretation. In: *2nd Ed. Ophthalmology Monograph 5. San Francisco: American Academy of Ophthalmology*. ; 1997.
13. Binotti WW, Nosé RM, Koseoglu ND, Dieckmann GM, Kenyon K, Hamrah P. The utility of anterior segment optical coherence tomography angiography for the assessment of limbal stem cell deficiency. *Ocul Surf*. Published online 2020. doi:10.1016/j.jtos.2020.04.007

14. Bizheva K, Hutchings N, Sorbara L, Moayed AA, Simpson T. In vivo volumetric imaging of the human corneo-scleral limbus with spectral domain OCT. *Biomed Opt Express*. 2011;2(7):1794. doi:10.1364/boe.2.001794
15. Böhringer D, Spierings E, Enczmann J, et al. Matching of the minor histocompatibility antigen HLA-A1/H-Y may improve prognosis in corneal transplantation. *Transplantation*. 2006;82(8):1037-1041. doi:10.1097/01.tp.0000235908.54766.44
16. Bron A, Easty D. Fluorescein angiography of the globe and anterior segment . *Trans Ophthalmol Soc U K*. 1970;90:339-367. Accessed October 6, 2020. https://pubmed.ncbi.nlm.nih.gov/4933929/
17. Bron A, Tripathi R, Tripathi B, Eds. *Wolff's Anatomy of the Eye and Orbit, 8th Ed. London, UK: Chapman and Hall Medical*.; 1997.
18. Bron AJ. A simple scheme for documenting corneal disease. *Br J Ophthalmol*. 1973;57(9):629-634. doi:10.1136/bjo.57.9.629
19. Bron AJ, Easty DL. Fluorescein angiography of the globe and anterior segment. *Trans Ophthalmol Soc U K*. 1970;90:339-367. Accessed September 12, 2020. https://pubmed.ncbi.nlm.nih.gov/4933929/
20. Brouwer NJ, Marinkovic M, Bleeker JC, Luyten GPM, Jager MJ. Anterior Segment OCTA of Melanocytic Lesions of the Conjunctiva and Iris. *Am J Ophthalmol*. 2021;222:137-147. doi:10.1016/j.ajo.2020.09.009
21. Brunner M, Romano V, Steger B, et al. Imaging of corneal neovascularization: Optical coherence tomography angiography and fluorescence angiography. *Investig Ophthalmol Vis Sci*. 2018;59(3):1263-1269. doi:10.1167/iovs.17-22035
22. Brunner M, Romano V, Steger B, et al. Imaging of corneal neovascularization: Optical coherence tomography angiography and fluorescence angiography. *Investig Ophthalmol Vis Sci*. 2018;59(3):1263-1269. doi:10.1167/iovs.17-22035
23. Brunner M, Steger B, Romano V, et al. Identification of Feeder Vessels in Ocular Surface Neoplasia Using Indocyanine Green Angiography: A Preliminary Report. *Curr Eye Res*. 2018;43(2):163-169. doi:10.1080/02713683.2017.1387273
24. Chan CML, Chew PTK, Alsagoff Z, Wong JS, Tan DTH. Vascular patterns in pterygium and conjunctival autografting: A pilot study using indocyanine green anterior segment angiography. *Br J Ophthalmol*. 2001;85(3):350-353. doi:10.1136/bjo.85.3.350
25. Chan G, Balaratnasingam C, Yu PK, et al. Quantitative morphometry of perifoveal capillary networks in the human retina. *Investig Ophthalmol Vis Sci*. 2012;53(9):5502-5514. doi:10.1167/iovs.12-10265
26. Chan SY, Pan CT, Feng Y. Localization of Corneal Neovascularization Using Optical Coherence Tomography Angiography. *Cornea*. 2019;38(7):888-895. doi:10.1097/ICO.0000000000001931
27. Chang JH, Gabison EE, Kato T, Azar DT. Corneal neovascularization. *Curr Opin Ophthalmol*. 2001;12(4):242-249. doi:10.1097/00055735-200108000-00002
28. Chen W, Batawi HIM, Alava JR, et al. Bulbar conjunctival microvascular responses in dry eye. *Ocul Surf*. 2017;15(2):193-201. doi:10.1016/j.jtos.2016.12.002
29. Chong T, Simpson T, Fonn D. The repeatability of discrete and continuous anterior segment grading scales. *Optom Vis Sci*. 2000;77(5):244-251. doi:10.1097/00006324-200005000-00011
30. Conjunctival circulation in relation to circulatory disorders - PubMed. Accessed September 10, 2020. https://pubmed.ncbi.nlm.nih.gov/5233050/
31. Cursiefen C, Cao J, Chen L, et al. Inhibition of hemangiogenesis and lymphangiogenesis after normal-risk corneal transplantation by neutralizing VEGF promotes graft survival. *Investig Ophthalmol Vis Sci*. 2004;45(8):2666-2673. doi:10.1167/iovs.03-1380
32. Cursiefen C, Chen L, Borges LP, et al. VEGF-A stimulates lymphangiogenesis and hemangiogenesis in inflammatory neovascularization via macrophage recruitment. *J Clin Invest*. 2004;113(7):1040-1050. doi:10.1172/JCI20465
33. Dana MR, Schaumberg DA, Kowal VO, et al. Corneal neovascularization after penetrating

keratoplasty. *Cornea*. 1995;14(6):604-609. doi:10.1097/00003226-199511000-00014

34. Deán-Ben XL, Bay E, Razansky D. Functional optoacoustic imaging of moving objects using microsecond-delay acquisition of multispectral three-dimensional tomographic data. *Sci Rep*. 2014;4. doi:10.1038/srep05878
35. Easty DL, Bron AJ. Fluorescein angiography of the anterior segment its value in corneal disease. *Br J Ophthalmol*. 1971;55(10):671-682. doi:10.1136/bjo.55.10.671
36. Ecoiffier T, Yuen D, Chen L. Differential distribution of blood and lymphatic vessels in the murine cornea. *Investig Ophthalmol Vis Sci*. 2010;51(5):2436-2440. doi:10.1167/iovs.09-4505
37. Efron N. Chapter 1 - Anterior eye examination. In: *In: Efron N, Editor. Contact Lens Complications (Third Edition). London: W.B. Saunders*. ; 2012:1-20.
38. Efron N. Grading scales. *Optician*. 2000;219:44-45.
39. Efron N. Grading scales for contact lens complications. In: *Ophthalmic and Physiological Optics*. Vol 18. Ophthalmic Physiol Opt; 1998:182-186. doi:10.1016/S0275-5408(97)00066-5
40. Efron N, Morgan PB, Katsara SS. Validation of grading scales for contact lens complications. *Ophthalmic Physiol Opt*. 2001;21(1):17-29. doi:10.1046/j.1475-1313.2001.00575.x
41. Ehrlich P. Dtsch, Med. Wschr. March 181. *Dtsch, Med Wschr*.
42. Evaluation of conjunctival inflammatory status by confocal scanning laser microscopy and conjunctival brush cytology in patients with atopic keratoconjunctivitis (AKC) - PubMed. Accessed September 10, 2020. https://pubmed.ncbi.nlm.nih.gov/19693288/
43. Faraj LA, Said DG, Al-Aqaba M, Otri AM, Dua HS. Clinical evaluation and characterisation of corneal vascularisation. *Br J Ophthalmol*. 2016;100(3):315-322. doi:10.1136/bjophthalmol-2015-306686
44. Fingler J, Schwartz D, Yang C, Fraser SE. Mobility and transverse flow visualization using phase variance contrast with spectral domain optical coherence tomography. *Opt Express*. 2007;15(20):12636. doi:10.1364/oe.15.012636
45. Fujimoto J, Huang D. Foreword: 25 years of optical coherence tomography. *Investig Ophthalmol Vis Sci*. 2016;57(9):OCTi-OCTii. doi:10.1167/iovs.16-20269
46. Fung SSM, Stewart RMK, Dhallu SK, et al. Anterior Segment Optical Coherence Tomographic Angiography Assessment of Acute Chemical Injury. *Am J Ophthalmol*. 2019;205:165-174. doi:10.1016/j.ajo.2019.04.021
47. Gao SS, Jia Y, Zhang M, et al. Optical coherence tomography angiography. *Investig Ophthalmol Vis Sci*. 2016;57(9):OCT27-OCT36. doi:10.1167/iovs.15-19043
48. Goldberg M, Bron A. Limbal palisades of Vogt . *Trans Am Ophthalmol Soc*. 1982;80:155-171.
49. Graves B. CERTAIN CLINICAL FEATURES OF THE NORMAL LIMBUS. *Br J Ophthalmol*. 1934;18(7):369-387. doi:10.1136/bjo.18.7.369
50. Guex-Crosier Y, Durig J. Anterior segment indocyanine green angiography in anterior scleritis and episcleritis. *Ophthalmology*. 2003;110(9):1756-1763. doi:10.1016/S0161-6420(03)00567-0
51. Guthoff RF, Zhivov A, Stachs O. In vivo confocal microscopy, an inner vision of the cornea - A major review. *Clin Exp Ophthalmol*. 2009;37(1):100-117. doi:10.1111/j.1442-9071.2009.02016.x
52. Harper RN, Moore MA, Marr MC, Watts LE, Hutchins PM. Arteriolar rarefaction in the conjunctiva of human essential hypertensives. *Microvasc Res*. 1978;16(3):369-372. doi:10.1016/0026-2862(78)90070-5
53. Hau SC, Devarajan K, Ang M. Anterior Segment Optical Coherence Tomography Angiography and Optical Coherence Tomography in the Evaluation of Episcleritis and Scleritis. *Ocul Immunol Inflamm*. Published online 2019. doi:10.1080/09273948.2019.1682617
54. Hope-Ross M, Yannuzzi LA, Gragoudas ES, et al. Adverse Reactions due to Indocyanine Green. *Ophthalmology*. 1994;101(3):529-533. doi:10.1016/S0161-6420(94)31303-0
55. Horak F, Berger U, Menapace R, Schuster N. Quantification of conjunctival vascular reaction by digital imaging. *J Allergy Clin Immunol*. 1996;98(3):495-500. doi:10.1016/S0091-

6749(96)70081-7

56. Hu S, Rao B, Maslov K, Wang L V. Label-free photoacoustic ophthalmic angiography. *Opt Lett*. 2010;35(1):1. doi:10.1364/ol.35.000001
57. Hu Y, Matsumoto Y, Adan ES, et al. Corneal In Vivo Confocal Scanning Laser Microscopy in Patients with Atopic Keratoconjunctivitis. *Ophthalmology*. 2008;115(11):2004-2012. doi:10.1016/j.ophtha.2008.05.010
58. Huang D, Swanson EA, Lin CP, et al. Optical coherence tomography. *Science*. 1991;254(5035):1178-1181. Accessed January 17, 2019. http://www.ncbi.nlm.nih.gov/pubmed/1957169
59. Indocyanine green angiography. American Academy of Ophthalmology. *Ophthalmology*. 1998;105(8):1564-1569.
60. Ivanov KP, Kalinina MK, Levkovich YI. Blood flow velocity in capillaries of brain and muscles and its physiological significance. *Microvasc Res*. 1981;22(2):143-155. doi:10.1016/0026-2862(81)90084-4
61. Jalbert I, Stapleton F, Papas E, Sweeney DF, Coroneo M. In vivo confocal microscopy of the human cornea. *Br J Ophthalmol*. 2003;87(2):225-236. doi:10.1136/bjo.87.2.225
62. Jensen VA, Lundbœk K. FLUORESCENSE ANGIOGRAPHY OF THE IRIS IN RECENT AND LONG-TERM DIABETES PRELIMINARY COMMUNICATION. *Acta Ophthalmol*. 1968;46(3):584-585. doi:10.1111/j.1755-3768.1968.tb02854.x
63. Jeon, M. & Kim C. Multimodal photoacoustic tomography. *IEEE Trans Multimed*. 2013;(15):975-982.
64. Jeon M, Kim J, Kim C. Multiplane spectroscopic whole-body photoacoustic imaging of small animals in vivo. *Med Biol Eng Comput*. 2016;54(2-3):283-294. doi:10.1007/s11517-014-1182-6
65. Jeon S, Kim J, Lee D, Baik JW, Kim C. Review on practical photoacoustic microscopy. *Photoacoustics*. 2019;15. doi:10.1016/j.pacs.2019.100141
66. Jeon S, Song HB, Kim J, et al. In Vivo Photoacoustic Imaging of Anterior Ocular Vasculature: A Random Sample Consensus Approach. *Sci Rep*. 2017;7(1). doi:10.1038/s41598-017-04334-z
67. Jia Y, Tan O, Tokayer J, et al. Split-spectrum amplitude-decorrelation angiography with optical coherence tomography. *Opt Express*. 2012;20(4):4710. doi:10.1364/oe.20.004710
68. Käsmann-Kellner B, Latta L, Fries FN, Viestenz A, Seitz B. Diagnostic impact of anterior segment angiography of limbal stem cell insufficiency in PAX6-related aniridia. *Clin Anat*. 2018;31(3):392-397. doi:10.1002/ca.22987
69. Kim YJ, Yoo SH, Chung JK. Reconstruction of the limbal vasculature after limbal-conjunctival autograft transplantation in pterygium surgery: An angiography study. *Investig Ophthalmol Vis Sci*. 2014;55(12):7925-7933. doi:10.1167/iovs.14-15288
70. Kirwan RP, Zheng Y, Tey A, Anijeet D, Sueke H, Kaye SB. Quantifying Changes in Corneal Neovascularization Using Fluorescein and Indocyanine Green Angiography. *Am J Ophthalmol*. 2012;154(5):850-858.e2. doi:10.1016/j.ajo.2012.04.021
71. Konerding MA, Fait E, Gaumann A. 3D microvascular architecture of pre-cancerous lesions and invasive carcinomas of the colon. *Br J Cancer*. 2001;84(10):1354-1362. doi:10.1054/bjoc.2001.1809
72. Kukreja I, Kapoor P, Deshmukh R, Kulkarni V. VEGF and CD 34: A correlation between tumor angiogenesis and microvessel density-an immunohistochemical study. *J Oral Maxillofac Pathol*. 2013;17(3):367-373. doi:10.4103/0973-029X.125200
73. Kwiterovich KA, Maguire MG, Murphy RP, et al. Frequency of Adverse Systemic Reactions after Fluorescein Angiography: Results of a Prospective Study. *Ophthalmology*. 1991;98(7):1139-1142. doi:10.1016/S0161-6420(91)32165-1
74. Lawman S, Dong Y, Williams BM, et al. High resolution corneal and single pulse imaging with line field spectral domain optical coherence tomography. *Opt Express*. 2016;24(11):12395. doi:10.1364/oe.24.012395

75. Lee P, Wang CC, Adamis AP. Ocular neovascularization: An epidemiologic review. *Surv Ophthalmol*. 1998;43(3):245-269. doi:10.1016/S0039-6257(98)00035-6
76. Lee W Di, Devarajan K, Chua J, Schmetterer L, Mehta JS, Ang M. Optical coherence tomography angiography for the anterior segment. *Eye Vis*. 2019;6(1). doi:10.1186/s40662-019-0129-2
77. Li P, An L, Reif R, Shen TT, Johnstone M, Wang RK. In vivo microstructural and microvascular imaging of the human corneo-scleral limbus using optical coherence tomography. *Biomed Opt Express*. 2011;2(11):3109. doi:10.1364/boe.2.003109
78. Ling S, Lin H, Liang L, et al. Development of new lymphatic vessels in alkali-burned corneas. *Acta Ophthalmol*. 2009;87(3):315-322. doi:10.1111/j.1755-3768.2008.01349.x
79. Liu S, Romano V, Steger B, Kaye SB, Hamill KJ, Willoughby CE. Gene-based antiangiogenic applications for corneal neovascularization. *Surv Ophthalmol*. 2018;63(2):193-213. doi:10.1016/j.survophthal.2017.10.006
80. Liu W, Schultz KM, Zhang K, et al. In vivo corneal neovascularization imaging by optical-resolution photoacoustic microscopy. *Photoacoustics*. 2014;2(2):81-86. doi:10.1016/j.pacs.2014.04.003
81. Liu W, Zhang HF. Photoacoustic imaging of the eye: A mini review. *Photoacoustics*. 2016;4(3):112-123. doi:10.1016/j.pacs.2016.05.001
82. Liu YC, Devarajan K, Tan TE, Ang M, Mehta JS. Optical Coherence Tomography Angiography for Evaluation of Reperfusion After Pterygium Surgery. *Am J Ophthalmol*. 2019;207:151-158. doi:10.1016/j.ajo.2019.04.003
83. Liu Z, Karp CL, Galor A, Al Bayyat GJ, Jiang H, Wang J. Role of optical coherence tomography angiography in the characterization of vascular network patterns of ocular surface squamous neoplasia. *Ocul Surf*. 2020;18(4):926-935. doi:10.1016/j.jtos.2020.03.009
84. Liu Z, Wang H, Jiang H, Gameiro GR, Wang J. Quantitative analysis of conjunctival microvasculature imaged using optical coherence tomography angiography. *Eye Vis*. 2019;6(1). doi:10.1186/s40662-019-0130-9
85. Lockard I, Debacker H. Conjunctival circulation in relation to circulatory disorders. *J S C Med Assoc*. 1967;63(6):201-206. Accessed October 6, 2020. https://pubmed.ncbi.nlm.nih.gov/5233050/
86. Mackman G, Polack F, Sidrys L. Fluorescein angiography of soft contact lens induced vascularization in penetrating keratoplasty - PubMed. *Ophthalmic Surg* . 1985;16(3):157-161. Accessed September 12, 2020. https://pubmed.ncbi.nlm.nih.gov/2581204/
87. Maguire MG, Stark WJ, Gottsch JD, et al. Risk factors for corneal graft failure and rejection in the collaborative corneal transplantation studies. Collaborative Corneal Transplantation Studies Research Group. *Ophthalmology*. 1994;101(9):1536-1547. Accessed October 20, 2018. http://www.ncbi.nlm.nih.gov/pubmed/8090456
88. Marvin Minsky, inventorMicroscopy apparatus. US1957 (filed), 1961 (granted).
89. McDonald DM, Choyke PL. Imaging of angiogenesis: From microscope to clinic. *Nat Med*. 2003;9(6):713-725. doi:10.1038/nm0603-713
90. McMonnies CW, Chapman-Davies A. Assessment of conjunctival hyperemia in contact lens wearers. part I. *Optom Vis Sci*. 1987;64(4):246-250. doi:10.1097/00006324-198704000-00003
91. Meyer PAR. Patterns of blood flow in episcleral vessels studied by low-dose fluorescein videoangiography. *Eye*. 1988;2(5):533-546. doi:10.1038/eye.1988.104
92. Meyer PAR, Watson PG. Low dose fluorescein angiography of the conjunctiva and episclera. *Br J Ophthalmol*. 1987;71(1):2-10. doi:10.1136/bjo.71.1.2
93. Mimura T, Amano S, Usui T, Kaji Y, Oshika T, Ishii Y. Expression of vascular endothelial growth factor C and vascular endothelial growth factor receptor 3 in corneal lymphangiogenesis. *Exp Eye Res*. 2001;72(1):71-78. doi:10.1006/exer.2000.0925
94. Mitsui Y, Matsubara M, Kanagawa M. Fluorescence irido-corneal photography. *Br J Ophthalmol*. 1969;53(8):505-512. doi:10.1136/bjo.53.8.505

95. Nagendran M, Chen Y, Lovejoy CA, et al. Artificial intelligence versus clinicians: Systematic review of design, reporting standards, and claims of deep learning studies in medical imaging. *BMJ*. 2020;368. doi:10.1136/bmj.m689
96. Nagy JA, Benjamin L, Zeng H, Dvorak AM, Dvorak HF. Vascular permeability, vascular hyperpermeability and angiogenesis. *Angiogenesis*. 2008;11(2):109-119. doi:10.1007/s10456-008-9099-z
97. Nieuwenhuizen J, Watson PG, Jager MJ, Emmanouilidis-van der Spek K, Keunen JEE. The value of combining anterior segment fluorescein angiography with indocyanine green angiography in scleral inflammation. *Ophthalmology*. 2003;110(8):1653-1666. doi:10.1016/S0161-6420(03)00487-1
98. Nuttall AL. Velocity of red blood cell flow in capillaries of the guinea pig cochlea. *Hear Res*. 1987;27(2):121-128. doi:10.1016/0378-5955(87)90013-X
99. Ocular lymphatics: state-of-the-art review - PubMed. Accessed September 10, 2020. https://pubmed.ncbi.nlm.nih.gov/19725271/
100. Oie Y, Nishida K. Evaluation of corneal neovascularization using optical coherence tomography angiography in patients with limbal stem cell deficiency. *Cornea*. 2017;36:S72-S75. doi:10.1097/ICO.0000000000001382
101. Olver JM, McCartney ACE. Anterior segment vascular casting. *Eye*. 1989;3(3):302-307. doi:10.1038/eye.1989.43
102. Owen CG, Newsom RSB, Rudnicka AR, Barman SA, Woodward EG, Ellis TJ. Diabetes and the Tortuosity of Vessels of the Bulbar Conjunctiva. *Ophthalmology*. 2008;115(6). doi:10.1016/j.ophtha.2008.02.009
103. Palme C, Ahmad S, Romano V, et al. En-face analysis of the human limbal lymphatic vasculature. *Exp Eye Res*. 2020;201:108278. doi:10.1016/j.exer.2020.108278
104. Palme C, Romano V, Brunner M, Vinciguerra R, Kaye SB, Steger B. Functional staging of corneal neovascularization using fluorescein and indocyanine green angiography. *Transl Vis Sci Technol*. 2018;7(5). doi:10.1167/tvst.7.5.15
105. Palme C, Wanner A, Romano V, et al. Indocyanine green angiographic assessment of melanocytic ocular surface neoplastic lesions. *Submitt Cornea Unpubl results*.
106. Palme C, Wanner A, Romano V, Haas G, Kaye S, Steger B. Observation of angiographic dye leakage in ocular surface squamous neoplasia. *Am J Ophthalmol Case Reports*. 2020;20. doi:10.1016/j.ajoc.2020.100912
107. Papas E. Key factors in the subjective and objective assessment of conjunctival erythema . *Invest Ophthalmol Vis Sci*. 2000;41(3):687-691.
108. Peebo BB, Fagerholm P, Lagali N. An in vivo method for visualizing flow dynamics of cells within corneal lymphatics. *Lymphat Res Biol*. 2013;11(2):93-100. doi:10.1089/lrb.2012.0023
109. Perlman HB, Kimura R. Cochlear blood flow in acoustic trauma. *Acta Otolaryngol*. 1962;54(1-6):99-110. doi:10.3109/00016486209126927
110. Peterson RC, Wolffsohn JS. Sensitivity and reliability of objective image analysis compared to subjective grading of bulbar hyperaemia. *Br J Ophthalmol*. 2007;91(11):1464-1466. doi:10.1136/bjo.2006.112680
111. Pharmacologic modulation of vascular permeability in ocular allergy in the rat - PubMed. Accessed September 10, 2020. https://pubmed.ncbi.nlm.nih.gov/2105283/
112. Pries AR, Cornelissen AJM, Sloot AA, et al. Structural adaptation and heterogeneity of normal and tumor microvascular networks. *PLoS Comput Biol*. 2009;5(5). doi:10.1371/journal.pcbi.1000394
113. Rocha De Lossada C, Pagano L, Gadhvi K, et al. Persistent loss of marginal corneal arcades after chemical injury. *Indian J Ophthalmol 2020 Press*.
114. Romano V, Spiteri N, Kaye SB. Angiographic-guided treatment of corneal neovascularization. *JAMA Ophthalmol*. 2015;133(3):e143544. doi:10.1001/jamaophthalmol.2014.3544
115. Romano V, Steger B, Brunner M, et al. Detecting Change in Conjunctival Hyperemia Using a

Pixel Densitometry Index. *Ocul Immunol Inflamm*. 2019;27(2):276-281. doi:10.1080/09273948.2017.1387276

116. Romano V, Steger B, Brunner M, Ahmad S, Willoughby CE, Kaye SB. Method for Angiographically Guided Fine-Needle Diathermy in the Treatment of Corneal Neovascularization. *Cornea*. 2016;35(7):1029-1032. doi:10.1097/ICO.0000000000000865
117. Romano V, Steger B, Kaye SB. Detection and Imaging of Lymphatic and Other Vessels in Corneal Neovascular Complexes. *Cornea*. 2018;37(4):e22-e23. doi:10.1097/ICO.0000000000001516
118. Romano V, Steger B, Kaye SB. Fine-Needle Diathermy Guided by Angiography. *Cornea*. 2015;34(9):e29-e30. doi:10.1097/ICO.0000000000000546
119. Romano V, Steger B, Zheng Y, Ahmad S, Willoughby CE, Kaye SB. Angiographic and in vivo confocal microscopic characterization of human corneal blood and presumed lymphatic neovascularization: A pilot study. *Cornea*. 2015;34(11):1459-1465. doi:10.1097/ICO.0000000000000609
120. Romano V, Steger B, Zheng Y, Ahmad S, Willoughby CE, Kaye SB. Angiographic and in vivo confocal microscopic characterization of human corneal blood and presumed lymphatic neovascularization: A pilot study. *Cornea*. 2015;34(11):1459-1465. doi:10.1097/ICO.0000000000000609
121. Schulze MM, Hutchings N, Simpson TL. Grading bulbar redness using cross-calibrated clinical grading scales. *Investig Ophthalmol Vis Sci*. 2011;52(8):5812-5817. doi:10.1167/iovs.10-7006
122. Schulze MM, Hutchings N, Simpson TL. The use of fractal analysis and photometry to estimate the accuracy of bulbar redness grading scales. *Investig Ophthalmol Vis Sci*. 2008;49(4):1398-1406. doi:10.1167/iovs.07-1306
123. Schulze MM, Jones DA, Simpson TL. The development of validated bulbar redness grading scales. *Optom Vis Sci*. 2007;84(10):976-983. doi:10.1097/OPX.0b013e318157ac9e
124. Shahidi M, Wanek J, Gaynes B, Wu T. Quantitative assessment of conjunctival microvascular circulation of the human eye. *Microvasc Res*. 2010;79(2):109-113. doi:10.1016/j.mvr.2009.12.003
125. Shields CL, Alset AE, Boal NS, et al. Conjunctival Tumors in 5002 Cases. Comparative Analysis of Benign Versus Malignant Counterparts. The 2016 James D. Allen Lecture. *Am J Ophthalmol*. 2017;173:106-133. doi:10.1016/j.ajo.2016.09.034
126. Shields CL, Chien JL, Surakiatchanukul T, Sioufi K, Lally SE, Shields JA. Conjunctival tumors: Review of clinical features, risks, biomarkers, and outcomes - The 2017 J. Donald M. Gass Lecture. *Asia-Pacific J Ophthalmol*. 2017;6(2):109-120. doi:10.22608/APO.201710
127. Shields JA, Kligman BE, Mashayekhi A, Shields CL. Acquired sessile hemangioma of the conjunctiva: A report of 10 cases. *Am J Ophthalmol*. 2011;152(1):55-59.e1. doi:10.1016/j.ajo.2011.01.013
128. Shields JA, Mashayekhi A, Kligman BE, et al. Vascular tumors of the conjunctiva in 140 cases. *Ophthalmology*. 2011;118(9):1747-1753. doi:10.1016/j.ophtha.2011.04.034
129. Shortt AJ, Secker GA, Munro PM, Khaw PT, Tuft SJ, Daniels JT. Characterization of the Limbal Epithelial Stem Cell Niche: Novel Imaging Techniques Permit In Vivo Observation and Targeted Biopsy of Limbal Epithelial Stem Cells. *Stem Cells*. 2007;25(6):1402-1409. doi:10.1634/stemcells.2006-0580
130. Shu X, Wang J, Hu L. A review of functional slit lamp biomicroscopy. *Eye Vis*. 2019;6(1). doi:10.1186/s40662-019-0140-7
131. Sirazitdinova E, Gijs M, Bertens CJF, Berendschot TTJM, Nuijts RMMA, Deserno TM. Validation of computerized quantification of ocular redness. *Transl Vis Sci Technol*. 2019;8(6). doi:10.1167/tvst.8.6.31
132. Spaide RF. Optical coherence tomography angiography signs of vascular abnormalization with antiangiogenic therapy for choroidal neovascularization. *Am J Ophthalmol*. 2015;160(1):6-16. doi:10.1016/j.ajo.2015.04.012

133. Spaide RF, Klancnik JM, Cooney MJ. Retinal vascular layers in macular telangiectasia type 2 imaged by optical coherence tomographic angiography. *JAMA Ophthalmol*. 2015;133(1):66-73. doi:10.1001/jamaophthalmol.2014.3950

134. Spiteri N, Romano V, Zheng Y, et al. Corneal angiography for guiding and evaluating fine-needle diathermy treatment of corneal neovascularization. *Ophthalmology*. 2015;122(6):1079-1084. doi:10.1016/j.ophtha.2015.02.012

135. Steger B, Romano V, Kaye SB. Angiographic Evaluation of Inflammation in Atopic Keratoconjunctivitis. *Ocul Immunol Inflamm*. 2018;26(5):685-688. doi:10.1080/09273948.2016.1247873

136. Steger B, Romano V, Kaye SB. Corneal Indocyanine Green Angiography to Guide Medical and Surgical Management of Corneal Neovascularization. *Cornea*. 2016;35(1):41-45. doi:10.1097/ICO.0000000000000683

137. Stewart R. Conjunctival-corneal melt in association with carotid artery stenosis. *Clin Ophthalmol*. 2008;2(3):649. doi:10.2147/opth.s2430

138. Structural aspects of the permeability of the microvascular endothelium - PubMed. Accessed September 10, 2020. https://pubmed.ncbi.nlm.nih.gov/382743/

139. Sugisaki K, Usui T, Nishiyama N, et al. Photodynamic therapy for corneal neovascularization using polymeric micelles encapsulating dendrimer porphyrins. *Investig Ophthalmol Vis Sci*. 2008;49(3):894-899. doi:10.1167/iovs.07-0389

140. Sun Y, Hua R. Ocular surface squamous neoplasia: Angiographic characteristics and response to subconjunctival/ perilesional 5-fluorouracil injections. *Drug Des Devel Ther*. 2019;13:1323-1334. doi:10.2147/DDDT.S191161

141. Talusan ED, Schwartz B. Fluorescein angiography: Demonstration of Flow Pattern of Anterior Ciliary Arteries. *Arch Ophthalmol*. 1981;99(6):1074-1080. doi:10.1001/archopht.1981.03930011074018

142. Terry R, Wong R, Papas E. Variability of clinical investigators in contact lens research. *Optom Vis Sci 1995;7216*. 1995;72:16.

143. Waring GO, Laibson PR. A Systematic Method of Drawing Corneal Pathologic Conditions. *Arch Ophthalmol*. 1977;95(9):1540-1542. doi:10.1001/archopht.1977.04450090062004

144. Watson PG, Bovey E. Anterior Segment Fluorescein Angiography in the Diagnosis of Scleral Inflammation. *Ophthalmology*. 1985;92(1):1-11. doi:10.1016/S0161-6420(85)34074-5

145. Wuest TR, Carr DJJ. VEGF-A expression by HSV-1-infected cells drives corneal lymphangiogenesis. *J Exp Med*. 2010;207(1):101-115. doi:10.1084/jem.20091385

146. Yadav S, Kaye S, Wilson N. An unusual presentation of generalized essential telangiectasia. *Clin Exp Dermatol*. 2015;40(5):513-515. doi:10.1111/ced.12568

147. Yaylali V, Ohta T, Kaufman SC, Maitchouk DY, Beuerman RW. In vivo confocal imaging of corneal neovascularization. *Cornea*. 1998;17(6):646-653. doi:10.1097/00003226-199811000-00013

148. Yuen D, Wu X, Kwan AC, et al. Live imaging of newly formed lymphatic vessels in the cornea. *Cell Res*. 2011;21(12):1745-1749. doi:10.1038/cr.2011.178

149. Zhang Y, Jeon M, Rich LJ, et al. Non-invasive multimodal functional imaging of the intestine with frozen micellar naphthalocyanines. *Nat Nanotechnol*. 2014;9(8):631-638. doi:10.1038/nnano.2014.130

150. Zhao F, Cai S, Huang Z, Ding P, Du C. Optical Coherence Tomography Angiography in Pinguecula and Pterygium. *Cornea*. 2020;39(1):99-103. doi:10.1097/ICO.0000000000002114

151. Zhao Z, Yue Y, Zhang S, et al. Optical coherence tomography angiography for marginal corneal vascular remodelling after pterygium surgery with limbal-conjunctival autograft. *Eye*. 2020;34(11):2054-2062. doi:10.1038/s41433-020-0773-8

152. Zheng Y, Kaye AE, Boker A, et al. Marginal corneal vascular arcades. *Investig Ophthalmol Vis Sci*. 2013;54(12):7470-7477. doi:10.1167/iovs.13-12614

1063

Table 1. Imaging techniques: application, benefit and limitations

Imaging technique	Benefit	Limitation
Drawing	Easy to perform Easy to document the lesion of interest Highlight features Inexpensive	Lack precision Subjective Time consuming Require annotation software (digital or analogue)
Photography	Easy to perform High magnification Capture colours Inexpensive	Operator dependent Dependent on camera quality Dependent on patient cooperation Reliant on contrast Limited by plane of focus
Angiography	Dynamic examination with high contrast Excellent visualisation of the vascular complex Excellent vessel staging Direction of flow Good reproducibility	Operator dependent Dependent on patient cooperation Time consuming Invasive Side-effects Expensive
In vivo confocal microscopy	Visualisation of the cell morphology Visualisation of the tissue morphology High magnification High resolution	Operator dependent Time consuming Dependent on patient cooperation Small field of view Need to physically contact the cornea Limited reproducibility Expensive
Optical coherence tomography angiography	Non-invasive Easy to perform	Dependent on patient cooperation Depend on intravascular cell movement Unable to show the dynamic patterns of leakage Insensitive to avascular vessels (ghost vessels) Expensive
Photoacoustic imaging	Non-invasive Novel	Need to physically contact the cornea Time consuming Low resolution and scanning depth Expensive

Table 2. ICG angiographic vascular features in ocular surface neoplastic lesions

Feature	Benign	Dysplastic / Malignant
Intrinsic tumor vessels	Rare	Frequent
Intralesional hemorrhage	No	Frequent
Feeder vessels	Rare	Frequent

Afferent-efferent vessel diameter ratio	0.3 - 0.9	0.9 - 1.3
Angiographic perfusion time	2.2 - 4.3 seconds	2.0 – 2.9 seconds
Angiographic malperfusion	No	Frequent
Angiographic time to ICG leakage	210 - ∞ seconds	50 – 160 seconds

Biomicroscopic and ICG angiographic vascular features differentiating benign from dysplastic or malignant ocular surface neoplastic lesions. ICG Indocyanine green [105]

Figure Legend

Figure 1. A. Anterior view of palpebral conjunctival blood supply. LPA – Lateral palpebral artery. LA – Lacrimal artery. LM – Lid margin. PTA – Peripheral tarsal arcade (Not always present inferiorly). MPA – Medial palpebral artery. OA – Ophthalmic artery. PCA – Posterior conjunctival artery. MTA – Marginal tarsal arcade.

B. Lateral view of anterior segment blood supply. OA – Ophthalmic artery. RMS – Rectus muscle supply. LPCA – Long posterior ciliary artery. EAA – Episcleral arterial arcade. IAA – Intraocular arterial arcade. MCA – Marginal corneal arcade. LMA – Limbal arcade. MTA – Marginal tarsal arcade. TP – Tarsal plate. OO – Orbicularis oculi. PTA – Peripheral tarsal arcade. PCA – Posterior conjunctival artery. ACA – Anterior ciliary artery. C. Anterior view of anterior segment blood supply. EAA – Episcleral arterial arcade. ACA – Anterior ciliary arteries

Figure 2. ICGA Details of the normal marginal corneal arcades (A) and early development of corneal neovascularization arising from the marginal corneal arcades (C). A) shows a regular pattern in vessel loop configuration, while in C there is limbal transvascular leakage and increasing loop irregularity. B)* represents an en face optical section collected from a corneal limbal wholemount stained with FITC-phalloidin (green) and anti-CD31 (platelet endothelial cell adhesion molecule-1) antibody (red) to identify blood vessels. This demonstrates the presence of a complex vascular plexus that is intimately associated with the limbal crypts (arrows). CO indicates the peripheral cornea.[129] C) Normal marginal arcades and development of Conv from MCA (white arrows). *Reproduced with permission of *Stem Cells*. Any reuse requires permission from *Stem Cells*

Figure 3. Lymphatic vessels as visualized by reuptake of leaked fluorescein dye on late fluorescein angiography (A). In B lymphatic vessels are seen on a composition of in vivo confocal microscopic images (B). C and D represent 10 min fluorescein and 1 min indocyanine green angiography respectively. E is a digital image obtained by subtracting the two previous images to show the ‘sausage‘ shaped lymphatic vessel (white arrow). [120] Reproduced with permission of *Cornea*. Any reuse requires permission from *Cornea*

Figure 4. Diagram of vasculature and vessel segments. Pixels in white represent segmented vessels and black means background. The red lines represent the centerlines computed from the segmented vessels. Blue squares denote branching points, green triangles the ending points and the yellow

circle an intersection point between two vessel segments. Note: Points on the edge of the images are not considered here. The locations of the centrelines and the landmark points are for demonstration and may not be accurate. (B) angiographic image with branching point in red

Figure 5. Color photograph of lipid kerathopathy (A) – efferent vessel seen (blue arrowhead) but not afferent vessel (red arrowhead). Fluorescein angiography (B) demonstrates transvascular leakage. Afferent vessel (artery - red arrow) and efferent vessel (vein - blue arrow) are highlighted. Indocyanine green angiography (C) demonstrates excellent vessel architecture (afferent vessel – arrow). Color photo of a central corneal scar (D). Indocyanine green angiography highlights corneal neovascularization (E), even when obscured by exudation and corneal scar tissue.

Figure 6. Color photograph of lipid keratopathy (A) with corresponding fluorescein angiography on the right showing transvascular dye leakage (B).

Figure 7. Color photographs, fluorescein angiography (FA) at 5 mins, indocyanine green angiography (ICGA) at 1 and 7 minutes for active, inactive and regressed corneal neovascularization (CoNV). Transvascular leakage is seen on FA and ICGA in active CoNV, while in inactive CoNV there is only leakage on FA, and no leakage on either angiography in regressed CoNV. [104]

Figure 8. Color photograph (A), fluorescein angiography (B) and OCT-angiography (C) for a case of corneal neovascularization. D, E and F show a segmentation analysis with OCT-angiography revealing vessel depth.[21]

Figure 9. Corneal neovascularization before (A and B) and after (C) fine-needle diathermy of the afferent vessels. Early- and late-phase indocyanine green angiography was performed to measure and distinguish the afferent (A) and more numerous efferent (B) vessels.[114] Reproduced with permission of *JAMA Ophthalmol*. Any reuse requires permission from *JAMA Ophthalmol*.

Figure 10. Arterial (A, D), arterial-venous (B, E) and venous phase (C, F). Red arrows represent arteries, while blue arrows represent veins. The pictures A, B and C represent a corneal neovascularization in patient with a herpes simplex keratitis, while pictures D, E and F represent a corneal neovascularization in patient with an Acanthamoeba sp. keratitis.

Figure 11. Fluorescein (left) and indocyanine (right) angiography of a chemical burn injury at different follow ups. Green arrows show vessel leakage while the orange line is delimitating the avascular zone on day 1 (A and B), and only partial consecutive re-perfusion at 3 months (C and D) and 6 years (E and F).[113]

Figure 12. Representative images of angiographic studies in patients and controls. In the active group, transepithelial fluorescein dye leakage and increasing extravascular ICG leakage are seen. In the inactive group, both of these findings are absent. In only one (here presented) control patient, late extravascular leakage of ICG at the lid margin but not from large tarsal conjunctival vessels was observed, corresponding to the presence of associated lid margin inflammation. FA, fluorescein angiography; ICGA, indocyanine green angiography; early images taken 1 min after injection; late image taken 5–10 min after injection.[135] Pending permission of *Ocul Immunol Inflamm*. for image reuse

Figure 13. Conjunctival hyperemia pre (A, C) and post application of topical phenylephrine (B, D) with color photographs and indocyanine green angiography. The graph (E) quantifies the intensity of fluorescent dye present in C (blue line) and D (red line).[115] Pending permission of *Ocul Immunol Inflamm*. for image reuse

Figure 14. Color pictures (A, C, E) and respective ICGA (B, D, F) showing teleangectatic vessels of the conjunctiva and the lid margin.

Figure 15. Subclinical limbus inflammation with absence of clear sign at slit lamp (A) in an atopic keratoconjunctivitis patient with limbus stem cell deficiency and fluorescein angiography (B) showing vessel leakage at the limbus, especially in the superior quadrants.

Figure 16. A. Biomicroscopic color photograph of conjunctival in-situ squamous carcinoma. B Early fluorescein angiography showing diffuse dye leakage within the neoplastic tissue, accentuated in the terminal vascular bulbs on the centripetal border of the lesion. C Early indocyanine green angiography showing diffuse dye leakage within the borders of the lesion, but not in surrounding conjunctival tissue.[106] Pending permission of *Am J Ophthalmol Case Reports* for image reuse

Figure 17. Color photographs and indocyanine green angiography (ICGA) of conjunctival papilloma

(A, B)*, in situ squamous cell carcinoma (C, D), conjunctival naevus (E, F) and conjunctival invasive melanoma (G, H)*. On color photographs, black arrows represent afferent vessels, while blue dots represent efferent vessels. On ICGA the red arrows represent afferent vessels, while blue dots represent efferent vessels.[23] *Reproduced with permission of *Curr Eye Res*. Any reuse requires permission from *Curr Eye Res*.

Supplementary figure. Early phase (1 minute) of ICG angiography of the eyelid that highlight the venous complex (arteries are deep and not visible).

April 25, 2021

Dear Editor,

We appreciate your suggestions to bring the text of our submitted Review paper, entitled "Imaging of vascular abnormalities in ocular surface disease" (SURVOPH-D-21-00026) more in line with Survey style. We accepted the suggested changes and a final clean copy has been submitted.

Yours Sincerely,

Vito Romano

University of Liverpool
Institute of Life Course and Medical Sciences,
Department of Eye and Vision Science,
William Henry Duncan Building,
Liverpool L7 8TX, United Kingdom
e-mail: vito.romano@gmail.com

Figure 1

Click here to access/download;Figure;1.tiff

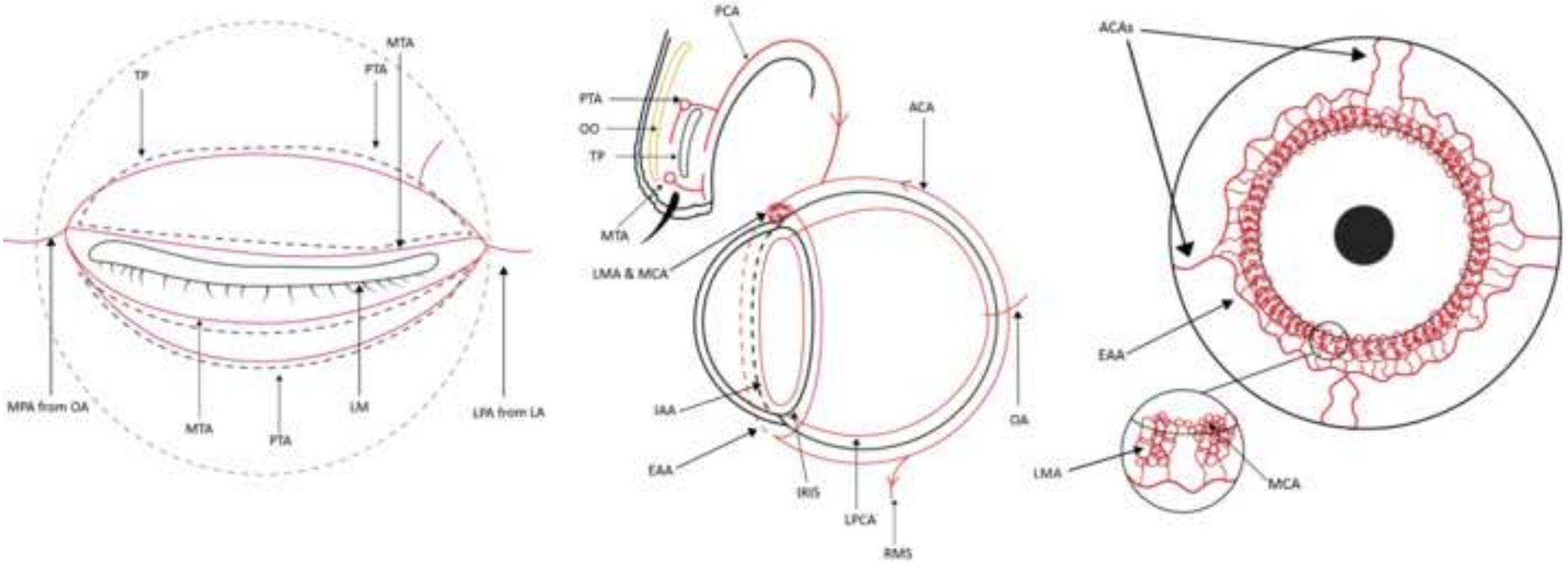

Figure 2

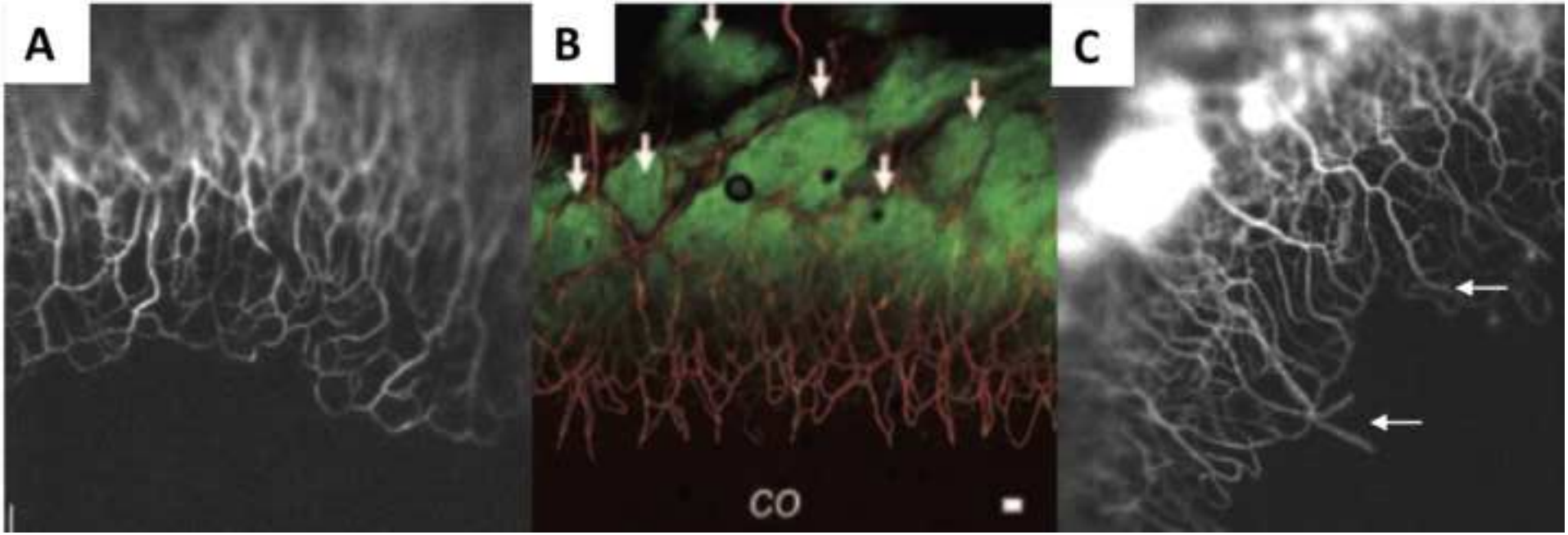

Figure 3

Click here to access/download;Figure;3.tiff

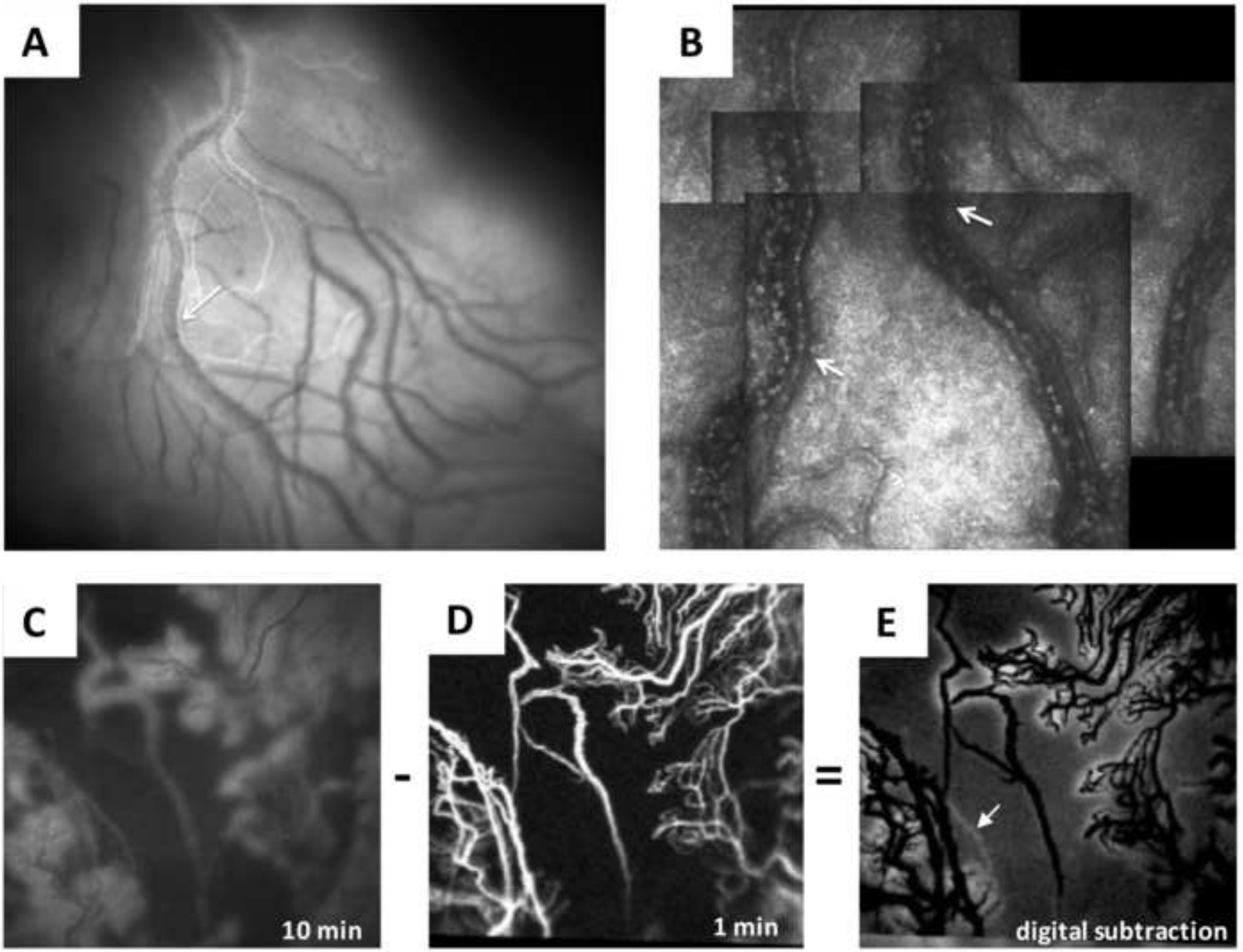

Figure 4

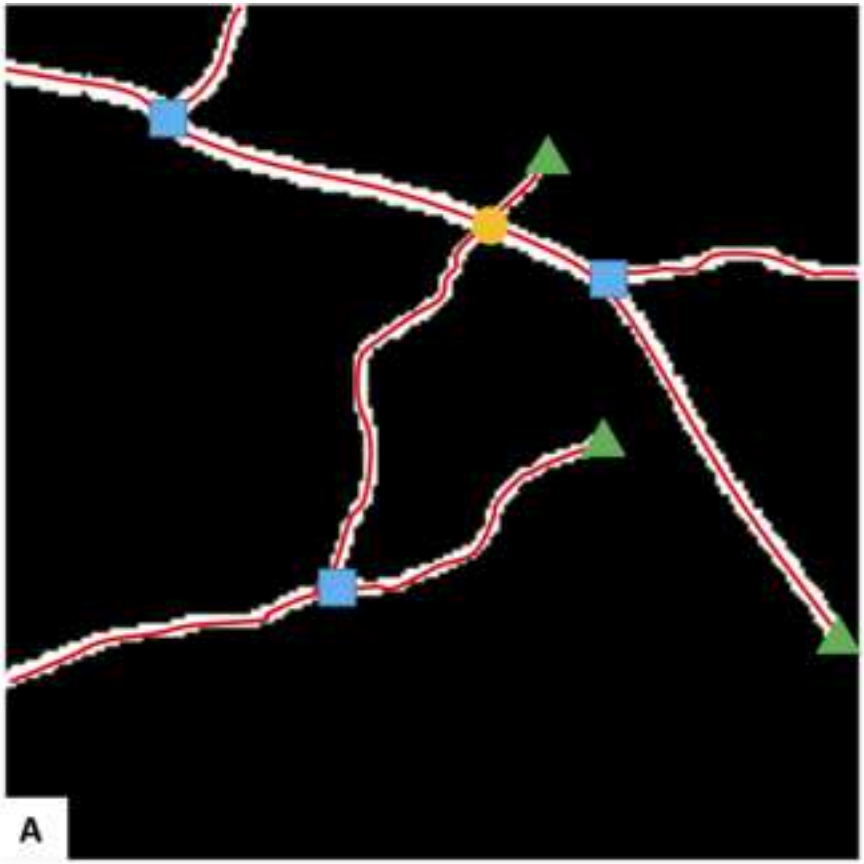

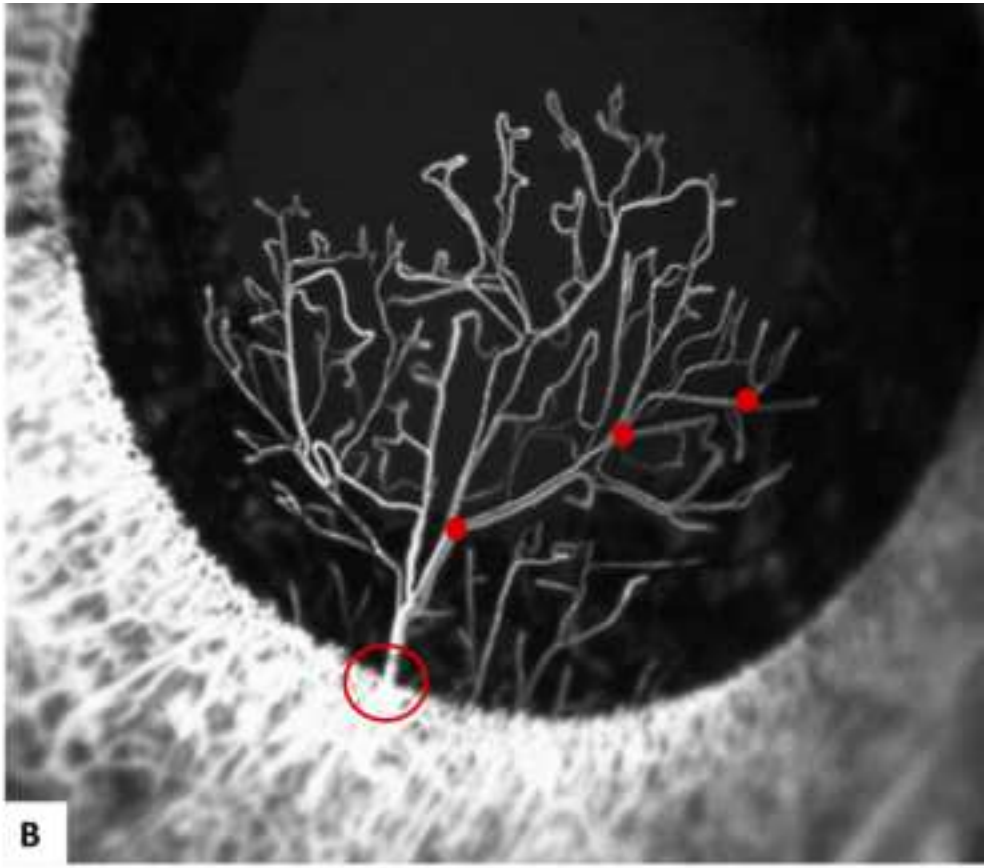

Figure 5

Click here to access/download;Figure;5.tiff

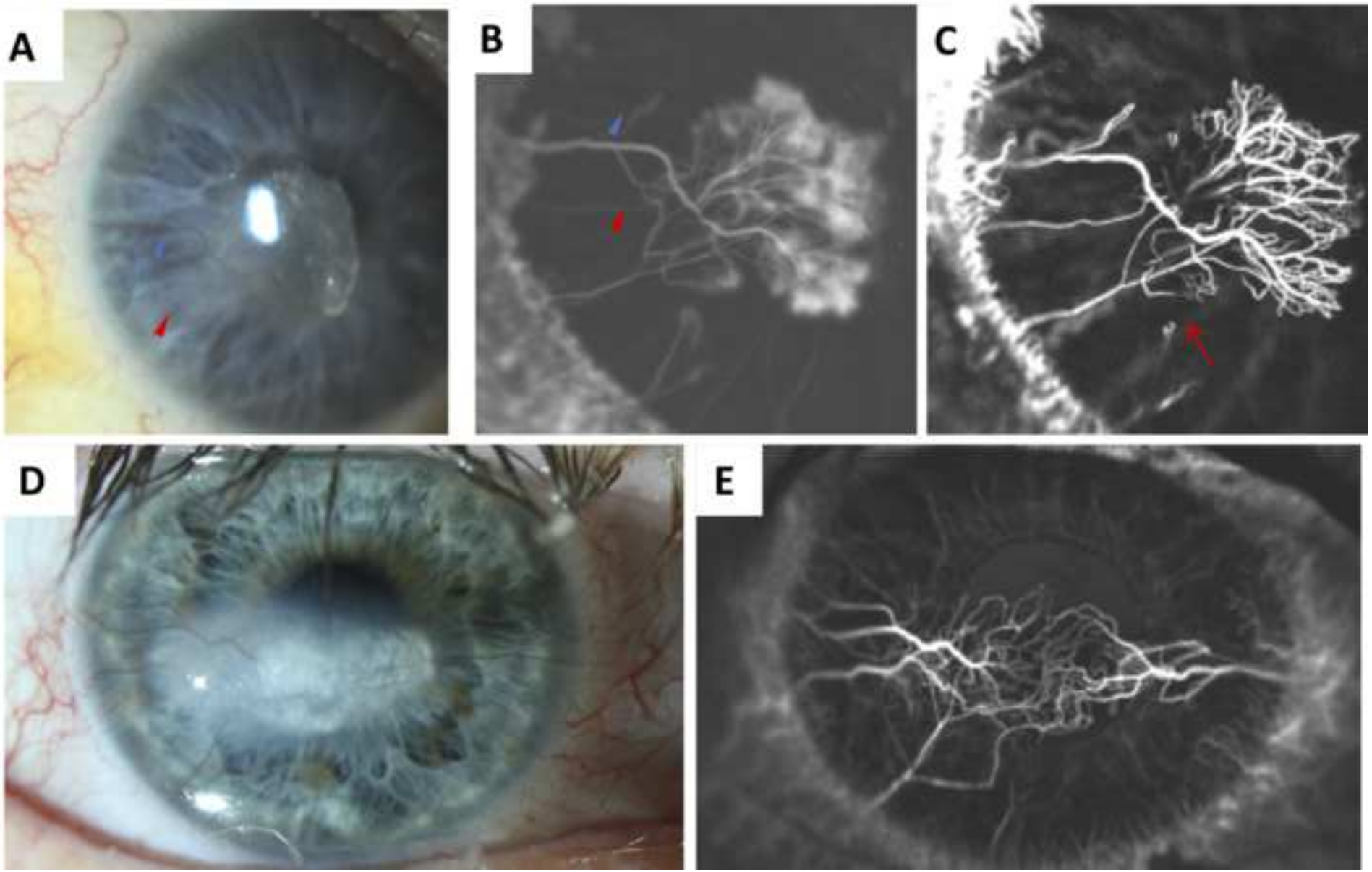

Figure 6

Click here to access/download;Figure;6.tiff

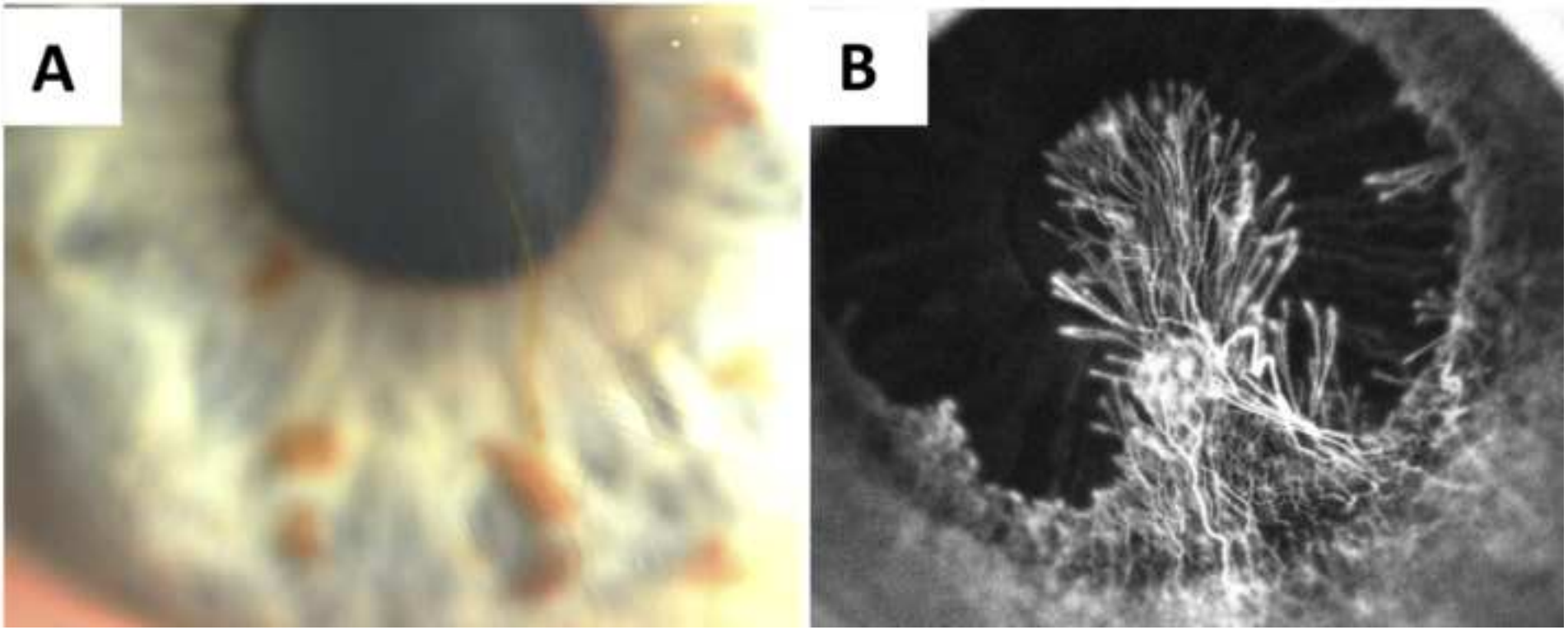

Figure 7

Click here to access/download;Figure;7.tiff

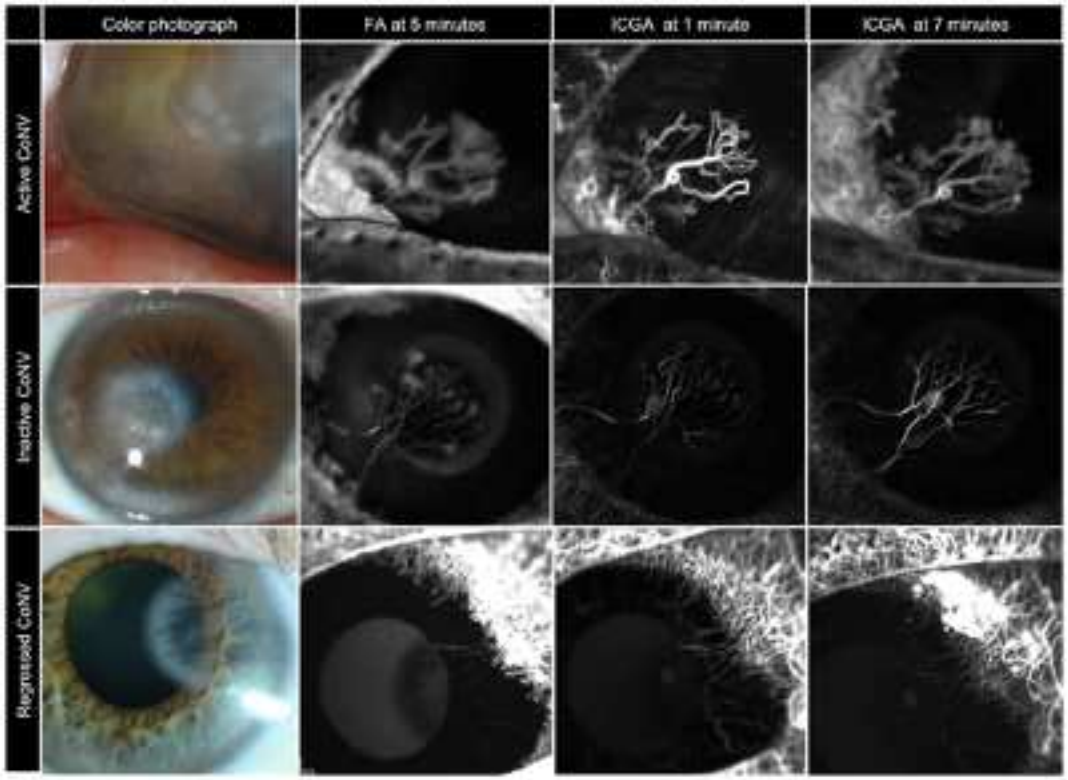

Figure 8

Click here to access/download;Figure;8.tiff

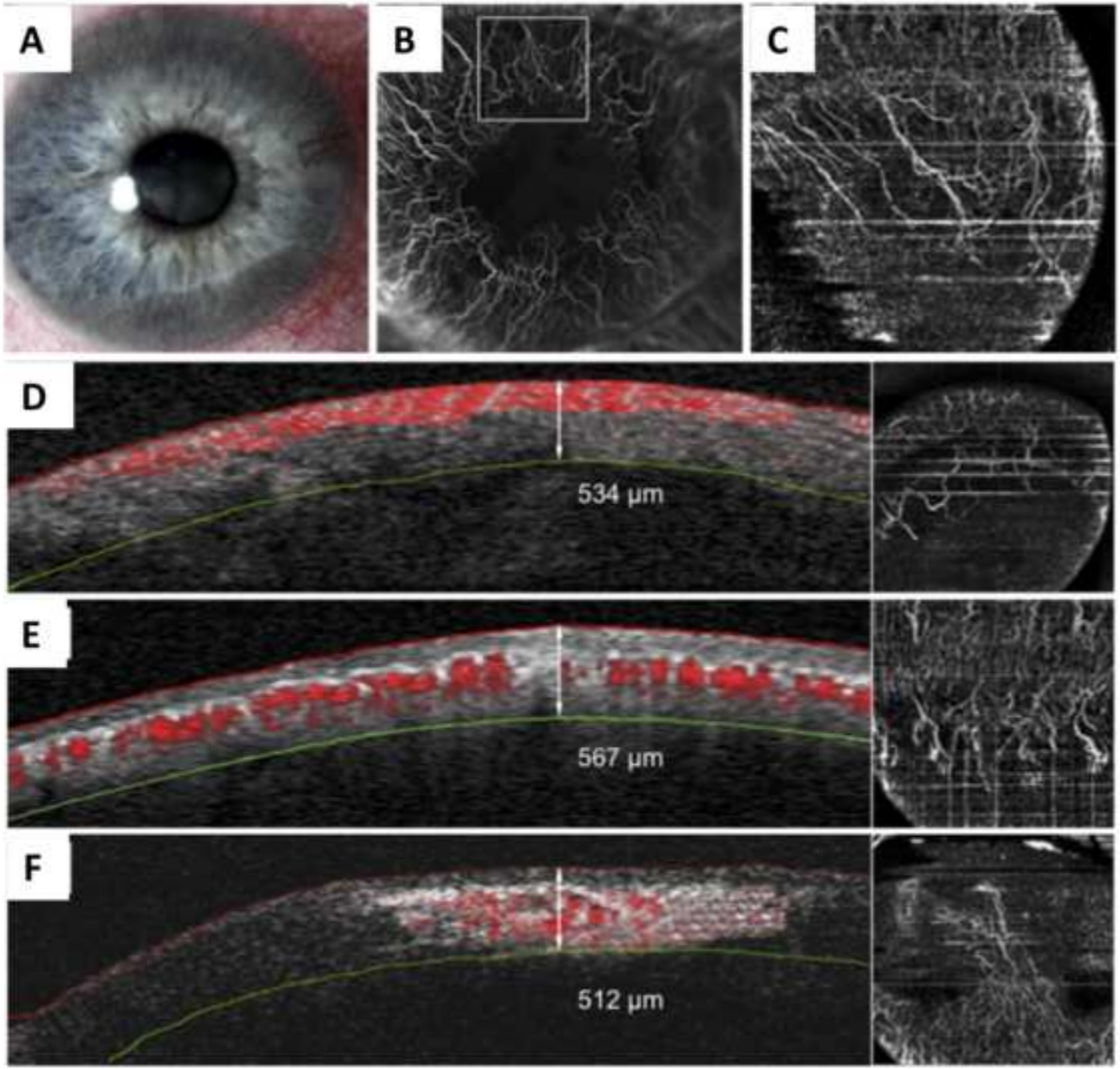

Figure 9

Click here to access/download;Figure;9..tiff

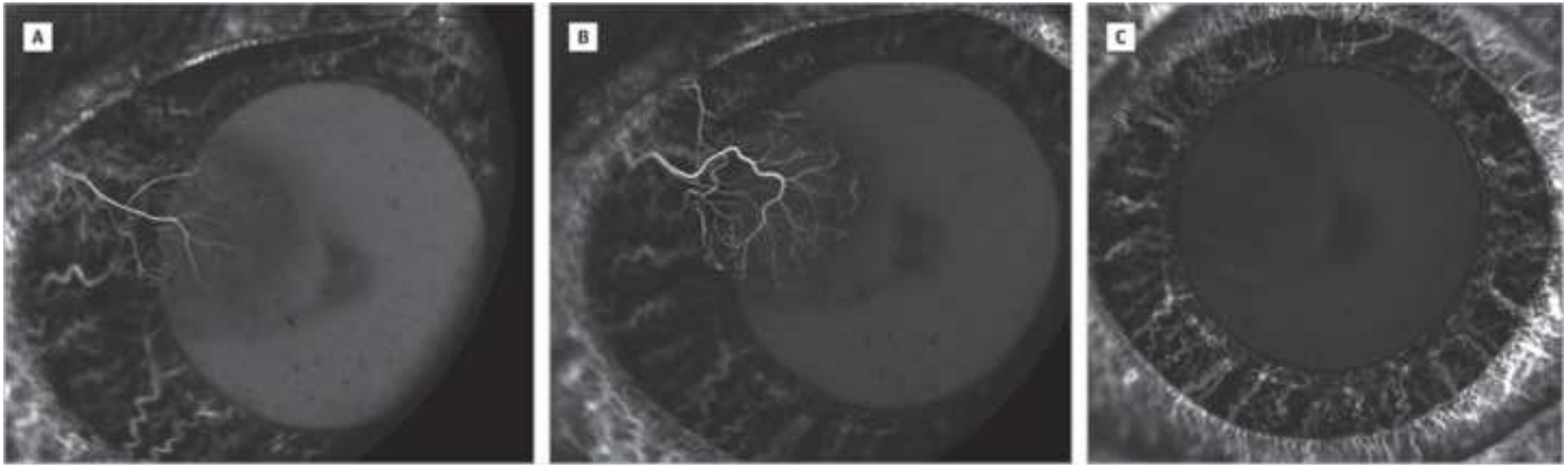

Figure 10

Click here to access/download;Figure;10..tiff

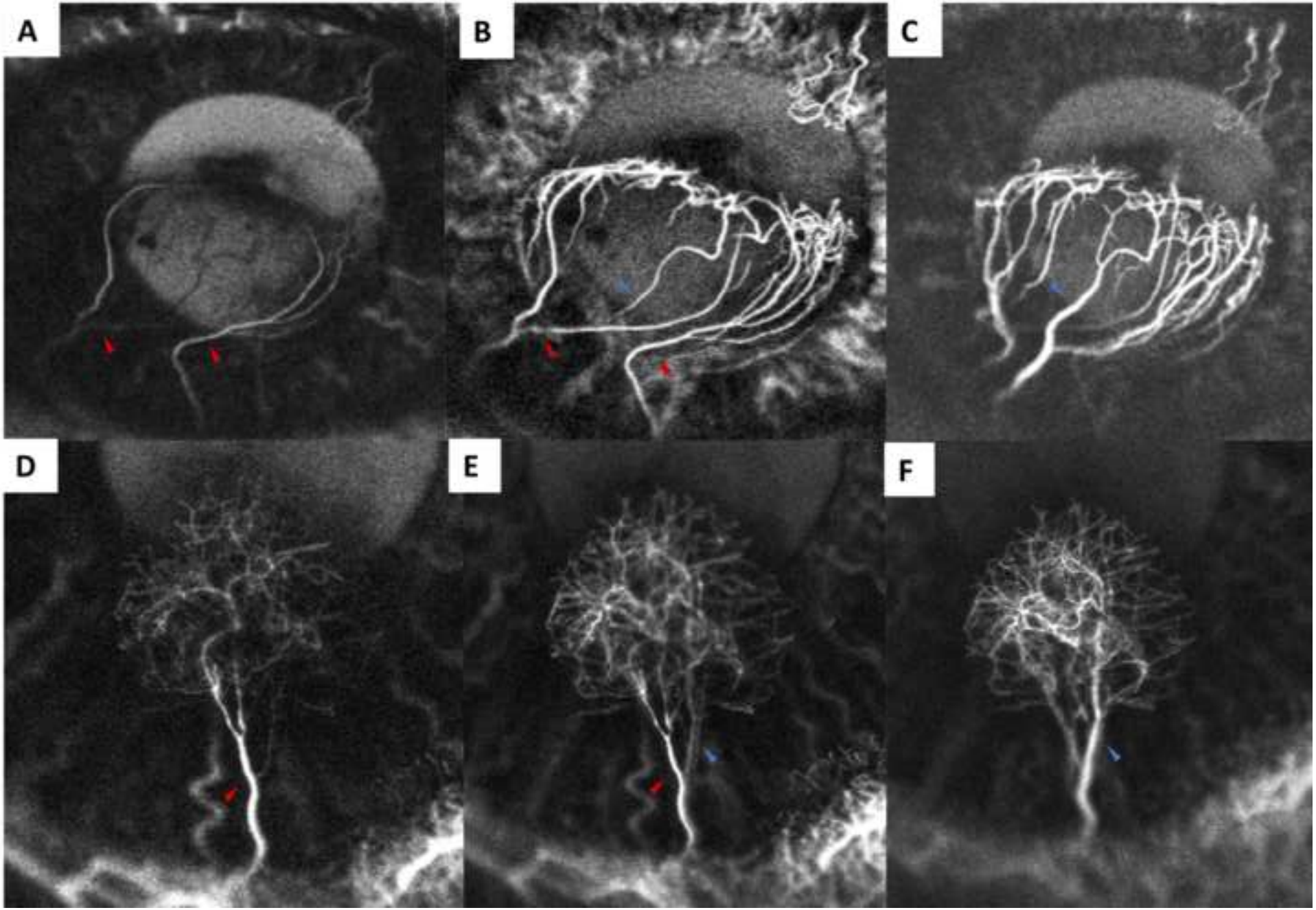

Figure 11

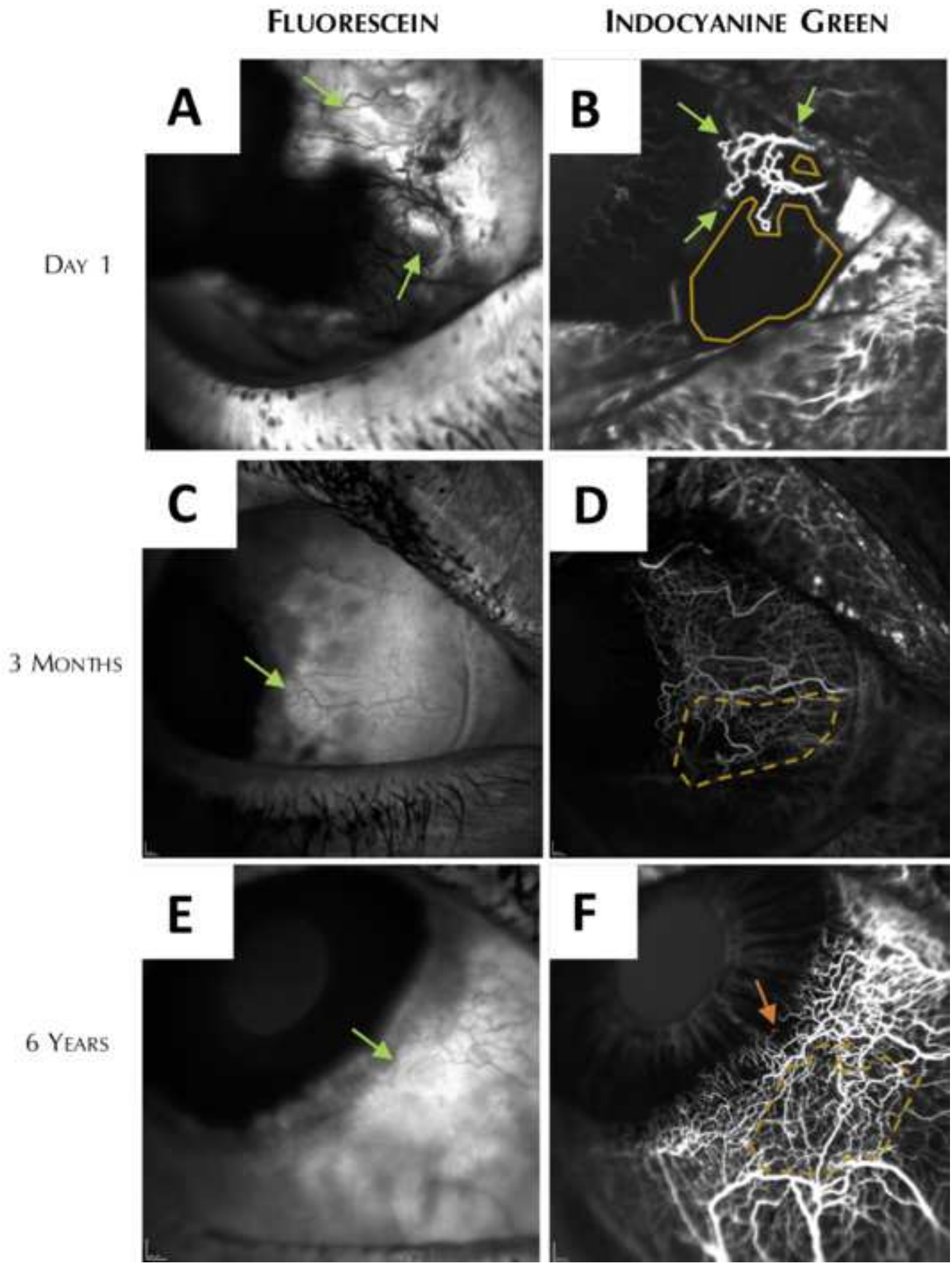

Figure 12

Click here to access/download;Figure;12..tiff

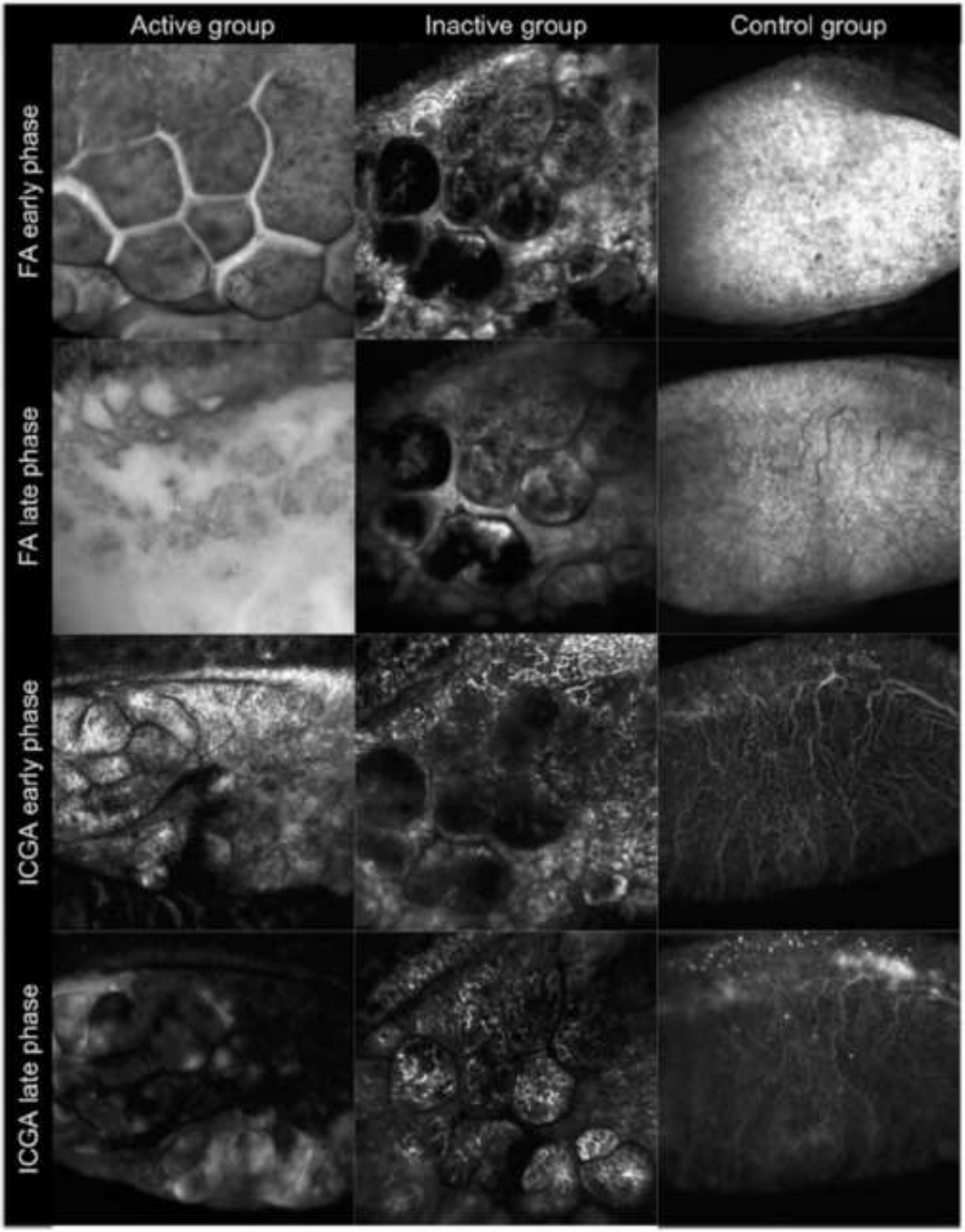

Figure 13

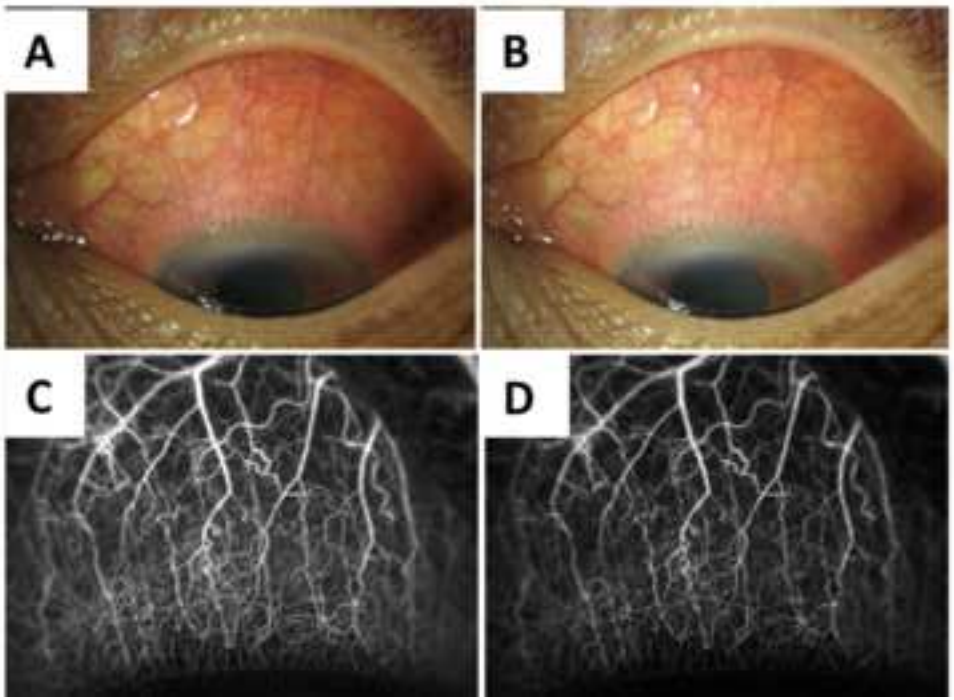

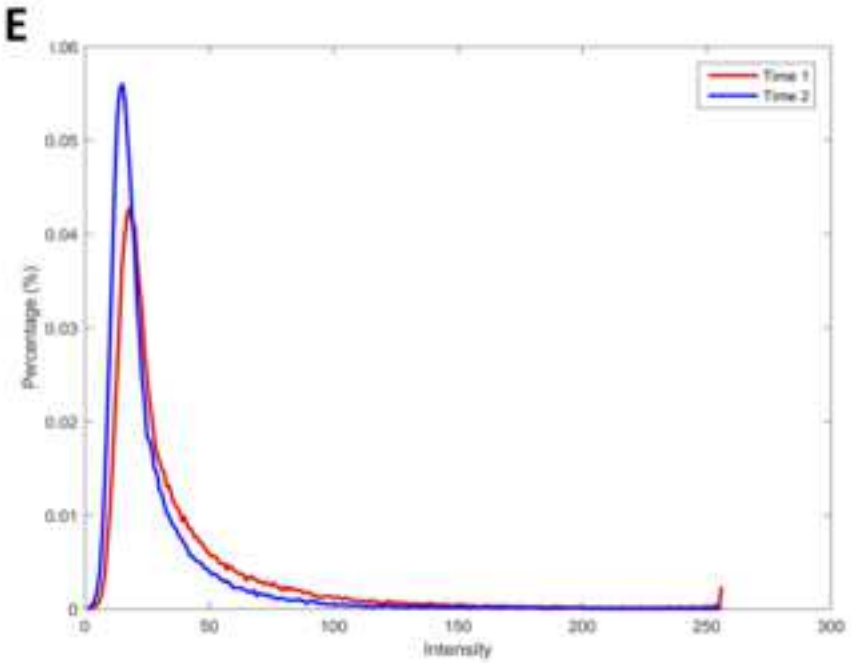

Figure 14

Click here to access/download;Figure;14..tiff

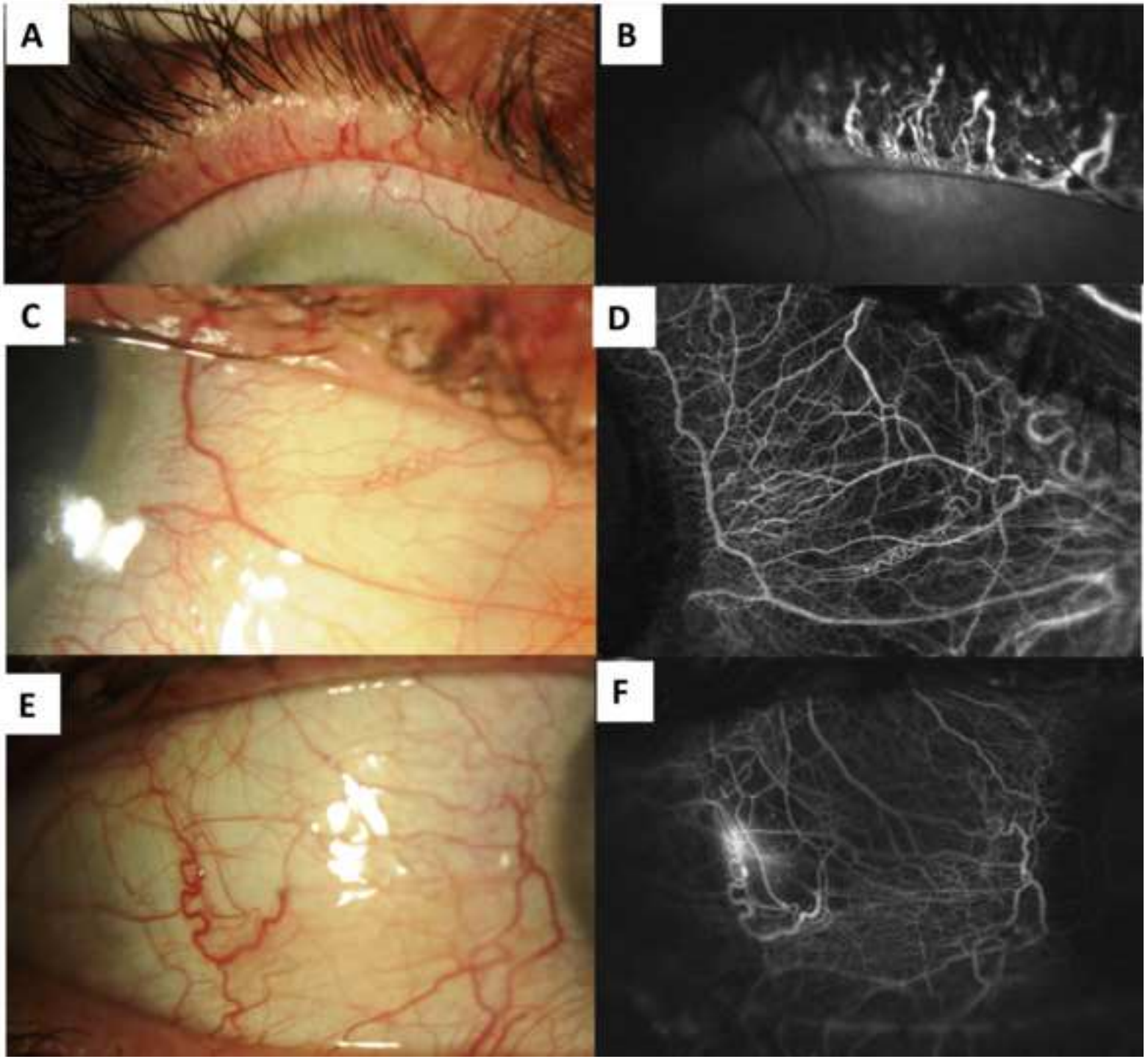

Figure 15

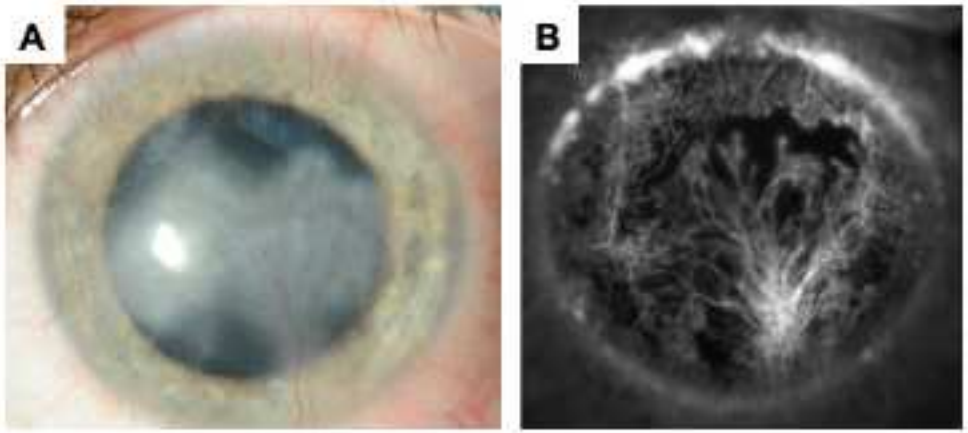

Figure 16

Click here to access/download;Figure;16..tiff

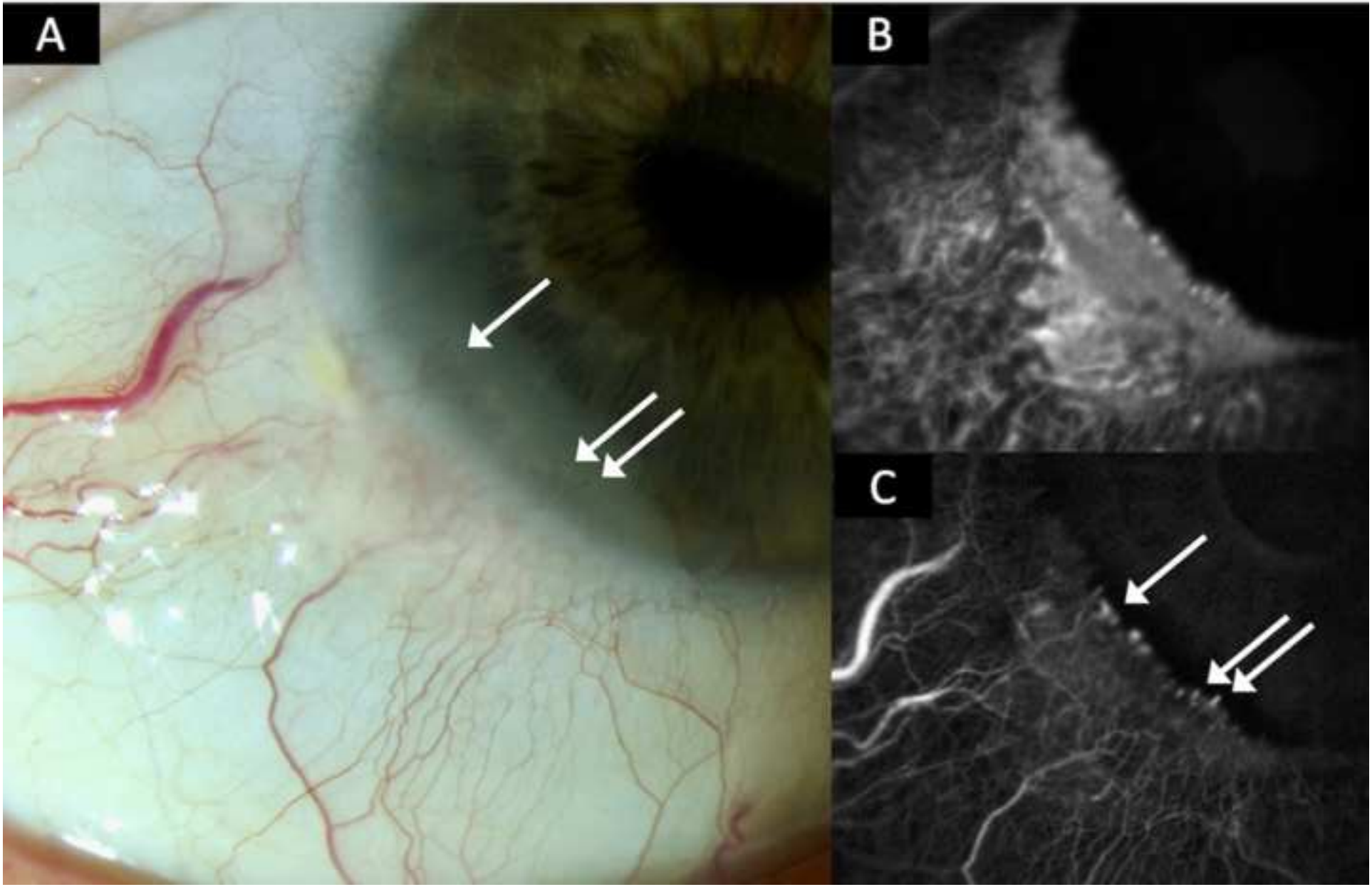

Figure 17

Click here to access/download;Figure;17.tiff

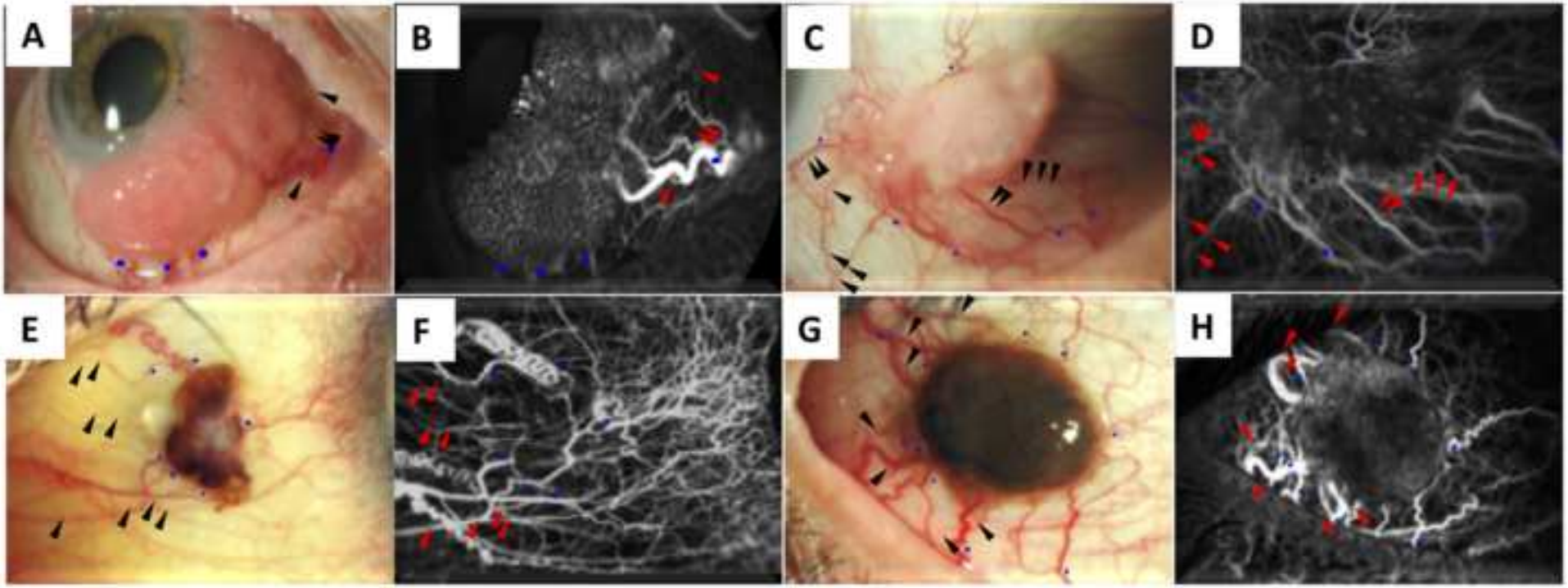

Figure suppl

Click here to access/download;Figure;supplementary Fig.tiff

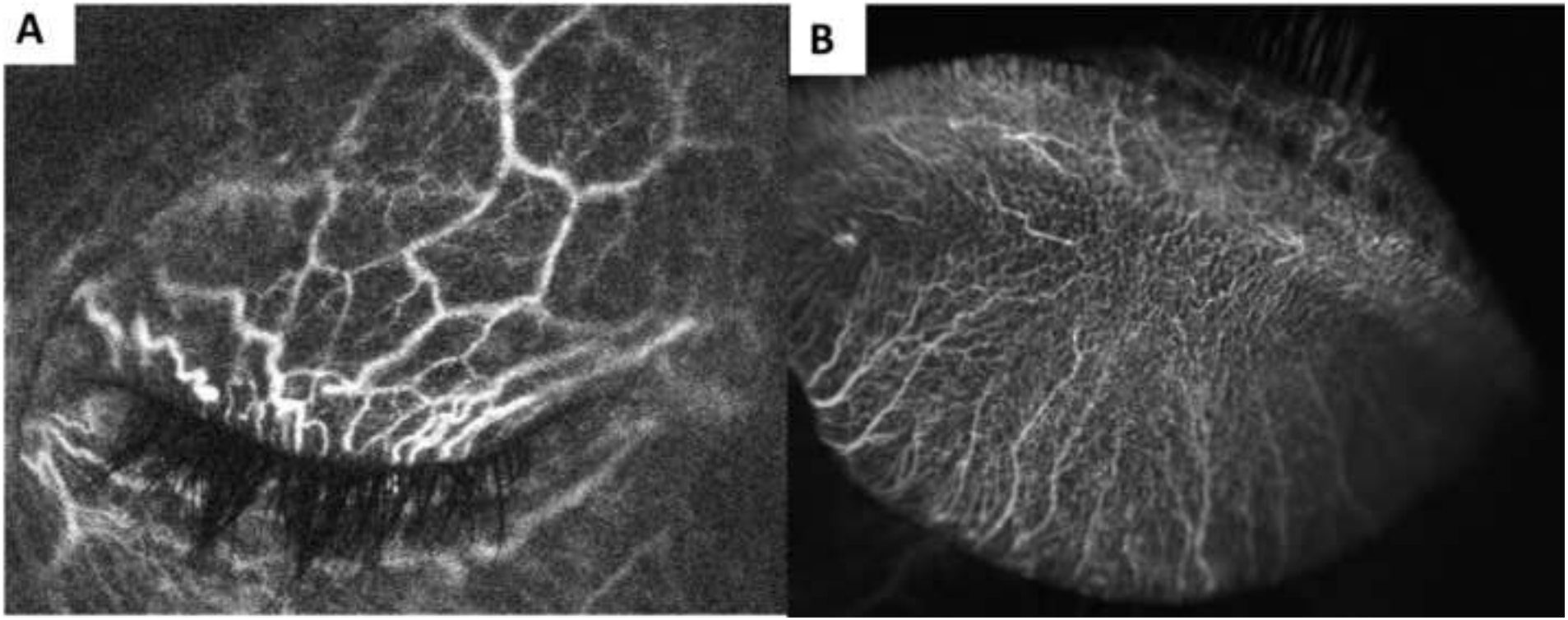

Table 1 . Applications, benefits, and limitations of each of the imaging modalities.

Imaging technique	Benefit	Limitation
Drawing	Easy to perform Easy to document the lesion of interest Highlight features Inexpensive	Lack precision Subjective Time consuming Require annotation software (digital or analogue)
Photography	Easy to perform High magnification Capture colours Inexpensive	Operator dependent Dependent on camera quality Dependent on patient cooperation Reliant on contrast Limited by plane of focus
Angiography	Dynamic examination with high contrast Excellent visualisation of the vascular complex Excellent vessel staging Direction of flow Good reproducibility	Operator dependent Dependent on patient cooperation Time consuming Invasive Side-effects Expensive
In vivo confocal microscopy	Visualisation of the cell morphology Visualisation of the tissue morphology High magnification High resolution	Operator dependent Time consuming Dependent on patient cooperation Small field of view Need to physically contact the cornea Limited reproducibility Expensive
Optical coherence tomography angiography	Non-invasive Easy to perform	Dependent on patient cooperation Depend on intravascular cell movement Unable to show the dynamic patterns of leakage Insensitive to avascular vessels (ghost vessels) Expensive
Photoacoustic imaging	Non-invasive Novel	Need to physically contact the cornea Time consuming Low resolution and scanning depth Expensive

Declaration of interests

☒ The authors declare that they have no known competing financial interests or personal relationships that could have appeared to influence the work reported in this paper.

☐The authors declare the following financial interests/personal relationships which may be considered as potential competing interests:

video 1

Click here to access/download
e-Component
Corneal Angiography 1.mp4

video 2

Click here to access/download

e-Component

Leukocyte rolling adhesion.mp4

Title: Imaging of vascular abnormalities in ocular surface disease

Short title: Ocular surface vascularity

Authors: Vito Romano[1,2*],MD, Bernhard Steger[3*],MD, Mohammad Ahmad[1], FRCOphth, Giulia Coco[1,4],MD, Luca Pagano[1,5], MD, Sajjad Ahmad[6],PhD, Yitian Zhao[2,7], PhD, Yalin Zheng[2], PhD, Stephen B Kaye[1,2] MD

*Vito Romano and Bernhard Steger contributed equally.

Affiliations:

[1] The Royal Liverpool University Hospital, Liverpool, UK

[2] Department of Eye and Vision Science, Institute of Life Course and Medical Sciences, University of Liverpool, Liverpool, UK

[3] Department of Ophthalmology, Medical University of Innsbruck, Innsbruck, Austria

[4] Department of Clinical Science and Translational Medicine, University of Rome Tor Vergata, Rome, Italy

[5] Humanitas Clinical and Research, via Manzoni 56, 20089 Rozzano (Mi) - Italy

[6] UCL Institute of Ophthalmology, London, UK

[7] Cixi Institute of Biomedical Engineering, Ningbo Institute of Materials Technology and Engineering, Chinese Academy of Sciences, Ningbo, 315300, China

Correspondence:

Vito Romano, MD

Corneal and External Eye Disease Service,

Royal Liverpool University Hospital,

Liverpool, United Kingdom L7 8XP

Email: Vito.Romano@liverpool.ac.uk

Tel: 0151 706 3997

Abbreviations: CoNV: Corneal neovascularization; FA: Fluorescein angiography; ICGA: Indocianin green angiography, ICG: Indicianin green; IVCM: *In vivo* confocal microscopy; OCT: Optical coherence tomography; OCT-A: Optical coherence tomography angiography; HSV: Herpes simplex virus; MCA: Marginal corneal arcades; LCA: Lymphatic corneal arcade ; FSLB: Functional slit lamp biomicroscocpy ; PAM: Photoacoustic microscopy; ROI: Region of interest ; DSA: Digital subtraction analysis ; VBR: Validated Bulbar Redness ; PDI: Pixel densitometry index ; HSK: Herpes simplex keratitis; LSCD: Limbal stem cell deficiency; OSN: Ocular surface neoplasia; AI: Artificial intelligence

Abstract

The vascular system of the ocular surface plays a central role in infectious, autoimmune, inflammatory, traumatic and neoplastic diseases. The development, application, and monitoring of treatments for vascular abnormalities depends on the *in vivo* analysis of the ocular surface vasculature. Until recently, ocular surface vascular imaging was confined to biomicroscopic and color photographic assessment, both limited by poor reproducibility and the inability to image lymphatic vasculature *in vivo*. The evolvement and clinical implementation of innovative imaging modalities including confocal microscopy, intravenous, and optical coherence tomography--based angiography now allows standardized quantitative and functional vascular assessment with potential applicability to automated analysis algorithms and diagnostics.

Keywords: Ocular surface; vascularization; corneal neovascularization; OCT-A; angiography; fine needle

Disclosure

None of the authors have any potential conflict of interest

1. Introduction

The vascular system of the ocular surface is essential for the homeostasis of the cornea and conjunctiva. It delivers nutrients and removes catabolites and aids the defense responses of the ocular surface to infectious, inflammatory, traumatic, and neoplastic disease. The vasculature normally covers the entire ocular surface except for the cornea, although it does extend into the corneal periphery. Pathologic vessel formation such as corneal neovascularization (CoNV) and abnormal neoplastic vessel formation or peri-limbal vessel loss [27,134] following chemical or radiation injury, represent significant causes of visual loss [9]. Although the global impact is not known, the incidence rate of CoNV has been estimated to be 1.4 million per year in the United States [33]. The development, application, and monitoring of treatments for vascular abnormalities depend on the *in vivo* analysis of the ocular surface vasculature. We provide a picture of current methods for imaging and quantifying vascular abnormalities in ocular surface diseases and their clinical applications and highlight future perspectives.

2. History of imaging of vascular abnormalities of the ocular surface

Documentation of vascular conditions of the ocular surface has been underpinned by accurate drawing and image annotation. Advances in ocular surface imaging follows the improvements in photography, such as lighting systems and magnification. Use of fluorescein in ophthalmology dates back to 1881 when Ehrlich observed that the dye appeared in the anterior chamber following injection into the blood stream [41]. Jensen and Lundbaek in 1968 described the use of fluorescein angiography (FA) for studying iris vascularization [62]. In 1969, Mitsui an co-workers used FA to study CoNV, highlighting the vascular patterns associated with trachoma and herpes simplex virus (HSV) [94]. In 1971, Bron and Easty, in a large study of 250 patients, concluded that 'fluorangiography', was the only investigation able to identify CoNV, which would otherwise be difficult to visualize with photography or slit lamp biomicroscopy. They also noted the ability of FA to identify vascular leakage and its limitation in visualizing vessels underneath corneal scars [86]. In the 1980's, Goldberg and Bron [48], Meyer and Watson, [92] and others [94,141,19,35] were able to describe in detail the features of the limbal palisades using FA. Image analysis programs and the dependency on analogue systems, limited the analysis that could be undertaken. Following improvements in digital imaging systems, corneal and anterior segment angiography gained new interest in the second decade of the 21st century, with the quality of image analysis software enabling more reliable and reproducible methods for quantifying CoNV [70,8,139]. Further steps in the imaging of the ocular surface vasculature came with developments of *in vivo* confocal microscopy (IVCM). In 1998, Yaylali and co-workers first described CoNV using IVCM, [147] followed In 2009 by Guthoff and co-workers who were able to obtain

depth selective high-resolution *in vivo* optical images [51]. More recently developments in optical coherence tomography angiography (OCT-A) have allowed visualization of blood flow in vessels via motion contrast imaging of blood cell movement across sequential B-scans [133,7,21].

3. Anatomy of the ocular surface vasculature

The blood supply to the anterior segment of the eye is derived from both an extraocular and an intraocular circulation [91]. The medial and lateral long posterior ciliary arteries that run within the globe arise from the ophthalmic artery and travel forward to supply the iris, ciliary body, and anterior part of the choroid. The external route consists of anterior ciliary arteries thatare continuations of the muscular arteries from the ophthalmic artery. The anterior ciliary arteries run forward along the tendons and divide within the episcleral tissue to form an anterior episcleral arterial arcade that supplies the anterior conjunctival and episcleral capillary bed. The anterior ciliary arteries give rise to the episcleral branches, which in turn give rise to the recurrent conjunctival arteries, the palisadal vessels and the marginal arcades (terminal capillary loops) of the cornea that are the most centrally located vessels [48,92] (Figure 1).

The superior and inferior medial palpebral arteries (from the ophthalmic artery) anastomose with the corresponding superior and inferior lateral palpebral arteries (from the lacrimal artery) to form the marginal and peripheral tarsal arcades in the upper and lower lid. These supply the palpebral conjunctiva and the fornixes. The ascending branches from the peripheral tarsal arcade pass around the fornixes as the posterior conjunctival arteries. These vessels anastomose with conjunctival arteries from the anterior ciliary arteries and supply the bulbar conjunctiva. The conjunctival veins largely accompany the corresponding arteries. The episcleral venous plexus also receives blood from the anterior uveal circulation as well as aqueous from the Schlemm canal. The venous blood then primarily drains into the superior ophthalmic vein, which empties into the cavernous sinus [17]. There is, however, significant anatomical variation among individuals [124].

3.1 Limbal vascular complex and the marginal corneal arcades (MCA)

The limbal vasculature helps to maintain the homeostasis of the limbal palisade stem cell niche. Biomicroscopy and anatomical methods such as vascular casting have informed much of our understanding of this vasculature [101,49]. In the 1980's, Goldberg and Bron used FA to demonstrate that the vessels of the palisades are derived from the anterior ciliary arteries, [48] and Meyer and Watson showed that the limbal arcades are supplied by anterior branches from the episcleral circle [92]. Peng Li and co-workers, using optical microangiography, suggested that a fraction of the

conjunctival plexus become terminal vessels which reach the palisades of Vogt to supply the peripheral corneal arcades [77]. They also noted recurrent vessels in the conjunctival plexus, which run posteriorly to supply the perilimbal area [77]. The vessels within the peripheral cornea (0.2 to 0.3mm) are the marginal corneal arcades [129] (MCA, Figure 1 and 2). Until recently, little was known about the MCA, particularly in the living human eye, because of limitations in image acquisition and analysis systems [16,35]. The introduction of indocyanine green angiography (ICGA) with increased magnification, computerized digital angiography, and image analysis systems [8] has greatly improved our understanding of the corneal marginal arcades *in vivo*. The MCA are a network of vessels rather than a vascular tree, consisting of vascular loops with between 3 and 4 branches, approximated by an elliptical shape with the major axis twice as long as the minor axis (Figure 2). There is, however, considerable variation in loop size and branching both within and between subjects and quadrants. The internal row of loops appears to have a slightly larger diameter than the average of the external 4-5 rows. It is possible that the larger diameter, together with an increased path length, leads to a reduced velocity of blood flow, allowing for better oxygen exchange. In fact, the total capillary loop area of the marginal capillaries varies between 10.44 $x10^{-3}mm^2$ and 11.87 $x10^{-3}mm^2$ (For comparison, the capillary loop area in the perifovea varies between 3.95$x10^{-3}mm^2$ and 6.87x10-$^{3}mm^2$ [25]).

While MCA are clinically visible and well described, lymphatic vessels are biomicroscopically invisible and therefore elude clinical observation [4]. The presence of limbal lymphatic vasculature has been visualized immunohistochemistry using LYVE-1 antibodies to selectively stain the lymphovascular endothelium in murine and human tissues [99,103]. High resolution, cross-sectional and volumetric images of the human corneoscleral limbus using spectral domain OCT has allowed the visualization, but not the differentiation, of limbal and scleral blood and lymph vasculature [14]. The lymphatic corneal arcade (LCA) is more pronounced in the nasal compared to the temporal limbal region [36]. *In vivo* confocal microscopy has been used to image corneal blood and lymphatic vasculature in human beings [119] (Figure 3). This technique was also applied to describe the LCA in human corneoscleral tissue [103]. Palme and coworker showed that the LCA overlaps with the MCA, but terminates slightly more peripherally, and is located at a mean depth of 43 ± 12 µm.This is deeper than the hematic arcade that has a mean depth of 24 ± 9 µm [103]. Morphometric characteristics as observed on *in vivo* confocal microscopy are useful to differentiate blood and lymphatic limbo corneal vasculature, with LCA showing shorter and larger vessel segments (Figure 3).

3.2 Conjunctival vascular complex [27,134]

The conjunctival vascular network is sensitive to local irritants including contact lenses, immune and allergic reactions, infections and systemic disease such as diabetes and hypertension [102,52,1,28]. Different methods, including digital imaging [55] and angiography, [144] have been used to try and image the conjunctival vascular network, such as digital imaging using serial displacement of red blood cells, etc.

Recently, OCT-A has been employed in imaging the anterior segment and for aiding the diagnosis of vascular lesions of the cornea and conjunctiva [7]. Akagi and co-workers investigated conjunctival and intrascleral vasculature using OCT-A and suggested comparable results with FA and ICGA [3]. Liu and co-workers carried out quantitative analysis of bulbar conjunctival microvascular density acquired using OCT-A and compared with vessel density using functional slit lamp biomicroscopy (FSLB). Vessel density measured by fractal analysis (box counting) as well as by pixel counting (per centage) was found to be significantly lower when using OCT-A compared with FSLB [84]. Although OCT-A is considered a promising tool for evaluating conjunctival and intrascleral vasculature, further developments are required to improve axial and lateral resolution.

4. Modalities of reporting vascular abnormalities

4.1. Drawing and annotating

Hand drawing or digital image annotation can be used to record vascular pathology, and with the advent and popularity of electronic patient records it is important to have a standard method to annotate images and notes. The observer can draw or annotate any ocular surface vascular abnormality visible on the slit lamp. A generally accepted convention for documentation of corneal conditions was standardized in 1973, with frontal and slit sketches of the cornea and color coding [18,143]. In the frontal view a black circle is used to represent the corneal limbus and a red color to represent vessels. Superficial corneal vessels are drawn as wavy lines originating from outside the limbus, while deep vessels are straight lines beginning at the limbus. Ghost vessels are represented as dashed lines. Corneal scars and degenerations, including lesions such as droplet keratopathy and lipoid degeneration, are black [18,143]. In the slit view a freehand drawing of two parallel curved lines indicating the corneal contour are first drawn. Corneal vessels are represented as red lines in the longitudinal section or as red dots in the cross section at the appropriate depth [143]. Annotation of digital images (manual, semi-automated or automated) can now be performed and may become the norm in the future (Figure 4). Hand drawings are easy to perform but are lack the precision or reproducibility of digital images. Digital annotations of color images can be time consuming if done

manually, but may be performed semi-automatically in the future with further developments in artificial intelligence.

4.2. Photography

Slit lamp biomicroscopy typically uses a white light source (>100,000 lux) modulated by different filters (such as red-free and polarization filters) and different illumination patterns. In general, slit lamp biomicroscopy can provide magnifications ranging from 6x to 40x and a best resolution of approximately 20 µm. Color photographic images are popular because they match to some extent what is seen clinically using slit lamp biomicroscopy. Advantages include speed and ease of acquisition, as well as superior reproducibility compared to hand annotations. Larger vascular abnormalities of the ocular surface such as feeder vessels of tumors, corneal neovascularization, and conjunctival hyperemia can be visualized. Current photography of ocular surface disease, including color, red free, and infrared, however, has limited reproducibility and image quality due to the convex ocular surface, lighting (environment, dimmer settings, diffuser, slit-beam angle), camera definition (magnification, number of pixels of the lens, diaphragm diameter and shutter speed), and patient-dependent factors [11]. Fine details however can be lost in transparent media, and slit lamp color photographs tend to favor larger venous vessels, as these vessels are more numerous, andhave a larger diameter with more red blood cells, thereby making them more prominent than the smaller, less abundant, faster flowing, and more deeply located arteries. As a consequence, many studies delineating the anatomy of the normal and abnormal ocular surface using color photography tend to evaluate the efferent or venous system. These limitations have meant that other techniques such as angiography and optical coherence tomography are more desirable because of their ability to highlight the presence of vessels, despite also their limitations in focusing on a convex surface [8] (Figure 5).

Photoacoustic microscopy (PAM) is another emerging imaging technology that allows vasculature visualization in 3D[64] as a result of its depth-resolving imaging capability [149]. It relies on a photoacoustic effect generated when light is absorbed by an exogenous contrast agents or endogenous molecules within a medium. It utilizes the inherent optical absorbance of hemoglobin itself to provide avascular image [34]. This can aid ophthalmic diagnosis by providing morphologic information on ocular vasculature[63]. Liu and co-workers previously demonstrated segmentation of corneal vascularization using this technique using local regression smoothing[80]. Jeon and co-workers combined *in vivo* PAM imaging and an ocular surface imaging estimation method using machine learning to visualize ocular vasculature[66]. Similar to OCTA, an advantage is the lack of side effects associated with contrast agents[56]. The presence of opaque and scarred tissue, however, affects

image quality, and imaging speed are slow [66]. On the other hand, current PAM imaging requires physical contact between the eye and its ultrasonic detector that may cause patient discomfort in a similar way as a confocal microscope, and resolution is not sufficient to image the capillaries. It is expected that technical advances will improve the speed, depth, resolution, and the need for physical contact [65,81]

4.3 Angiography

Anterior segment angiography using FA and or ICGA provides accurate images of the vascular network of the ocular surface. It has been shown that anterior segment angiography allows for a 3 to 4 times greater visibility of ocular surface vessels compared to color photographs [8]. Fluorescein is an orange-red crystalline hydrocarbon thattravels through vascular structures 80% bound to plasma proteins, mainly to plasma albumin, and 20% unbound. This latter component transits freely and spreads rapidly in tissues where blood-tissue barriers are altered and can therefore be visualized. Fluorescein fluoresces in the green light spectrum (520–530 nm) when the molecule is excited by a blue light (465–490 nm). Following injection into a peripheral vein of 3 ml of 20% fluorescein (Martindale Pharmaceuticals, Essex, United Kingdom), the mean time to appearance of fluorescein in CoNV is approximately 20 ± 7 seconds ,depending on the age and cardiovascular status of the patient. A combination of videography and single images acquired every three to five seconds for three minutes and late images at 5 and 10 minutes provides good detail [73,12] usually with the most informative images acquired at 47 ± 19 seconds [8] (Figures 5, 6 and 7).

ICGA uses a water-soluble tricarbocyanine dye that travels almost completely bound to plasma proteins (98%) after intravenous injection. This limits its diffusion through small capillary fenestrations, thus remaining confined into the intravascular space [59]. This accounts for the absence of leakage (before 10 minutes) and excellent vessel delineation [70,8]. After injection of 5 ml of indocyanine green at a concentration of 5mg/ml (Pulsion Medical Systems, Feldkirchen, Germany) into a peripheral vein, images are similarly acquired by videography every three or five seconds for three minutes, followed by later acquisitions at five and ten minutes. ICG in the corneal vessels appears approximately 17 ± 6 seconds after injection. Best image quality is obtained at 64 ± 41 seconds [8]. It fluoresces in the near-infrared range (790–805 nm), less than fluorescein, and can therefore be detected only with specialized infrared angiography systems [59]. Owing to the peak of indocyanine absorption in the near-infrared range, ICGA images allow a better visualization of corneal vessels in opaque corneas and corneal scars compared to color photographs and FA [70,8] (Figure 5). ICG is then metabolized in the liver and excreted in the bile [59]. Given the different characteristics of FA and ICGA, angiography that uses both fluorescein and indocyanine green

provides better visualization of CoNVs and vessel maturity [8]. As fluorescein and ICG both travel within the vessel lumen, the differences in vessel diameter seen on angiographic images compared to color photographs may reflect vessel wall thickness [11,70,8]. Unfortunately, both FA and ICGA require intravenous dye injection and are therefore invasive, time-consuming, and can be associated with adverse reactions such as nausea, itching, and rarely anaphylaxis [73,54].

FA and ICG are particularly useful in delineating abnormal corneal vessels, extent of limbal ischemia following injury, as well as vascular supply of surface tumors.

Fluorescein angiography provides important information on time to leakage, which is useful when assessing vessel maturity and late reuptake by lymphatics. Although leakage can affect image quality, the extent of leakage can help decide between medical and surgical treatment, as timing and extent of leakage are an indirect indicator of vessel maturity.

4.4 *In vivo* confocal microscopy (IVCM)

IVCM is a noninvasive imaging technique for imaging the cornea at high resolution. IVCM is based on the confocal principle discovered by Marvin Minsky in the 1950s [88]. Using point illumination, a pinhole is introduced in an optically conjugate plane to selectively allow only light reflected from the focal plane to pass through. This configuration blocks the light that is out-of-focus and significantly improves the axial and lateral resolution. Depending on the scanning pattern, there are slit-based systems such as the Nidek instrument and laser scanning such as the Heidelberg HRT3 [61,37]. TheHRT3 uses spotlights at near infrared range (about 670 nm) to scan the tissues in a raster scan pattern. IVCM can normally provide a magnification >400x and a lateral resolution of about 1um/pixel. It requires the lens or a cap to applanate the cornea of the patients in order to achieve high resolution. By moving the focal points in the axial direction, a series of images of the corneal structures at different depths can be acquired. Romano and co-workers showed larger corneal vessels filled with erythrocytes using IVCM, while the intravascular cell types could not be determined in the small vessels [120]. Figure 3 shows an exemplary IVCM image of large corneal vessels. Although the resolution is high, image quality is limited by low contrast. IVCM also requires contact with the cornea provides a small field of view that can be of limited value when assessing large area of vascularization. Moreover, while IVCM allows in vivo microscopic evaluation of the cornea, it only provides morphologic information and requires careful interpretation and clinical correlation. Limited reproducibility means that, at present, it is not routinely used to evaluate ocular surface vascular abnormalities such as staging or differentiating corneal vascularization, tumor progression, or ischemic changes following chemical injury.

4.5. Optical coherence tomography angiography

OCT-A is an innovative application of the OCT technique that was initially introduced in 1991 [58] as part of the rapid development of OCT [45]. OCT uses an interference principle similar to ultrasound to acquire high-resolution images of biological tissues with near infrared light in a non-invasive manner. It can provide axial resolution down to 1-2 µm [74] (Figure 8). OCT-A, is a functional extension of OCT imaging that enables visualization of microvasculature down to capillary level [132]. OCT-A reconstructs blood vessels by detecting moving particles such as red blood cells in the tissue by detecting phase [44] or amplitude [67] differences from the repeated OCT scans at the same location. By conducting continuous cross-sectional OCT-A scans of the tissue, a 3-dimensional OCT-A map can be produced. In order to facilitate the visualization of retinal vessels, projections of the acquired 3D OCT-A map into 2D enface images are frequently used. Compared with FA and ICGA, OCT-A is preferred for its non-invasive nature, however, it is not able to show the dynamic patterns of leakage offered by FA and ICGA especially when assessing corneal vascularization. Recent studies have suggested that measurement of ocular surface vessel density by OCTA in eyes with pterygia and pinguecula is repeatable [150]. It should be noted that, while the scan only takes a few seconds, involuntary movements of the eye could affect the quality of CoNV images. Although at present, its main applications clinically are in retinal imaging [47], a recent literature has demonstrated applicability of OCT-A in assessing abnormal vasculature in pterygium and corneal neovascularization invading corneal graft [7,26]. Currently there are four OCT-A devices: AngioVue RTVue XR Avanti (Optovue, Fremont, California, USA), Angioscan RS-3000 Advance (Nidek, Gamagori, Aichi, Japan), Triton Prototype DRI-OCT (Topcon Corporation, Tokyo, Japan), and PLEX Elite 9000 (Carl Zeiss Meditec, Dublin, California, USA) [76]. Figure 8 shows an OCTA image obtained with AngioVue and a FA/ICG angiograph of CoNV [22]. Table 1 summarizes the applications, benefits, and limitations of each of the imaging modalities.

5.0 Analysis

5.1 Quantitative image analysis

Quantitative analysis of images is essential for the characterization of lesions and in aiding management plans [134,8,70]. In general, these analyses involve a number of techniques in the field of image analysis [8]. First, image enhancement or restoration may be required when the image quality is poor or there is too much noise for the subsequent analysis. Following image enhancement, an automated process of threshold binarization allows enhancement of the vessel's pixels compared to the surrounding pixels. Vessel segmentation is then applied to the enhanced images so as to separate the pixels of vessels from the background. The segmentation is often represented by a

binary image where white pixels represent vessels and black pixels represent non-vessels. After the segmentation a skeletonization process is often required in order to extract the center lines of the vessels for the detailed analysis of vessel parameters (Figure 4).

In the situations where there are several images of the same structure or pathology taken at different times, a process called image registration can be applied to align them into the same spatial coordinates. This process is essential to obtain digital subtractions (subtraction between images after alignment) [119] or to measure flow by detecting the movement of particles in the same vessel [152].

5.2 Definitions of vessel parameters

Ocular surface vessels often appear as a vascular network. In order to characterize these networks, a top-down approach is generally adopted, and the whole vascular segmentation is divided into individual vessel segments by the knowledge of branching or intersection points. Once we derive the center lines of the vessels, then the tail (end) points are defined as the pixels that only have one neighbor vessel pixel, while branching points are defined by pixels that have three neighboring vessel pixels. Due to projection artefacts, intersections (pixels with more than three vessel pixel neighbors) between vessels may appear, and ideally these need to be removed. Figure 4 illustrates the segmented vessels with center lines, branching, tail and intersection points. For each segment then we can then measure its length, diameter and tortuosity. For instance, the length of a segment is the length along the path between its two end points. Given the vessels are often not straight, tortuosity is used to measure the curviness of a vessel segment. There are many definitions, however, the one defined by the ratio of the path length against the Euclidian distance between the two end points is most commonly used (the smallest value is 1 when it is a straight line) [8]. The diameter at each point along the path is the distance between two intersection points on the edge of the vessels of the perpendicular line passing the point under consideration. The mean diameter can then be estimated by averaging the diameters along the path. The area of a segment is the total number of pixels between the two end points of a segment. After all the parameters of each individual vessels are extracted, an overall picture of the whole vasculature can be produced using statistical analysis [152].

5.3. Program, software design and datasets

At present, there are no proprietary programs that can be used for the quantitative analysis of vessel parameters. Programs described in the literature are often semi-automated, customized for specific applications, or even certain types of images. In addition there are no publicly available datasets to

evaluate the programs, thus it is difficult to validate these techniques and widen their applications. Future developments in technology may overcome these limitations.

6. Vascular parameters

A multimodal approach is very helpful in providing most of the detail needed to adequately delineate the vascular abnormality. Slit lamp biomicroscopy and drawing or annotating color images are necessary to ask the clinical question and then to define what is known as the region of interest (ROI). Functional slit lamp biomicroscopy consists of a slit lamp and digital camera. It can assess vessel diameter, blood flow velocity and also generate vascular perfusion maps. It is typically used in contact lens and dry eye disease to study change in microvasculature on the ocular surface. [130] ICGA delineates the anatomy of the vascular network, location and number of afferent vessels and FA vessel maturity. OCT-A differentiates between superficial and deep CoNV [21] (Figure 8).
Changes in the area of CoNV, vessel diameter, branching, and tortuosity have been shown to be particularly evident on angiography, and analysis provides a reliable measure of change. [70,11]
Although some of these parameters may be present in color images, they are much less evident and are inconsistent. Angiography and OCT-A in conjunction with computer-assisted automated analysis, have enabled the measurement of individual vessels across ROI for each patient before and after treatment. This type of analysis enables construction of frequency histograms and statistical testing of changes in vessel parameters for each patient. For example, following treatment of microbial keratitis, the frequency distributions of individual vessel parameters such as diameter and tortuosity for an individual patient show a reduction in vascular parameters accompanied by a reduction in the spread of vessel size.

6.1 Filling patterns

Angiographic methods have shown that limbal vessels and MCAs do not fill at the same rate around the circumference of the cornea [152]. The inferior vessels fill first, followed by those of the superior, nasal, and temporal regions [152]. There is a 6 second difference in filling of the inferior MCAs to those of the temporal region. In cases of carotid stenosis, delays in filling of the limbus and surrounding conjunctiva may be expected [137].

6.2 Origins of corneal neovascular complexes

Angiography is essential for the investigation of the origin of the vascular complex. Arterioles or afferent vessels may be differentiated clinically from venules or efferent vessels, as they are a

usually thinner, straighter, deeper and less tortuous. There are generally fewer afferent than efferent vessels and, in the presence of large vascular complex, they can be very difficult to find. CoNV may potentially arise from the MCA, the limbal vessels and or the surrounding conjunctival and episcleral vascular arcades. The location and severity of the disease will usually determine their respective origin. For example, CoNV resulting from disease confined to the cornea, such as inflammatory or infective conditions, may arise from the intact limbal and MCA. In situations where there is injury to the MCA and limbal arcades, such as in a chemical injury resulting in limbal ischemia, CoNV may develop from the in-growth and or originate from conjunctival and episcleral vessels. Determining the origin of the vascular complex helps plan treatment, especially for selective fine needle diathermy. [116136118114] (Figure 9 and 10, video 1 and 2)

6.3 Area

Defining and measuring the area of an abnormal vascular network is important for both characterizing the condition and measuring the response to treatment [79]. For example, the number of 'quadrants' of CoNV is significantly associated with an increased risk of corneal graft rejection [87]. Corneal angiography compliments slit lamp biomicroscopy as it has a wide field of view which helps to precisely quantify the area of CoNV. At present, OCT-A has a limited field of 6x6 mm and still presents artifacts that limit its ability to quantify the area (Figure 8).

6.4 Drop-out

Defining an area of ischemia and or vessel loss following a chemical injury is essential for planning clinical management. It can be very difficult to discern between the unaffected and damaged vessels with no blood flow by simple observation on slit lamp biomicroscopy and accompanying photography. Determining the extent of limbal ischemia for example, is crucial for assessing the risk of limbal stem cell failure or neovascular response following a chemical injury. Using anterior segment angiography (OCT-A, FA and ICGA) provides the best definition of the ischemic area, residual vascular damage with leakage, degree of flow, and capillary drop out [113,46](Figure 11).

6.5 Vessel parameters (diameter, branching, tortuosity)

ICGA provides excellent vessel delineation even in the presence of stromal scars to measure vessel parameters such as branch pattern, segment length, diameter, and tortuosity. Appropriate computer software is essential for this type of analysis. Kirwan and co-workers found a statistically significant reduction in mean vessel diameter in patients treated for active keratitis, that was more

evident when analyzed with ICGA (reduction from 44.77μm to 33.29μm), compared to color images (reduction from 29.10μm to 25.17μm [70]).

6.7 Flow

Digital angiography measures vascular flow (rate and direction), which is useful for disease monitoring. For example, direction of flow is important in planning treatment such as fine needle diathermy. Digital angiography is gaining importance especially in cases of ocular surface neoplastic lesions where the intralesional formation of shunt vessels and the filling time can be considered as a parameter in malignant lesions [23]. Tissue perfusion is proportional to the transit time across a capillary bed which in turn governs the time available for the exchange of respiratory gases. Alfred and Nuttal noted that the greatest velocities occurred in feeder vessels, which are vessels that divide into two or more capillaries at the apical border [98]. A problem in measuring blood flow velocity through capillaries by observation is the need for a mark by which blood motion along the vessel can be observed [60]. Ivanov used gaps (plasma) between erythrocyte flow to measure velocity [60]. It is difficult, however, to appreciate gaps with the use of dyes such as ICG and FA. Although only based upon one patient, the average speed of flow in the marginal corneal arcade of 0.22 mm/second or 0.79m/hour, is similar to the velocity of blood flow in the capillaries of the cochlea which has been measured from below 0.1 mm/s to about 0.3-0.4 mm/s with an average velocity of 0.22 mm/s [98,109]. Although the flow velocity in the limbal vessels is unknown, it would be expected to be greater than in the MCA.

6.8 Angiographic dye leakage

6.8.1 Corneal neovascular complex (CoNV)

Apart from the MCA, all corneal vascularization is pathological. CoNV evolves as a result of a disruption of the balance between pro- and anti-angiogenic factors, with loss of the corneal angiogenic and immune privilege [27,93]. The time to leakage of FA or ICGA provides a measure of vessel staging and maturity. Fluorescein usually leaks at 42 ± 23 seconds depending on the maturity of the CoNV. The earlier the leakage (about 30 seconds), the more immature the vessel and the later the leakage (about 50 seconds), and the more mature and stable the vessel [8] (Figure 7). For example, time to first appearance of FA dye leakage significantly increases following treatment and resolution of the keratitis and is consistent with the clinical impression of reduced vascular leakage as the inflammation responds to treatment. Topical fluorescein before intravenous fluorescein injection interferes with good angiographic image quality and should be avoided [8]. Palme and co-workers demonstrated a significant association between the time to ICG leakage and clinical staging of CoNV

and the age of CoNV [104]. ICG leakage within 10 minutes was observed significantly more frequently in cases with active compared to inactive CoNV (100% vs 9%, p<0.001), supporting the use of FA and ICGA to stage objectively the activity of CoNV and to guide treatment.

The use of a five-grade biomicroscopic staging scale of CoNV by Faraj and co-workers was found to be of limited value due to reliance on easily seen large vessels which are usually efferent (venous) with little attention to afferent (arterial) vessels that are fewer and much more difficult to discern [43]. This limitation underlines the need for objective measures reflecting functional stages and maturity of CoNV and the need to distinguish afferent and efferent vessels, especially for guiding treatment [116]. Palme and co-workers therefore suggested 3 clinical stages of CoNV: active CoNV, inactive CoNV and regressed CoNV (ghost vessels) (Figure 6 and 7).

This simplified clinical three-stage classification was found to be supported by the angiographic features (leakage, pattern, and size) and age of CoNV. In both patients with active and inactive CoNV, there is perfusion of the corneal vessel plexuses on angiography with no differences in segment length, branching, and tortuosity. Time to leakage of both fluorescein and ICG helps to define active from inactive CoNV. For example, leakage of ICG dye within 10 minutes was identified in 100% of active, but only in 6.3% of inactive or regressed CoNV.

At late stages of inactive CoNV, angiography showed cessation of red blood cell traffic but persistent acellular flow in corneal plasma vessels confirmed by IVCM. The intravascular lumen of plasma vessels was found to be large enough to potentially carry red blood cells (average diameter, 21 mm), and the mean vessel diameters did not differ between plasma vessels and active CoNV.

Corneal hematic angiogenesis is mostly accompanied by the formation of lymphatic neovessels.[78,32,145,31] These lymphatic vessels, however, have long eluded *in vivo* detection because of the transparency of lymphatic endothelial cells and the lymph fluid [108]. Based on these findings Romano and co-workers [120] proposed to image corneal lymphatic vessels using IVCM and digital subtraction analysis of intravenous angiograms, showing that dye leaks out from vessels into the surrounding tissues and is then reabsorbed into the venous or lymphatic system or both [117] (Figure 3). They suggested that uptake into the lymphatic micro vessels in the cornea will occur in less than an hour, enabling the visualization of microlymphatic vessels. Digital subtraction analysis (DSA) was used to objectively identify newly appeared corneal vessels with reuptake of ICG from the interstitial space. It was shown that, similar to the mouse model used by Yuen and co-workers, corneal neovascular lymphatic vessels are co-localized to blood vessels [148]. This method, however, has limitations such as imaging at exactly the same angle and focus of a 3-dimensional CoNV on the

spherical cornea, which can be difficult to perform. Technological developments to improve alignment may enhance the ability to more consistently identify such a vascular structure with DSA.

6.8.2 Conjunctival vessels and inflammation

Conjunctival capillaries are fenestrated, allowing more rapid passage of luminal contents in inflammation [138]. After intravenous injection of fluorescein, conjunctival vessels leak in a time and concentration sequence similar to that of the choroidal capillaries. The vessels at the palisades of Vogt may be more competent and leak less than conjunctival vessels elsewhere. Conjunctival inflammation, infections, irritation, or severe intraorbital inflammation cause the conjunctival capillaries to leak plasma proteins faster than the fluid can pass between the epithelial cells [30,96,85]. This phenomenon can be used to stage the activity of ocular surface inflammatory disease such as e.g. cicatrizing keratoconjunctivitis [57,42]. Steger and co-workers [135] described new angiographic parameters that may help evaluate inflammatory activity using IVCM and anterior segment angiography. In cases with active inflammation, the transvascular migration of inflammatory cells into the interstitial tissue, known as leukocyte diapedesis, can be observed (Video 2). Using tarsal conjunctival FA and ICGA there was both increased transvascular and even transepithelial leakage of intravenous dyes on FA and ICGA in active atopic keratoconjunctivitis, which correlated closely with the clinical degree of disease activity [135] (Figure 12). This is supported by reports using a rat model, where the activity of allergic conjunctivitis correlated with the degree of Evans blue-albumin complex extravasation from conjunctival vessels [111]. Invasive angiography should, however, be used with caution in non-vision threatening mild inflammatory disease as it has side effects, including allergic reactions ranging from mild to anaphylaxis.

Clinical grading of conjunctival redness is used for monitoring inflammatory ocular surface disease [90,39]. Biomicroscopic grading of vascular alterations is widely based on the assessment of conjunctival redness but is limited by intra- and interobserver variability, poor reproducibility and image quality [10,110,142,29].

Frequently used photographic scales for estimating bulbar redness include the McMonnies and Chapman-Davies scale (M-CD scale) [90], the Efron scale [38], and the Validated Bulbar Redness (VBR) grading scale. [123] There are many differences among these scales, including the number of reference images, the range of redness, the linearity of the scores as a measure of redness, and the conjunctival region displayed in the reference images [40,107,121,110,29,122]. To overcome these limitations, the ocular redness index and CLAHE algorithm (contrast-limited adaptive histogram equalization) have been proposed based on automated digital analysis of nasal conjunctival digital slit lamp photographs [5,131]. Both indices are observer-independent but cannot correct for quality and color

519 deficiencies of the conjunctival photographs used. Recent literature has suggested that OCTA maybe
520 useful when assessing ocular surface vasculature when compared with invasive angiograph [6] and slit
521 lamp photography [2]. The quality of OCTA images however may be limited by artefacts [21,6]. Ang and
522 co-workers observed underestimation of corneal vessel area on ICGA compared with OCTA was
523 likely of minimal clinical significance and may need reconfirming in further studies. It may be due to
524 fundamental differences in image acquisition techniques and discrepancies in image analysis like
525 non-parallel segmentation or projection artefacts that can cause a superficial vessel to appear
526 thicker that it actually is. Furthermore, light scatter from corneal scars can also overestimate areas
527 of vascularisation.[6] Romano and co-workers proposed a pixel densitometry index (PDI) based on
528 early ICG angiographic images to quantify obkectively ocular hyperemia. PDI is calculated from the
529 number of white and black pixels in analyzed angiograms, where vessels with dye are seen as white
530 pixels [115] (Figure 13). Use of FA or ICGA enables the assessment of additional vascular parameters
531 including flow direction and vascular permeability, [104,119] which can be helpful in disease activity and
532 differentiating episcleritis, scleritis and scleral necrosis [50,97,53,144]. ICGA in particular provides
533 anatomical details of the ocular vessels giving the opportunity to highlight even systemic conditions
534 such as generalized essential telangiectasia [146] (Figure 14).
535
536 **7. Imaging vascular features of specific conditions**
537 **7.1 Vascular abnormalities associated with infective conditions**
538 Corneal neovascularization (CoNV) is a common accompaniment of microbial keratitis. This is
539 typically seen in *Herpes simplex* keratitis (HSK), *Pseudomonas aeruginosa* and *Staphylococcus aureus*
540 keratitis, and acanthamoeba-associated keratitis. Herpetic keratitis has been associated with the
541 most severe CoNV and with more frequent lipid keratopathy while acanthamoeba keratitis leads to
542 less severe CoNV;[43] however, a more detailed analysis on the extent of variation of the pattern of
543 development of CoNV between these microbiological causes is unclear. Typically, with recurrent
544 disease as in HSK and *Staphylococcus aureus* further CoNV occurs adjacent to or in a new area of the
545 cornea. The associated exudation and scarring associated with the keratitis and CoNV leads to loss
546 of vision. [75] Identifying and characterizing the neovascular complex enables one to monitor the
547 disease and plan treatment aimed at reducing the exudation and scarring associated with the CoNV.
548 It can be difficult to determine whether the CoNV is helping to negate the infection, and or is
549 contributing to loss of vision. This is often dependent on the stage of the microbial keratitis.
550 Corneal angiography in the presence of microbial keratitis, provides information on many aspects of
551 the neovascular complex so that the clinician is able to make a decision on whether and when to
552 treat the CoNV. Time is important as CoNV may be an important part of the host's immune response

to helping clear the infection and too soon an intervention may be deleterious. Treatment may comprise medical treatment, for example the response of immature vessels to steroids or antivascular treatment or response of mature vessels to angiographically assisted fine needle diathermy of the feeder vessel. Analysis of the neovascular complex (area, vessel length, tortuosity, leakage times) can be used to monitor the response of the disease to treatment as in the following examples of an HSK, bacterial and acanthamoeba keratitis [134], although potential side effects and time required for repeated corneal angiographies should be kept in mind and careful evaluation of their appropriateness performed [73,54]. (Figure 10).

7.2. Noninfectious diseases.

FA and ICGA are particularly suited to delineating vessels in congenital lesions of the cornea, assessing corneal grafts or pre-corneal transplantation, or in determining the prognosis of nasal conjunctival disorders [150]. ICGA has also been used to show that the fan-shape vascular plexus of a pterygium forms from a single feeder vessel of the anterior conjunctival circulation [24]. Both ICGA and OCTA have also been utilized to investigate the progress and pattern of vascularization of autografts used for conjunctival reconstruction after pterygium excision [69,82,151].

7.2.5 Limbal stem cell deficiency

Limbal stem cell deficiency (LSCD) is a clinical and or cytological diagnosis where the corneal epithelium is replaced by conjunctival tissue, including conjunctival epithelium and blood vessels. Conversely, chemical burns and radiation damage to the limbus can result in limbal ischemic changes and subsequent LSCD. There are many causes of LSCD including genetic, trauma (chemical burns), inflammatory and iatrogenic causes. The presence of superficial corneal vascularization as well as the loss of limbal vessels is important in the grading and therefore subsequent management of LSCD using limbal stem cell therapies. CoNV in LSCD has been studied using slit lamp biomicroscopy, as well as more recently fluorescein and OCT angiography [100,46,103,68,13]. Without angiography it can be very difficult to detect and quantify the associated vascularization and plan treatment. (Figure 15) Reconstructive surgery in LSCD requires limbal transplants (either whole tissue or cultured cells), and for these to succeed the vascular supply to the ocular surface is important in bringing blood borne growth factors and cytokines to the transplanted limbal stem cells.

7.2.6 Neoplasms (benign and malignant)

Pathological angiogenesis is a known hallmark of tumor growth. High densities of new vessel formation in neoplastic tissues are associated with aggressive invasive growth and metastatic disease

[72]. Both vascular architecture and function are impaired in malignant neoplastic disease. Nonhomogeneous Videovessel density, decreased regularity, loss of vessel hierarchy, shunt vessel formation [112], and blind ending capillaries are seen in a variety of malignant tissues [71]. Defective angiogenesis leads to an anomalous vessel wall structure with multi-layered basement membrane, incomplete and loose pericyte coverage leading to chronic transvascular hyperpermeability.

Clinical assessment of ocular surface neoplasia (OSN) includes the identification of risk factors associated with dysplastic or malignant disease, including vascular features such as the presence of hemorrhage, feeder vessels or visible intrinsic tumor vasculature [125,126].

FA, ICGA and OCT angiography have been used to characterize both vascular patterns and functional alterations seen in vascular OSN [127,128,83]. Using ICGA, afferent feeders can clearly be discerned from efferent vessels [23]. Under physiologic circumstances arterioles can be differentiated clinically from venules by thinner vessel diameter and less tortuosity. This, however, is not always possible with ocular surface vessels in OSN. Flow velocity and vessel diameter in efferent venules are increased due to the frequent intralesional formation of shunt vessels, bypassing the capillary system [112]. Thus, flow and pressure differences between arterioles and venules are reduced, leading to morphologically similar appearance of these vessels, as shown by Brunner et al. [23]. They reported that the vessel diameter ratio of afferent to efferent vessels was significantly different between benign and malignant melanocytic OSN and that the angiographic filling time was significantly shorter in benign and non-invasive lesions compared to invasive melanocytic and squamous cell OSN [23]. In a further recent study, the angiographic characteristics of OSN included focal or sea fan-shaped intra-tumoral and conjunctival feeding vessels on ICGA, and angiography proved useful to monitor vessel regression as a measure of treatment response to subconjunctival and perilesional 5-fluorouracil injection [140]. Additionally, the observation of ICG dye leakage has proved to be useful in the diagnostic evaluation of OSN. While ICG does not usually leak from conjunctival vessels, a recent report describes extensive ICG leakage from intrinsic but not feeding conjunctival tumor vessels or surrounding healthy conjunctival tissues in a case of in situ conjunctival squamous carcinoma [106,105](Figure 16). Likewise, the extravascular leakage of ICG was significantly associated with conjunctival melanoma in a series of 32 cases of melanocytic OSN [15] (Figure 17). The observed increased dye leakage on intravenous angiography is likely to be caused by trans-vascular hyperpermeability in tumor vessels [96] due to pathological tumor angiogenesis with incomplete or absent pericyte coverage, and abnormal basement membrane structure [89]. OCT angiography has recently been proposed as a non-invasive method for visualizing and quantifying vessel structure and density within, under, and surrounding ocular surface squamous neoplasia [83] and melanocytic lesions of the conjunctiva and iris. [20] Angiographic assessment of OSN thus enables early diagnosis and grading of OSN in vivo by the

detecting active intralesional tumor angiogenesis and abnormal transvascular permeability. The most notable vascular features differentiating benign from dysplastic or malignant OSN are summarized in Table 2.

8.0 Conclusion

Over the past several decades, ophthalmology as a whole has witnessed a rapid development in terms of new imaging technologies and novel analysis techniques. Recent advances in artificial intelligence (AI) offers further potential in developing new imaging technologies for the management of ocular surface disease. While predicting the future is difficult, we expect that new hardware development will allow improved imaging of the structures of interest and their functions (e.g. flow velocity) in real time at much higher resolution with a deeper and wider field of view. A single device may eventually be capable of providing all the diagnostic information needed currently provided by multiple devices and reduce the need for multimodal imaging. We expect that there will be improved image analysis programs that will be able to automatically extract useful clinical information from the large volume of raw data on the device for the clinician. AI will be the key enabler for the invention of new camera devices and novel analysis algorithms. In order, however, to reach the full potential of AI, some key issues have to be addressed, such as availability of data, interpretation, validation, and reliability [95], regulatory approval and ethical considerations, as well as acceptance by patients and clinicians. This should lead to improvements in the management and treatment of conditions associated with abnormal ocular surface vascularization.

Funding: This research did not receive any specific grant from funding agencies in the public, commercial, or not-for-profit sectors.

Methods of Literature Search

Literature search was conducted on PUBMED and Google Scholar for the topic “corneal neovascularization”. The authors analyzed original studies, reviews, and case reports. Keywords used were: corneal neovascularization/neovascularisation (CoNV), CoNV imaging, CoNV review, CoNV angiography, CoNV fluorescein angiography/FA, CoNV indicianine green angiography/ICGA, CoNV in vivo confocal microscopy/IVCM, CoNV optical coherence tomography, CoNV optical coherence tomography angiography/OCT-A, CoNV photography, CoNV drawing. Animal and human studies were included in this review and adhered to the Helsinki Declaration.

References:

1. Abelson MB, Schaefer K. Conjunctivitis of allergic origin: Immunologic mechanisms and current approaches to therapy. *Surv Ophthalmol*. 1993;38(SUPPL. 2):115-132. doi:10.1016/0039-6257(93)90036-7
2. Aicher NT, Nagahori K, Inoue M, Itoh Y, Hirakata A. Vascular density of anterior segment of eye determined by optical coherence tomography angiography and slit-lamp photography. *Ophthalmic Res*. 2020;63(6). doi:10.1159/000506953
3. Akagi T, Uji A, Huang AS, et al. Conjunctival and Intrascleral Vasculatures Assessed Using Anterior Segment Optical Coherence Tomography Angiography in Normal Eyes. *Am J Ophthalmol*. 2018;196:1-9. doi:10.1016/j.ajo.2018.08.009
4. Albuquerque RJC, Hayashi T, Cho WG, et al. Alternatively spliced vascular endothelial growth factor receptor-2 is an essential endogenous inhibitor of lymphatic vessel growth. *Nat Med*. 2009;15(9):1023-1030. doi:10.1038/nm.2018
5. Amparo F, Wang H, Emami-Naeini P, Karimian P, Dana R. The ocular redness index: A novel automated method for measuring ocular injection. *Investig Ophthalmol Vis Sci*. 2013;54(7):4821-4826. doi:10.1167/iovs.13-12217
6. Ang M, Cai Y, Macphee B, et al. Optical coherence tomography angiography and indocyanine green angiography for corneal vascularisation. *Br J Ophthalmol*. 2016;100(11):1557-1563. doi:10.1136/bjophthalmol-2015-307706
7. Ang M, Sim DA, Keane PA, et al. Optical Coherence Tomography Angiography for Anterior Segment Vasculature Imaging. *Ophthalmology*. 2015;122(9):1740-1747. doi:10.1016/j.ophtha.2015.05.017
8. Anijeet DR, Zheng Y, Tey A, Hodson M, Sueke H, Kaye SB. Imaging and evaluation of corneal vascularization using fluorescein and indocyanine green angiography. *Investig Ophthalmol Vis Sci*. 2012;53(2):650-658. doi:10.1167/iovs.11-8014
9. Bachmann B, Taylor RS, Cursiefen C. Corneal neovascularization as a risk factor for graft failure and rejection after keratoplasty: An evidence-based meta-analysis. *Ophthalmology*. 2010;117(7). doi:10.1016/j.ophtha.2010.01.039
10. Baudouin C, Barton K, Cucherat M, Traverso C. The measurement of bulbar hyperemia: Challenges and pitfalls. *Eur J Ophthalmol*. 2015;25(4):273-279. doi:10.5301/ejo.5000626
11. Benayoun Y, Rosenberg R, Casse G, Dallaudière B, Robert PY. Imagerie et quantification de la néovascularisation cornéenne. *J Fr Ophtalmol*. 2013;36(8):693-703. doi:10.1016/j.jfo.2013.04.006
12. Berkow J, Flower R, Orth D, Kelley J. Fluorescein and Indocyanine Green Angiography: Technique and Interpretation. In: *2nd Ed. Ophthalmology Monograph 5. San Francisco: American Academy of Ophthalmology*. ; 1997.
13. Binotti WW, Nosé RM, Koseoglu ND, Dieckmann GM, Kenyon K, Hamrah P. The utility of anterior segment optical coherence tomography angiography for the assessment of limbal stem cell deficiency. *Ocul Surf*. Published online 2020. doi:10.1016/j.jtos.2020.04.007
14. Bizheva K, Hutchings N, Sorbara L, Moayed AA, Simpson T. In vivo volumetric imaging of the human corneo-scleral limbus with spectral domain OCT. *Biomed Opt Express*. 2011;2(7):1794. doi:10.1364/boe.2.001794
15. Böhringer D, Spierings E, Enczmann J, et al. Matching of the minor histocompatibility antigen HLA-A1/H-Y may improve prognosis in corneal transplantation. *Transplantation*. 2006;82(8):1037-1041. doi:10.1097/01.tp.0000235908.54766.44
16. Bron A, Easty D. Fluorescein angiography of the globe and anterior segment . *Trans Ophthalmol Soc U K*. 1970;90:339-367. Accessed October 6, 2020. https://pubmed.ncbi.nlm.nih.gov/4933929/
17. Bron A, Tripathi R, Tripathi B, Eds. *Wolff's Anatomy of the Eye and Orbit, 8th Ed. London, UK:*

Chapman and Hall Medical.; 1997.
18. Bron AJ. A simple scheme for documenting corneal disease. *Br J Ophthalmol*. 1973;57(9):629-634. doi:10.1136/bjo.57.9.629
19. Bron AJ, Easty DL. Fluorescein angiography of the globe and anterior segment. *Trans Ophthalmol Soc U K*. 1970;90:339-367. Accessed September 12, 2020. https://pubmed.ncbi.nlm.nih.gov/4933929/
20. Brouwer NJ, Marinkovic M, Bleeker JC, Luyten GPM, Jager MJ. Anterior Segment OCTA of Melanocytic Lesions of the Conjunctiva and Iris. *Am J Ophthalmol*. 2021;222:137-147. doi:10.1016/j.ajo.2020.09.009
21. Brunner M, Romano V, Steger B, et al. Imaging of corneal neovascularization: Optical coherence tomography angiography and fluorescence angiography. *Investig Ophthalmol Vis Sci*. 2018;59(3):1263-1269. doi:10.1167/iovs.17-22035
22. Brunner M, Romano V, Steger B, et al. Imaging of corneal neovascularization: Optical coherence tomography angiography and fluorescence angiography. *Investig Ophthalmol Vis Sci*. 2018;59(3):1263-1269. doi:10.1167/iovs.17-22035
23. Brunner M, Steger B, Romano V, et al. Identification of Feeder Vessels in Ocular Surface Neoplasia Using Indocyanine Green Angiography: A Preliminary Report. *Curr Eye Res*. 2018;43(2):163-169. doi:10.1080/02713683.2017.1387273
24. Chan CML, Chew PTK, Alsagoff Z, Wong JS, Tan DTH. Vascular patterns in pterygium and conjunctival autografting: A pilot study using indocyanine green anterior segment angiography. *Br J Ophthalmol*. 2001;85(3):350-353. doi:10.1136/bjo.85.3.350
25. Chan G, Balaratnasingam C, Yu PK, et al. Quantitative morphometry of perifoveal capillary networks in the human retina. *Investig Ophthalmol Vis Sci*. 2012;53(9):5502-5514. doi:10.1167/iovs.12-10265
26. Chan SY, Pan CT, Feng Y. Localization of Corneal Neovascularization Using Optical Coherence Tomography Angiography. *Cornea*. 2019;38(7):888-895. doi:10.1097/ICO.0000000000001931
27. Chang JH, Gabison EE, Kato T, Azar DT. Corneal neovascularization. *Curr Opin Ophthalmol*. 2001;12(4):242-249. doi:10.1097/00055735-200108000-00002
28. Chen W, Batawi HIM, Alava JR, et al. Bulbar conjunctival microvascular responses in dry eye. *Ocul Surf*. 2017;15(2):193-201. doi:10.1016/j.jtos.2016.12.002
29. Chong T, Simpson T, Fonn D. The repeatability of discrete and continuous anterior segment grading scales. *Optom Vis Sci*. 2000;77(5):244-251. doi:10.1097/00006324-200005000-00011
30. Conjunctival circulation in relation to circulatory disorders - PubMed. Accessed September 10, 2020. https://pubmed.ncbi.nlm.nih.gov/5233050/
31. Cursiefen C, Cao J, Chen L, et al. Inhibition of hemangiogenesis and lymphangiogenesis after normal-risk corneal transplantation by neutralizing VEGF promotes graft survival. *Investig Ophthalmol Vis Sci*. 2004;45(8):2666-2673. doi:10.1167/iovs.03-1380
32. Cursiefen C, Chen L, Borges LP, et al. VEGF-A stimulates lymphangiogenesis and hemangiogenesis in inflammatory neovascularization via macrophage recruitment. *J Clin Invest*. 2004;113(7):1040-1050. doi:10.1172/JCI20465
33. Dana MR, Schaumberg DA, Kowal VO, et al. Corneal neovascularization after penetrating keratoplasty. *Cornea*. 1995;14(6):604-609. doi:10.1097/00003226-199511000-00014
34. Deán-Ben XL, Bay E, Razansky D. Functional optoacoustic imaging of moving objects using microsecond-delay acquisition of multispectral three-dimensional tomographic data. *Sci Rep*. 2014;4. doi:10.1038/srep05878
35. Easty DL, Bron AJ. Fluorescein angiography of the anterior segment its value in corneal disease. *Br J Ophthalmol*. 1971;55(10):671-682. doi:10.1136/bjo.55.10.671
36. Ecoiffier T, Yuen D, Chen L. Differential distribution of blood and lymphatic vessels in the murine cornea. *Investig Ophthalmol Vis Sci*. 2010;51(5):2436-2440. doi:10.1167/iovs.09-4505
37. Efron N. Chapter 1 - Anterior eye examination. In: *In: Efron N, Editor. Contact Lens Complications (Third Edition). London: W.B. Saunders*. ; 2012:1-20.

38. Efron N. Grading scales. *Optician*. 2000;219:44-45.
39. Efron N. Grading scales for contact lens complications. In: *Ophthalmic and Physiological Optics*. Vol 18. Ophthalmic Physiol Opt; 1998:182-186. doi:10.1016/S0275-5408(97)00066-5
40. Efron N, Morgan PB, Katsara SS. Validation of grading scales for contact lens complications. *Ophthalmic Physiol Opt*. 2001;21(1):17-29. doi:10.1046/j.1475-1313.2001.00575.x
41. Ehrlich P. Dtsch, Med. Wschr. March 181. *Dtsch, Med Wschr*.
42. Evaluation of conjunctival inflammatory status by confocal scanning laser microscopy and conjunctival brush cytology in patients with atopic keratoconjunctivitis (AKC) - PubMed. Accessed September 10, 2020. https://pubmed.ncbi.nlm.nih.gov/19693288/
43. Faraj LA, Said DG, Al-Aqaba M, Otri AM, Dua HS. Clinical evaluation and characterisation of corneal vascularisation. *Br J Ophthalmol*. 2016;100(3):315-322. doi:10.1136/bjophthalmol-2015-306686
44. Fingler J, Schwartz D, Yang C, Fraser SE. Mobility and transverse flow visualization using phase variance contrast with spectral domain optical coherence tomography. *Opt Express*. 2007;15(20):12636. doi:10.1364/oe.15.012636
45. Fujimoto J, Huang D. Foreword: 25 years of optical coherence tomography. *Investig Ophthalmol Vis Sci*. 2016;57(9):OCTi-OCTii. doi:10.1167/iovs.16-20269
46. Fung SSM, Stewart RMK, Dhallu SK, et al. Anterior Segment Optical Coherence Tomographic Angiography Assessment of Acute Chemical Injury. *Am J Ophthalmol*. 2019;205:165-174. doi:10.1016/j.ajo.2019.04.021
47. Gao SS, Jia Y, Zhang M, et al. Optical coherence tomography angiography. *Investig Ophthalmol Vis Sci*. 2016;57(9):OCT27-OCT36. doi:10.1167/iovs.15-19043
48. Goldberg M, Bron A. Limbal palisades of Vogt . *Trans Am Ophthalmol Soc*. 1982;80:155-171.
49. Graves B. CERTAIN CLINICAL FEATURES OF THE NORMAL LIMBUS. *Br J Ophthalmol*. 1934;18(7):369-387. doi:10.1136/bjo.18.7.369
50. Guex-Crosier Y, Durig J. Anterior segment indocyanine green angiography in anterior scleritis and episcleritis. *Ophthalmology*. 2003;110(9):1756-1763. doi:10.1016/S0161-6420(03)00567-0
51. Guthoff RF, Zhivov A, Stachs O. In vivo confocal microscopy, an inner vision of the cornea - A major review. *Clin Exp Ophthalmol*. 2009;37(1):100-117. doi:10.1111/j.1442-9071.2009.02016.x
52. Harper RN, Moore MA, Marr MC, Watts LE, Hutchins PM. Arteriolar rarefaction in the conjunctiva of human essential hypertensives. *Microvasc Res*. 1978;16(3):369-372. doi:10.1016/0026-2862(78)90070-5
53. Hau SC, Devarajan K, Ang M. Anterior Segment Optical Coherence Tomography Angiography and Optical Coherence Tomography in the Evaluation of Episcleritis and Scleritis. *Ocul Immunol Inflamm*. Published online 2019. doi:10.1080/09273948.2019.1682617
54. Hope-Ross M, Yannuzzi LA, Gragoudas ES, et al. Adverse Reactions due to Indocyanine Green. *Ophthalmology*. 1994;101(3):529-533. doi:10.1016/S0161-6420(94)31303-0
55. Horak F, Berger U, Menapace R, Schuster N. Quantification of conjunctival vascular reaction by digital imaging. *J Allergy Clin Immunol*. 1996;98(3):495-500. doi:10.1016/S0091-6749(96)70081-7
56. Hu S, Rao B, Maslov K, Wang L V. Label-free photoacoustic ophthalmic angiography. *Opt Lett*. 2010;35(1):1. doi:10.1364/ol.35.000001
57. Hu Y, Matsumoto Y, Adan ES, et al. Corneal In Vivo Confocal Scanning Laser Microscopy in Patients with Atopic Keratoconjunctivitis. *Ophthalmology*. 2008;115(11):2004-2012. doi:10.1016/j.ophtha.2008.05.010
58. Huang D, Swanson EA, Lin CP, et al. Optical coherence tomography. *Science*. 1991;254(5035):1178-1181. Accessed January 17, 2019. http://www.ncbi.nlm.nih.gov/pubmed/1957169
59. Indocyanine green angiography. American Academy of Ophthalmology. *Ophthalmology*.

1998;105(8):1564-1569.
60. Ivanov KP, Kalinina MK, Levkovich YI. Blood flow velocity in capillaries of brain and muscles and its physiological significance. *Microvasc Res*. 1981;22(2):143-155. doi:10.1016/0026-2862(81)90084-4
61. Jalbert I, Stapleton F, Papas E, Sweeney DF, Coroneo M. In vivo confocal microscopy of the human cornea. *Br J Ophthalmol*. 2003;87(2):225-236. doi:10.1136/bjo.87.2.225
62. Jensen VA, Lundbœk K. FLUORESCENSE ANGIOGRAPHY OF THE IRIS IN RECENT AND LONG-TERM DIABETES PRELIMINARY COMMUNICATION. *Acta Ophthalmol*. 1968;46(3):584-585. doi:10.1111/j.1755-3768.1968.tb02854.x
63. Jeon, M. & Kim C. Multimodal photoacoustic tomography. *IEEE Trans Multimed*. 2013;(15):975-982.
64. Jeon M, Kim J, Kim C. Multiplane spectroscopic whole-body photoacoustic imaging of small animals in vivo. *Med Biol Eng Comput*. 2016;54(2-3):283-294. doi:10.1007/s11517-014-1182-6
65. Jeon S, Kim J, Lee D, Baik JW, Kim C. Review on practical photoacoustic microscopy. *Photoacoustics*. 2019;15. doi:10.1016/j.pacs.2019.100141
66. Jeon S, Song HB, Kim J, et al. In Vivo Photoacoustic Imaging of Anterior Ocular Vasculature: A Random Sample Consensus Approach. *Sci Rep*. 2017;7(1). doi:10.1038/s41598-017-04334-z
67. Jia Y, Tan O, Tokayer J, et al. Split-spectrum amplitude-decorrelation angiography with optical coherence tomography. *Opt Express*. 2012;20(4):4710. doi:10.1364/oe.20.004710
68. Käsmann-Kellner B, Latta L, Fries FN, Viestenz A, Seitz B. Diagnostic impact of anterior segment angiography of limbal stem cell insufficiency in PAX6-related aniridia. *Clin Anat*. 2018;31(3):392-397. doi:10.1002/ca.22987
69. Kim YJ, Yoo SH, Chung JK. Reconstruction of the limbal vasculature after limbal-conjunctival autograft transplantation in pterygium surgery: An angiography study. *Investig Ophthalmol Vis Sci*. 2014;55(12):7925-7933. doi:10.1167/iovs.14-15288
70. Kirwan RP, Zheng Y, Tey A, Anijeet D, Sueke H, Kaye SB. Quantifying Changes in Corneal Neovascularization Using Fluorescein and Indocyanine Green Angiography. *Am J Ophthalmol*. 2012;154(5):850-858.e2. doi:10.1016/j.ajo.2012.04.021
71. Konerding MA, Fait E, Gaumann A. 3D microvascular architecture of pre-cancerous lesions and invasive carcinomas of the colon. *Br J Cancer*. 2001;84(10):1354-1362. doi:10.1054/bjoc.2001.1809
72. Kukreja I, Kapoor P, Deshmukh R, Kulkarni V. VEGF and CD 34: A correlation between tumor angiogenesis and microvessel density-an immunohistochemical study. *J Oral Maxillofac Pathol*. 2013;17(3):367-373. doi:10.4103/0973-029X.125200
73. Kwiterovich KA, Maguire MG, Murphy RP, et al. Frequency of Adverse Systemic Reactions after Fluorescein Angiography: Results of a Prospective Study. *Ophthalmology*. 1991;98(7):1139-1142. doi:10.1016/S0161-6420(91)32165-1
74. Lawman S, Dong Y, Williams BM, et al. High resolution corneal and single pulse imaging with line field spectral domain optical coherence tomography. *Opt Express*. 2016;24(11):12395. doi:10.1364/oe.24.012395
75. Lee P, Wang CC, Adamis AP. Ocular neovascularization: An epidemiologic review. *Surv Ophthalmol*. 1998;43(3):245-269. doi:10.1016/S0039-6257(98)00035-6
76. Lee W Di, Devarajan K, Chua J, Schmetterer L, Mehta JS, Ang M. Optical coherence tomography angiography for the anterior segment. *Eye Vis*. 2019;6(1). doi:10.1186/s40662-019-0129-2
77. Li P, An L, Reif R, Shen TT, Johnstone M, Wang RK. In vivo microstructural and microvascular imaging of the human corneo-scleral limbus using optical coherence tomography. *Biomed Opt Express*. 2011;2(11):3109. doi:10.1364/boe.2.003109
78. Ling S, Lin H, Liang L, et al. Development of new lymphatic vessels in alkali-burned corneas. *Acta Ophthalmol*. 2009;87(3):315-322. doi:10.1111/j.1755-3768.2008.01349.x

79. Liu S, Romano V, Steger B, Kaye SB, Hamill KJ, Willoughby CE. Gene-based antiangiogenic applications for corneal neovascularization. *Surv Ophthalmol*. 2018;63(2):193-213. doi:10.1016/j.survophthal.2017.10.006
80. Liu W, Schultz KM, Zhang K, et al. In vivo corneal neovascularization imaging by optical-resolution photoacoustic microscopy. *Photoacoustics*. 2014;2(2):81-86. doi:10.1016/j.pacs.2014.04.003
81. Liu W, Zhang HF. Photoacoustic imaging of the eye: A mini review. *Photoacoustics*. 2016;4(3):112-123. doi:10.1016/j.pacs.2016.05.001
82. Liu YC, Devarajan K, Tan TE, Ang M, Mehta JS. Optical Coherence Tomography Angiography for Evaluation of Reperfusion After Pterygium Surgery. *Am J Ophthalmol*. 2019;207:151-158. doi:10.1016/j.ajo.2019.04.003
83. Liu Z, Karp CL, Galor A, Al Bayyat GJ, Jiang H, Wang J. Role of optical coherence tomography angiography in the characterization of vascular network patterns of ocular surface squamous neoplasia. *Ocul Surf*. 2020;18(4):926-935. doi:10.1016/j.jtos.2020.03.009
84. Liu Z, Wang H, Jiang H, Gameiro GR, Wang J. Quantitative analysis of conjunctival microvasculature imaged using optical coherence tomography angiography. *Eye Vis*. 2019;6(1). doi:10.1186/s40662-019-0130-9
85. Lockard I, Debacker H. Conjunctival circulation in relation to circulatory disorders. *J S C Med Assoc*. 1967;63(6):201-206. Accessed October 6, 2020. https://pubmed.ncbi.nlm.nih.gov/5233050/
86. Mackman G, Polack F, Sidrys L. Fluorescein angiography of soft contact lens induced vascularization in penetrating keratoplasty - PubMed. *Ophthalmic Surg* . 1985;16(3):157-161. Accessed September 12, 2020. https://pubmed.ncbi.nlm.nih.gov/2581204/
87. Maguire MG, Stark WJ, Gottsch JD, et al. Risk factors for corneal graft failure and rejection in the collaborative corneal transplantation studies. Collaborative Corneal Transplantation Studies Research Group. *Ophthalmology*. 1994;101(9):1536-1547. Accessed October 20, 2018. http://www.ncbi.nlm.nih.gov/pubmed/8090456
88. Marvin Minsky, inventorMicroscopy apparatus. US1957 (filed), 1961 (granted).
89. McDonald DM, Choyke PL. Imaging of angiogenesis: From microscope to clinic. *Nat Med*. 2003;9(6):713-725. doi:10.1038/nm0603-713
90. McMonnies CW, Chapman-Davies A. Assessment of conjunctival hyperemia in contact lens wearers. part I. *Optom Vis Sci*. 1987;64(4):246-250. doi:10.1097/00006324-198704000-00003
91. Meyer PAR. Patterns of blood flow in episcleral vessels studied by low-dose fluorescein videoangiography. *Eye*. 1988;2(5):533-546. doi:10.1038/eye.1988.104
92. Meyer PAR, Watson PG. Low dose fluorescein angiography of the conjunctiva and episclera. *Br J Ophthalmol*. 1987;71(1):2-10. doi:10.1136/bjo.71.1.2
93. Mimura T, Amano S, Usui T, Kaji Y, Oshika T, Ishii Y. Expression of vascular endothelial growth factor C and vascular endothelial growth factor receptor 3 in corneal lymphangiogenesis. *Exp Eye Res*. 2001;72(1):71-78. doi:10.1006/exer.2000.0925
94. Mitsui Y, Matsubara M, Kanagawa M. Fluorescence irido-corneal photography. *Br J Ophthalmol*. 1969;53(8):505-512. doi:10.1136/bjo.53.8.505
95. Nagendran M, Chen Y, Lovejoy CA, et al. Artificial intelligence versus clinicians: Systematic review of design, reporting standards, and claims of deep learning studies in medical imaging. *BMJ*. 2020;368. doi:10.1136/bmj.m689
96. Nagy JA, Benjamin L, Zeng H, Dvorak AM, Dvorak HF. Vascular permeability, vascular hyperpermeability and angiogenesis. *Angiogenesis*. 2008;11(2):109-119. doi:10.1007/s10456-008-9099-z
97. Nieuwenhuizen J, Watson PG, Jager MJ, Emmanouilidis-van der Spek K, Keunen JEE. The value of combining anterior segment fluorescein angiography with indocyanine green angiography in scleral inflammation. *Ophthalmology*. 2003;110(8):1653-1666. doi:10.1016/S0161-6420(03)00487-1

98. Nuttall AL. Velocity of red blood cell flow in capillaries of the guinea pig cochlea. *Hear Res*. 1987;27(2):121-128. doi:10.1016/0378-5955(87)90013-X
99. Ocular lymphatics: state-of-the-art review - PubMed. Accessed September 10, 2020. https://pubmed.ncbi.nlm.nih.gov/19725271/
100. Oie Y, Nishida K. Evaluation of corneal neovascularization using optical coherence tomography angiography in patients with limbal stem cell deficiency. *Cornea*. 2017;36:S72-S75. doi:10.1097/ICO.0000000000001382
101. Olver JM, McCartney ACE. Anterior segment vascular casting. *Eye*. 1989;3(3):302-307. doi:10.1038/eye.1989.43
102. Owen CG, Newsom RSB, Rudnicka AR, Barman SA, Woodward EG, Ellis TJ. Diabetes and the Tortuosity of Vessels of the Bulbar Conjunctiva. *Ophthalmology*. 2008;115(6). doi:10.1016/j.ophtha.2008.02.009
103. Palme C, Ahmad S, Romano V, et al. En-face analysis of the human limbal lymphatic vasculature. *Exp Eye Res*. 2020;201:108278. doi:10.1016/j.exer.2020.108278
104. Palme C, Romano V, Brunner M, Vinciguerra R, Kaye SB, Steger B. Functional staging of corneal neovascularization using fluorescein and indocyanine green angiography. *Transl Vis Sci Technol*. 2018;7(5). doi:10.1167/tvst.7.5.15
105. Palme C, Wanner A, Romano V, et al. Indocyanine green angiographic assessment of melanocytic ocular surface neoplastic lesions. *Submitt Cornea Unpubl results*.
106. Palme C, Wanner A, Romano V, Haas G, Kaye S, Steger B. Observation of angiographic dye leakage in ocular surface squamous neoplasia. *Am J Ophthalmol Case Reports*. 2020;20. doi:10.1016/j.ajoc.2020.100912
107. Papas E. Key factors in the subjective and objective assessment of conjunctival erythema . *Invest Ophthalmol Vis Sci*. 2000;41(3):687-691.
108. Peebo BB, Fagerholm P, Lagali N. An in vivo method for visualizing flow dynamics of cells within corneal lymphatics. *Lymphat Res Biol*. 2013;11(2):93-100. doi:10.1089/lrb.2012.0023
109. Perlman HB, Kimura R. Cochlear blood flow in acoustic trauma. *Acta Otolaryngol*. 1962;54(1-6):99-110. doi:10.3109/00016486209126927
110. Peterson RC, Wolffsohn JS. Sensitivity and reliability of objective image analysis compared to subjective grading of bulbar hyperaemia. *Br J Ophthalmol*. 2007;91(11):1464-1466. doi:10.1136/bjo.2006.112680
111. Pharmacologic modulation of vascular permeability in ocular allergy in the rat - PubMed. Accessed September 10, 2020. https://pubmed.ncbi.nlm.nih.gov/2105283/
112. Pries AR, Cornelissen AJM, Sloot AA, et al. Structural adaptation and heterogeneity of normal and tumor microvascular networks. *PLoS Comput Biol*. 2009;5(5). doi:10.1371/journal.pcbi.1000394
113. Rocha De Lossada C, Pagano L, Gadhvi K, et al. Persistent loss of marginal corneal arcades after chemical injury. *Indian J Ophthalmol 2020 Press*.
114. Romano V, Spiteri N, Kaye SB. Angiographic-guided treatment of corneal neovascularization. *JAMA Ophthalmol*. 2015;133(3):e143544. doi:10.1001/jamaophthalmol.2014.3544
115. Romano V, Steger B, Brunner M, et al. Detecting Change in Conjunctival Hyperemia Using a Pixel Densitometry Index. *Ocul Immunol Inflamm*. 2019;27(2):276-281. doi:10.1080/09273948.2017.1387276
116. Romano V, Steger B, Brunner M, Ahmad S, Willoughby CE, Kaye SB. Method for Angiographically Guided Fine-Needle Diathermy in the Treatment of Corneal Neovascularization. *Cornea*. 2016;35(7):1029-1032. doi:10.1097/ICO.0000000000000865
117. Romano V, Steger B, Kaye SB. Detection and Imaging of Lymphatic and Other Vessels in Corneal Neovascular Complexes. *Cornea*. 2018;37(4):e22-e23. doi:10.1097/ICO.0000000000001516
118. Romano V, Steger B, Kaye SB. Fine-Needle Diathermy Guided by Angiography. *Cornea*. 2015;34(9):e29-e30. doi:10.1097/ICO.0000000000000546

119. Romano V, Steger B, Zheng Y, Ahmad S, Willoughby CE, Kaye SB. Angiographic and in vivo confocal microscopic characterization of human corneal blood and presumed lymphatic neovascularization: A pilot study. *Cornea*. 2015;34(11):1459-1465. doi:10.1097/ICO.0000000000000609

120. Romano V, Steger B, Zheng Y, Ahmad S, Willoughby CE, Kaye SB. Angiographic and in vivo confocal microscopic characterization of human corneal blood and presumed lymphatic neovascularization: A pilot study. *Cornea*. 2015;34(11):1459-1465. doi:10.1097/ICO.0000000000000609

121. Schulze MM, Hutchings N, Simpson TL. Grading bulbar redness using cross-calibrated clinical grading scales. *Investig Ophthalmol Vis Sci*. 2011;52(8):5812-5817. doi:10.1167/iovs.10-7006

122. Schulze MM, Hutchings N, Simpson TL. The use of fractal analysis and photometry to estimate the accuracy of bulbar redness grading scales. *Investig Ophthalmol Vis Sci*. 2008;49(4):1398-1406. doi:10.1167/iovs.07-1306

123. Schulze MM, Jones DA, Simpson TL. The development of validated bulbar redness grading scales. *Optom Vis Sci*. 2007;84(10):976-983. doi:10.1097/OPX.0b013e318157ac9e

124. Shahidi M, Wanek J, Gaynes B, Wu T. Quantitative assessment of conjunctival microvascular circulation of the human eye. *Microvasc Res*. 2010;79(2):109-113. doi:10.1016/j.mvr.2009.12.003

125. Shields CL, Alset AE, Boal NS, et al. Conjunctival Tumors in 5002 Cases. Comparative Analysis of Benign Versus Malignant Counterparts. The 2016 James D. Allen Lecture. *Am J Ophthalmol*. 2017;173:106-133. doi:10.1016/j.ajo.2016.09.034

126. Shields CL, Chien JL, Surakiatchanukul T, Sioufi K, Lally SE, Shields JA. Conjunctival tumors: Review of clinical features, risks, biomarkers, and outcomes - The 2017 J. Donald M. Gass Lecture. *Asia-Pacific J Ophthalmol*. 2017;6(2):109-120. doi:10.22608/APO.201710

127. Shields JA, Kligman BE, Mashayekhi A, Shields CL. Acquired sessile hemangioma of the conjunctiva: A report of 10 cases. *Am J Ophthalmol*. 2011;152(1):55-59.e1. doi:10.1016/j.ajo.2011.01.013

128. Shields JA, Mashayekhi A, Kligman BE, et al. Vascular tumors of the conjunctiva in 140 cases. *Ophthalmology*. 2011;118(9):1747-1753. doi:10.1016/j.ophtha.2011.04.034

129. Shortt AJ, Secker GA, Munro PM, Khaw PT, Tuft SJ, Daniels JT. Characterization of the Limbal Epithelial Stem Cell Niche: Novel Imaging Techniques Permit In Vivo Observation and Targeted Biopsy of Limbal Epithelial Stem Cells. *Stem Cells*. 2007;25(6):1402-1409. doi:10.1634/stemcells.2006-0580

130. Shu X, Wang J, Hu L. A review of functional slit lamp biomicroscopy. *Eye Vis*. 2019;6(1). doi:10.1186/s40662-019-0140-7

131. Sirazitdinova E, Gijs M, Bertens CJF, Berendschot TTJM, Nuijts RMMA, Deserno TM. Validation of computerized quantification of ocular redness. *Transl Vis Sci Technol*. 2019;8(6). doi:10.1167/tvst.8.6.31

132. Spaide RF. Optical coherence tomography angiography signs of vascular abnormalization with antiangiogenic therapy for choroidal neovascularization. *Am J Ophthalmol*. 2015;160(1):6-16. doi:10.1016/j.ajo.2015.04.012

133. Spaide RF, Klancnik JM, Cooney MJ. Retinal vascular layers in macular telangiectasia type 2 imaged by optical coherence tomographic angiography. *JAMA Ophthalmol*. 2015;133(1):66-73. doi:10.1001/jamaophthalmol.2014.3950

134. Spiteri N, Romano V, Zheng Y, et al. Corneal angiography for guiding and evaluating fine-needle diathermy treatment of corneal neovascularization. *Ophthalmology*. 2015;122(6):1079-1084. doi:10.1016/j.ophtha.2015.02.012

135. Steger B, Romano V, Kaye SB. Angiographic Evaluation of Inflammation in Atopic Keratoconjunctivitis. *Ocul Immunol Inflamm*. 2018;26(5):685-688. doi:10.1080/09273948.2016.1247873

136. Steger B, Romano V, Kaye SB. Corneal Indocyanine Green Angiography to Guide Medical and

Surgical Management of Corneal Neovascularization. *Cornea*. 2016;35(1):41-45. doi:10.1097/ICO.0000000000000683

137. Stewart R. Conjunctival-corneal melt in association with carotid artery stenosis. *Clin Ophthalmol*. 2008;2(3):649. doi:10.2147/opth.s2430
138. Structural aspects of the permeability of the microvascular endothelium - PubMed. Accessed September 10, 2020. https://pubmed.ncbi.nlm.nih.gov/382743/
139. Sugisaki K, Usui T, Nishiyama N, et al. Photodynamic therapy for corneal neovascularization using polymeric micelles encapsulating dendrimer porphyrins. *Investig Ophthalmol Vis Sci*. 2008;49(3):894-899. doi:10.1167/iovs.07-0389
140. Sun Y, Hua R. Ocular surface squamous neoplasia: Angiographic characteristics and response to subconjunctival/ perilesional 5-fluorouracil injections. *Drug Des Devel Ther*. 2019;13:1323-1334. doi:10.2147/DDDT.S191161
141. Talusan ED, Schwartz B. Fluorescein angiography: Demonstration of Flow Pattern of Anterior Ciliary Arteries. *Arch Ophthalmol*. 1981;99(6):1074-1080. doi:10.1001/archopht.1981.03930011074018
142. Terry R, Wong R, Papas E. Variability of clinical investigators in contact lens research. *Optom Vis Sci 1995;7216*. 1995;72:16.
143. Waring GO, Laibson PR. A Systematic Method of Drawing Corneal Pathologic Conditions. *Arch Ophthalmol*. 1977;95(9):1540-1542. doi:10.1001/archopht.1977.04450090062004
144. Watson PG, Bovey E. Anterior Segment Fluorescein Angiography in the Diagnosis of Scleral Inflammation. *Ophthalmology*. 1985;92(1):1-11. doi:10.1016/S0161-6420(85)34074-5
145. Wuest TR, Carr DJJ. VEGF-A expression by HSV-1-infected cells drives corneal lymphangiogenesis. *J Exp Med*. 2010;207(1):101-115. doi:10.1084/jem.20091385
146. Yadav S, Kaye S, Wilson N. An unusual presentation of generalized essential telangiectasia. *Clin Exp Dermatol*. 2015;40(5):513-515. doi:10.1111/ced.12568
147. Yaylali V, Ohta T, Kaufman SC, Maitchouk DY, Beuerman RW. In vivo confocal imaging of corneal neovascularization. *Cornea*. 1998;17(6):646-653. doi:10.1097/00003226-199811000-00013
148. Yuen D, Wu X, Kwan AC, et al. Live imaging of newly formed lymphatic vessels in the cornea. *Cell Res*. 2011;21(12):1745-1749. doi:10.1038/cr.2011.178
149. Zhang Y, Jeon M, Rich LJ, et al. Non-invasive multimodal functional imaging of the intestine with frozen micellar naphthalocyanines. *Nat Nanotechnol*. 2014;9(8):631-638. doi:10.1038/nnano.2014.130
150. Zhao F, Cai S, Huang Z, Ding P, Du C. Optical Coherence Tomography Angiography in Pinguecula and Pterygium. *Cornea*. 2020;39(1):99-103. doi:10.1097/ICO.0000000000002114
151. Zhao Z, Yue Y, Zhang S, et al. Optical coherence tomography angiography for marginal corneal vascular remodelling after pterygium surgery with limbal-conjunctival autograft. *Eye*. 2020;34(11):2054-2062. doi:10.1038/s41433-020-0773-8
152. Zheng Y, Kaye AE, Boker A, et al. Marginal corneal vascular arcades. *Investig Ophthalmol Vis Sci*. 2013;54(12):7470-7477. doi:10.1167/iovs.13-12614

Table 1. Imaging techniques: application, benefit and limitations

Imaging technique	Benefit	Limitation
Drawing	Easy to perform Easy to document the lesion of interest Highlight features Inexpensive	Lack precision Subjective Time consuming Require annotation software (digital or analogue)
Photography	Easy to perform High magnification Capture colours Inexpensive	Operator dependent Dependent on camera quality Dependent on patient cooperation Reliant on contrast Limited by plane of focus
Angiography	Dynamic examination with high contrast Excellent visualisation of the vascular complex Excellent vessel staging Direction of flow Good reproducibility	Operator dependent Dependent on patient cooperation Time consuming Invasive Side-effects Expensive
In vivo confocal microscopy	Visualisation of the cell morphology Visualisation of the tissue morphology High magnification High resolution	Operator dependent Time consuming Dependent on patient cooperation Small field of view Need to physically contact the cornea Limited reproducibility Expensive
Optical coherence tomography angiography	Non-invasive Easy to perform	Dependent on patient cooperation Depend on intravascular cell movement Unable to show the dynamic patterns of leakage Insensitive to avascular vessels (ghost vessels) Expensive
Photoacoustic imaging	Non-invasive Novel	Need to physically contact the cornea Time consuming Low resolution and scanning depth Expensive

Table 2. ICG angiographic vascular features in ocular surface neoplastic lesions

Feature	**Benign**	**Dysplastic / Malignant**
Intrinsic tumor vessels	Rare	Frequent
Intralesional hemorrhage	No	Frequent
Feeder vessels	Rare	Frequent

Afferent-efferent vessel diameter ratio	0.3 - 0.9	0.9 - 1.3
Angiographic perfusion time	2.2 - 4.3 seconds	2.0 – 2.9 seconds
Angiographic malperfusion	No	Frequent
Angiographic time to ICG leakage	210 - ∞ seconds	50 – 160 seconds

Biomicroscopic and ICG angiographic vascular features differentiating benign from dysplastic or malignant ocular surface neoplastic lesions. ICG Indocyanine green [105]

Figure Legend

Figure 1. A. Anterior view of palpebral conjunctival blood supply. LPA – Lateral palpebral artery. LA – Lacrimal artery. LM – Lid margin. PTA – Peripheral tarsal arcade (Not always present inferiorly). MPA – Medial palpebral artery. OA – Ophthalmic artery. PCA – Posterior conjunctival artery. MTA – Marginal tarsal arcade.
B. Lateral view of anterior segment blood supply. OA – Ophthalmic artery. RMS – Rectus muscle supply. LPCA – Long posterior ciliary artery. EAA – Episcleral arterial arcade. IAA – Intraocular arterial arcade. MCA – Marginal corneal arcade. LMA – Limbal arcade. MTA – Marginal tarsal arcade. TP – Tarsal plate. OO – Orbicularis oculi. PTA – Peripheral tarsal arcade. PCA – Posterior conjunctival artery. ACA – Anterior ciliary artery. C. Anterior view of anterior segment blood supply. EAA – Episcleral arterial arcade. ACA – Anterior ciliary arteries

Figure 2. ICGA Details of the normal marginal corneal arcades (A) and early development of corneal neovascularization arising from the marginal corneal arcades (C). A) shows a regular pattern in vessel loop configuration, while in C there is limbal transvascular leakage and increasing loop irregularity. B)* represents an en face optical section collected from a corneal limbal wholemount stained with FITC-phalloidin (green) and anti-CD31 (platelet endothelial cell adhesion molecule-1) antibody (red) to identify blood vessels. This demonstrates the presence of a complex vascular plexus that is intimately associated with the limbal crypts (arrows). CO indicates the peripheral cornea.[129] C) Normal marginal arcades and development of Conv from MCA (white arrows). *Reproduced with permission of *Stem Cells*. Any reuse requires permission from *Stem Cells*

Figure 3. Lymphatic vessels as visualized by reuptake of leaked fluorescein dye on late fluorescein angiography (A). In B lymphatic vessels are seen on a composition of in vivo confocal microscopic images (B). C and D represent 10 min fluorescein and 1 min indocyanine green angiography respectively. E is a digital image obtained by subtracting the two previous images to show the ‘sausage‘ shaped lymphatic vessel (white arrow). [120] Reproduced with permission of *Cornea*. Any reuse requires permission from *Cornea*

Figure 4. Diagram of vasculature and vessel segments. Pixels in white represent segmented vessels and black means background. The red lines represent the centerlines computed from the segmented vessels. Blue squares denote branching points, green triangles the ending points and the yellow

circle an intersection point between two vessel segments. Note: Points on the edge of the images are not considered here. The locations of the centrelines and the landmark points are for demonstration and may not be accurate. (B) angiographic image with branching point in red

Figure 5. Color photograph of lipid kerathopathy (A) – efferent vessel seen (blue arrowhead) but not afferent vessel (red arrowhead). Fluorescein angiography (B) demonstrates transvascular leakage. Afferent vessel (artery - red arrow) and efferent vessel (vein - blue arrow) are highlighted. Indocyanine green angiography (C) demonstrates excellent vessel architecture (afferent vessel – arrow). Color photo of a central corneal scar (D). Indocyanine green angiography highlights corneal neovascularization (E), even when obscured by exudation and corneal scar tissue.

Figure 6. Color photograph of lipid keratopathy (A) with corresponding fluorescein angiography on the right showing transvascular dye leakage (B).

Figure 7. Color photographs, fluorescein angiography (FA) at 5 mins, indocyanine green angiography (ICGA) at 1 and 7 minutes for active, inactive and regressed corneal neovascularization (CoNV). Transvascular leakage is seen on FA and ICGA in active CoNV, while in inactive CoNV there is only leakage on FA, and no leakage on either angiography in regressed CoNV. [104]

Figure 8. Color photograph (A), fluorescein angiography (B) and OCT-angiography (C) for a case of corneal neovascularization. D, E and F show a segmentation analysis with OCT-angiography revealing vessel depth.[21]

Figure 9. Corneal neovascularization before (A and B) and after (C) fine-needle diathermy of the afferent vessels. Early- and late-phase indocyanine green angiography was performed to measure and distinguish the afferent (A) and more numerous efferent (B) vessels.[114] Reproduced with permission of *JAMA Ophthalmol*. Any reuse requires permission from *JAMA Ophthalmol*.

Figure 10. Arterial (A, D), arterial-venous (B, E) and venous phase (C, F). Red arrows represent arteries, while blue arrows represent veins. The pictures A, B and C represent a corneal neovascularization in patient with a herpes simplex keratitis, while pictures D, E and F represent a corneal neovascularization in patient with an Acanthamoeba sp. keratitis.

Figure 11. Fluorescein (left) and indocyanine (right) angiography of a chemical burn injury at different follow ups. Green arrows show vessel leakage while the orange line is delimitating the avascular zone on day 1 (A and B), and only partial consecutive re-perfusion at 3 months (C and D) and 6 years (E and F).[113]

Figure 12. Representative images of angiographic studies in patients and controls. In the active group, transepithelial fluorescein dye leakage and increasing extravascular ICG leakage are seen. In the inactive group, both of these findings are absent. In only one (here presented) control patient, late extravascular leakage of ICG at the lid margin but not from large tarsal conjunctival vessels was observed, corresponding to the presence of associated lid margin inflammation. FA, fluorescein angiography; ICGA, indocyanine green angiography; early images taken 1 min after injection; late image taken 5–10 min after injection.[135] Pending permission of *Ocul Immunol Inflamm*. for image reuse

Figure 13. Conjunctival hyperemia pre (A, C) and post application of topical phenylephrine (B, D) with color photographs and indocyanine green angiography. The graph (E) quantifies the intensity of fluorescent dye present in C (blue line) and D (red line).[115] Pending permission of *Ocul Immunol Inflamm*. for image reuse

Figure 14. Color pictures (A, C, E) and respective ICGA (B, D, F) showing teleangectatic vessels of the conjunctiva and the lid margin.

Figure 15. Subclinical limbus inflammation with absence of clear sign at slit lamp (A) in an atopic keratoconjunctivitis patient with limbus stem cell deficiency and fluorescein angiography (B) showing vessel leakage at the limbus, especially in the superior quadrants.

Figure 16. A. Biomicroscopic color photograph of conjunctival in-situ squamous carcinoma. B Early fluorescein angiography showing diffuse dye leakage within the neoplastic tissue, accentuated in the terminal vascular bulbs on the centripetal border of the lesion. C Early indocyanine green angiography showing diffuse dye leakage within the borders of the lesion, but not in surrounding conjunctival tissue.[106] Pending permission of *Am J Ophthalmol Case Reports* for image reuse

Figure 17. Color photographs and indocyanine green angiography (ICGA) of conjunctival papilloma

(A, B)*, in situ squamous cell carcinoma (C, D), conjunctival naevus (E, F) and conjunctival invasive melanoma (G, H)*. On color photographs, black arrows represent afferent vessels, while blue dots represent efferent vessels. On ICGA the red arrows represent afferent vessels, while blue dots represent efferent vessels.[23] *Reproduced with permission of *Curr Eye Res*. Any reuse requires permission from *Curr Eye Res*.

Supplementary figure. Early phase (1 minute) of ICG angiography of the eyelid that highlight the venous complex (arteries are deep and not visible).